

The Jordan Journal of Earth and Environmental Sciences (JJEEES)

JJEEES is an international peer-reviewed research journal, issued by the Deanship of Academic Research and Graduate Studies, the Hashemite University, in corporation with, the Jordanian Scientific Research Support Fund, the Ministry of Higher Education and Scientific Research.

EDITORIAL BOARD

Editor-in-Chief

Professor Abdul Rahim A. Hamdan
The Hashemite University

Editorial board

- **Professor Abdulkader M. Abed**
University of Jordan
- **Professor Hani N. Khoury**
University of Jordan
- **Professor Zuhair H. El-Isa**
University of Jordan
- **Professor Sameh Gharaibeh**
Yarmouk University
- **Professor Ahmad Abu Hilal**
Yarmouk University
- **Professor Issa Makhlof**
The Hashemite University
- **Professor Tayel M. El-hasan**
Mu'tah University

THE INTERNATIONAL ADVISORY BOARD

- **Prof. Sayed Abdul Rahman,**
Cairo University, Egypt.
- **Prof. Abdullah Al-Amri,**
King Saud University, Saudi Arabia.
- **Prof. Waleed Al-Zubair,**
Arabian Gulf University, Bahrain.
- **Prof. Ute Austermann-Haun,**
Fachhochschule Lippe und Hoexter, Germany.
- **Prof. Ibrahim Banat,**
University of Ulster, UK.
- **Prof. Matthias Barjenbruch,**
Technisch Universitat Berlin, Germany.
- **Prof. Mohamed Boukhary,**
Ain Shams University, Egypt.
- **Prof. Mohammad El-Sharkawy,**
Cairo University, Egypt.
- **Prof. Venugopalan Ittekkot.**
Center for Tropical Marine Ecology, Bremen,
Germany.
- **Prof. Christopher Kendall,**
University of North Carolina, U.S.A.
- **Prof. Elias Salameh,**
University of Jordan, Jordan.
- **Prof. V. Subramanian,**
Jawaharlal Nehru University, India.
- **Prof. Omar Rimawy,**
University of Jordan, Jordan.
- **Prof. Hakam Mustafa,**
Yarmouk University, Jordan.
- **Dr. Michael Crosby,**
The National Science Board, National Science
Foundation, Virginia, U.S.A.
- **Dr. Brian Turner,**
Durham University, U.K..
- **Dr. Friedhelm Krupp,**
Senckenberg Research Institute and Natural History
Museum, Germany.
- **Dr. Richard Lim,**
University of Technology, Australia.

EDITORIAL BOARD SUPPORT TEAM

Language Editor

Dr. Qusai Al-Debyan

Publishing Layout

MCPD. Osama AlShareet

SUBMISSION ADDRESS:

Professor **Abdul Rahim A. Hamdan**
Deanship of Academic Research and Higher Studies
Hashemite University, P.O. Box 330127, Postal Code 13133, Zarqa, Jordan.

Phone: +962-5-3903333 ext. 4151
E-Mail: jjees@hu.edu.jo , hamdan@hu.edu.jo



Hashemite Kingdom of Jordan



Hashemite University

Jordan Journal of
Earth and Environmental Sciences

JJEEES

An International Peer-Reviewed Scientific Journal □ □

<http://jjees.hu.edu.jo/>

ISSN 1995-6681

PAGES	PAPERS
63 – 78	Application of Chemometric Technique in the Assessment of Groundwater Quality in Udi and its Environs, South-eastern Nigeria <i>S.O. Onwuka, C. S Ezeh and A.C. Ekwe</i>
79 – 98	Sedimentology and Morphology of Quaternary Alluvial Fans in Wadi Araba, Southwest Jordan <i>Issa M. Makhlof, Belal S. Amireh, Abdulkader M. Abed</i>
99 – 110	Geology and Mineralogy of Jabal Kabid Phosphorite Deposits, Southeastern Jordan <i>SAEB Al-SHEREIDEH, Khaled Tarawneh, Hani Nawafleh, NAZEM El-RADAIDEH and Khaled Moumani</i>
111 – 120	Eutrophication Process in the Mujib Dam <i>Sura T. Al-Harahsheh, Hani R. Al-Amoush</i>

Application of Chemometric Technique in the Assessment of Groundwater Quality in Udi and its Environs, South-eastern Nigeria

S.O. Onwuka, C. S Ezeh and A.C. Ekwe

Department of Geology, University of Nigeria Nsukka

Abstract

This paper examines the factors controlling the hydrochemical facies of groundwater in the shallow marine Plain Sands aquifer in Udi and its environs, in Enugu State, Southeastern Nigeria. Twelve water samples were collected from Udi and its environs and analyzed for twenty-one parameters. The data obtained were subjected to R-mode factor analysis. Factor 1 reflects the signature of pollution factors resulting from seepages into the aquifer from the Ama Brewery and the tide-influenced Ajali River. Factor 2 has high loading values and represents the processes of natural rainwater recharge and water-soil/rock interaction. Factor 3 can be related to the dissolution of sulphides from interstratified peat within the geological formation and from heavy vehicular and brewery activities in Ama town. A broad zone of groundwater contact between water species represented by Factors 1 and 2 is thus created towards the Ajali River. The inference is that ionic concentration in the water decreases away from the banks of the river, an indication that the quality of groundwater improves away from the river. Factor 3 is enhanced in the southeastern area of the town where it is deemed to be caused by the dissolution of sulphur-bearing minerals within the geological formation, and also in the central and northwestern parts of the town, where it could be related to the rain-dissolution of sulphur-bearing compounds from gaseous emission arising from vehicular and brewery activities.

© 2010 Jordan Journal of Earth and Environmental Sciences. All rights reserved

Keywords: Aquifer, Factor Analysis (FA), Factor Loading (FL), Pollution, Water Quality Index (WQI).

1. Introduction

The study area spans the entire Udi North Local Government Area (LGA) in Enugu State, southeastern Nigeria. Udi is in the Anambra basin, a depocentre filled with Cretaceous to Recent sedimentary materials. Several boreholes exist in Udi, all tapping the prolific aquifers of the Ajali Sandstone. The quality of groundwater depends on several factors, including climate, soil characteristics, manner of circulation of groundwater through the rock type and topography of area (Rajesh et al., 2002). Chemistry of water is one of the important factors for determining its use for domestic, agricultural or industrial purposes. The chemical composition of groundwater depends not only on natural factors such as lithology of aquifer, the quality of recharge waters and types of interactions between water and aquifer, but also on human (anthropogenic) factors (activities), which can alter fragile ground water systems either by polluting them or by changing hydrological cycle (Helena et al., 2000). Several graphical methods were used to facilitate the interpretation and presentation of chemical analysis data from this study. The methods include the piper, stiff or shape and ionic

concentration diagrams. Because these methods consider only major ionic constituents, multivariate technique, such as factor analysis (FA) has been widely used as unbiased methods in the analysis of groundwater quality data to characterize groundwater composition influenced by natural and anthropogenic factors. In this work, the large dataset obtained from the hydrochemical analysis of groundwater samples collected from Udi and its immediate environs were subjected to Factor Analysis (FA), with the objective of assessing the groundwater quality as well as the hidden factors explaining the various processes that influence the water quality. Physical and chemical parameters of groundwater play a significant role in classifying and assessing water quality. Water Quality Indices (WQI) permits us to access changes in the water quality and to identify water trends (Silvia and Daniel, 2000).

1.1. Local geographic setting

The area under study covers about sixteen towns that comprise the Udi North L.G.A in Enugu State, southeastern Nigeria, and lies roughly between latitudes $6^{\circ}17'N$ and $6^{\circ}23'N$ of the equator, and longitudes $7^{\circ}16'E$ and $7^{\circ}21'E$ of GMT (Fig. 1). Udi has undulating topography. The area is drained by Oji and Dodo Rivers on the southwestern and central parts respectively while the Ajali River drains the northwest part of the area. The preferred orientation of the tributaries and subtributaries

* Corresponding author. amobiekwe@yahoo.com

gives a dendritic drainage pattern, with water sources occurring as contact springs at the valley of the Udi cuesta,

joining up with other seepages to flow as streams along river valleys and extensive gully channels.

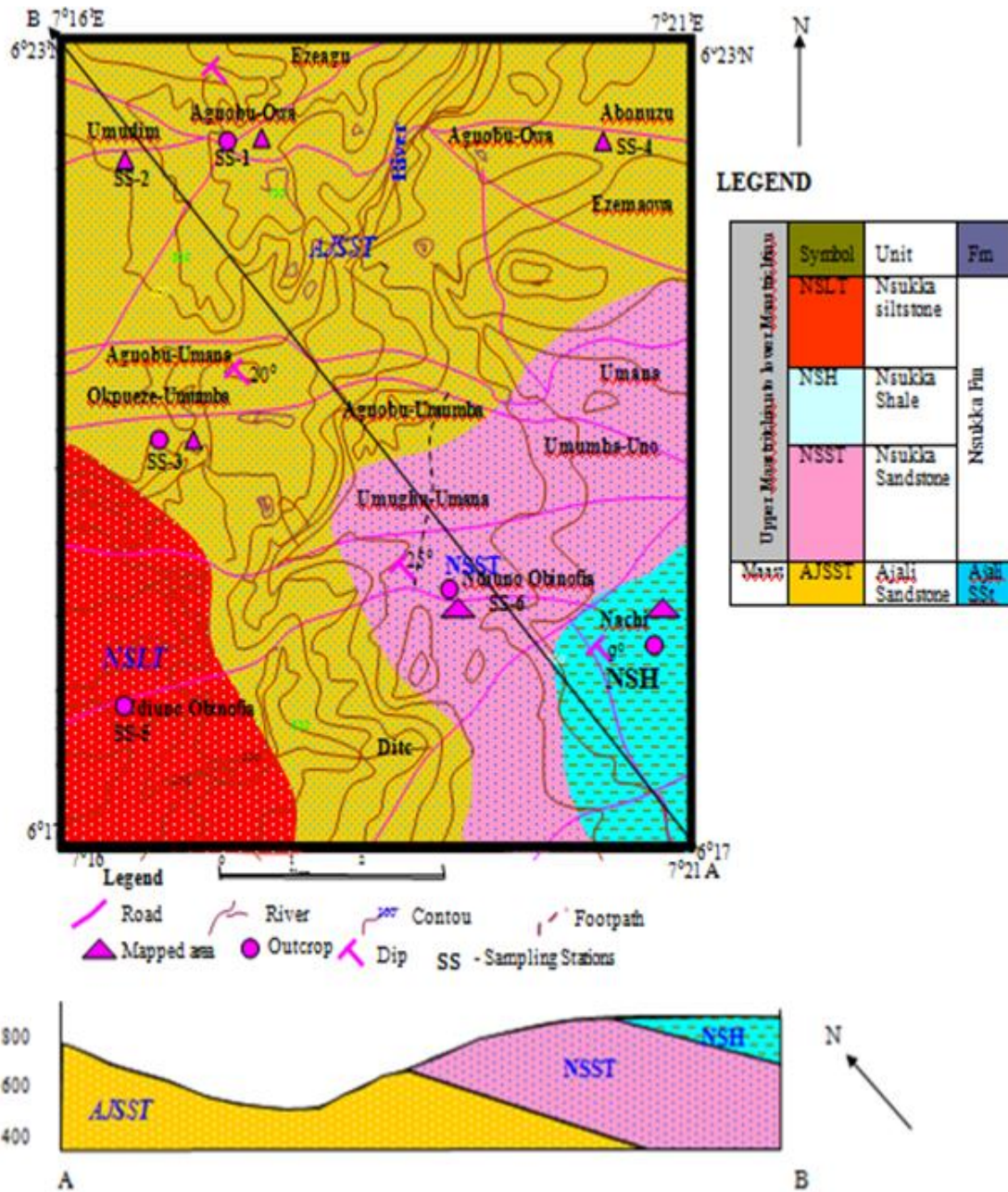


Fig. 1: Geologic map of the study area.

2. Geology and Hydrogeology

The study area is in the Anambra basin and is directly underlain by the Ajali Sandstone (Kogbe, 1976). It is dotted in places by the Nsukka Formation, which consists of tidal estuarine deposits (Reyment, 1965). The Ajali Sandstone lies unconformably on the Mamu Formation which, in turn, is underlain by the Nkporo group. The

Nkporo group is the basal unit of the Anambra stratigraphic pile (Fig. 2). The Ajali Sandstone is a thick, friable, poorly sorted, poorly cemented and unconsolidated sandstone sequence, generally covered by lateritic soil and thick red earth overburden, typically white in colour. (Ladipo, 1987; Nwajide and Reijers, 1996). The age of the formation is Maastrichtian.

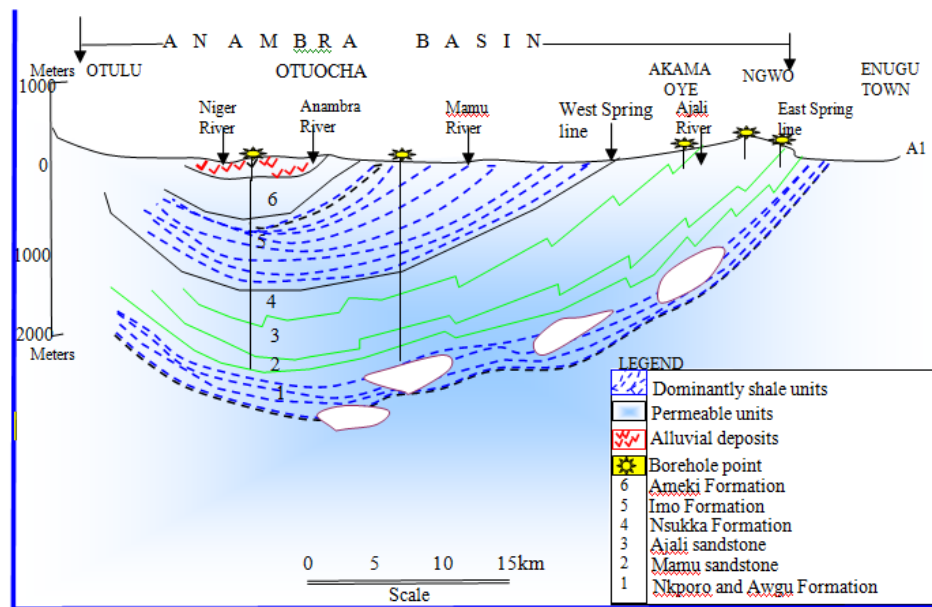


Fig 2: Schematic geological section across the Anambra basin showing the study area (Based on Reymont, 1965; Whiteman, 1982).

The Ajali Sandstone is up to 400m in places and constitutes the most prolific aquifer in the Anambra Basin (Ezeigbo, 1987). It comprises mainly a water table aquifer, but also has semi-confined aquifers where fingers of clays occur in appreciable thicknesses (Offodile, 2002). The existence of impermeable materials in the Ajali Sandstone makes possible the accumulation of groundwater at shallow depths that constitute perched aquifer system; hence the existence of hand-dug wells in parts of the study area. A number of boreholes exist in several parts of Udi, including those at the well fields that supply water to Enugu town which is basically underlain by shales. Uma *et al.* (1989) have given the hydraulic conductivity of the Ajali Sandstone to range from $1-10 \times 10^{-6}$.

3. Sampling and Analytical Procedures

3.1. Sampling and Analysis of Groundwater

The sampling network and strategy were designed to cover a wide range of determinants at key sites, which reasonably represent the groundwater quality in the study area. The representative sampling sites were chosen in order to cover areas of various anthropogenic activities, including waste disposal. The gathered background information provides sufficient details on these aspects. Groundwater samples (12 samples) were collected from hand-dug wells, springs, stream and an artesian well in March 2009 and July 2009, representing dry and rainy seasons sampling respectively. Samples for major ions and other inorganics were collected in one-liter pre-cleaned polypropylene bottles. The samples were immediately transported to the laboratory under low-temperature conditions in iceboxes and stored in the laboratory at 4°C until analysis. All the samples were analyzed for 21 parameters according to the standard methods of APHA–AWWA– WEF (1998). Details of analytical methodology followed are given in Table 1.

3.2. Factor Analysis (FA)

According to Ouyang *et al.* (2006), the purpose of FA is to reduce large analytical data of samples which are intercorrelated to a small set of ‘factors’ that are then interpretable. The factors group correlated concentrations together and they can be associated directly or indirectly with some specific source or process. The method consists of three steps, namely data standardization, factor extraction, and rotation of factor axes. Prior to analysis, the initial data are standardized by z -scale transformation as

$$Z = \frac{X_{ji} - \bar{X}_j}{S_j}$$

Where x_{ji} indicates the original value of the measured parameter, \bar{x}_j the average value of the parameter j and s_j the standard deviation of j . FA takes data contained in a correlation matrix and rearranges them in a manner that better explains the structure of the underlying system that produced the data. The starting point of FA is to generate a new group of variables from the initial dataset (the so-called factors) that are a linear combination of the original variables. The first factor obtained explains the biggest part of the variance. The following factors explain repeatedly smaller parts of the variance (Ruiz *et al.*, 1990).

Factor loadings show how the factors characterize the variables. High factor loadings (close to 1 or -1) indicate strong relationship (positive or negative) between the variable and the factor describing the variable. Then the factor loadings matrix is rotated to an orthogonal simple structure according to the varimax rotation technique. Finally, factor scores are calculated for each sample and plotted as a scatter diagram. Extreme positive factor scores ($>+1$) reflect sampling stations most affected by the process and extreme negative score (<-1) reflect those unaffected by the process explained by the factor. Near-zero scores reflect sampling stations affected to an average degree by the process (Kennel *et al.*, 2007).

3.3. Data Treatment and Chemometric Analysis

Chemometric analysis of the data was performed using FA techniques. FA is performed on standardized (z -scale transformation) experimental datasets in order to avoid misclassification due to wide differences in data dimensionality. The z -scale transformation renders the data normalized with mean and variance of zero and one

respectively. Standardization tends to increase the influence of variables whose variance is small and reduce the influence of variables whose variance is large (Lui *et al.*, 2003). Furthermore, standardization procedure eliminates the influence of different units of measurement and renders the data dimensionless. All the statistical computations were made using the SPSS 10.1 software.

Table 1: Details of analytical methodology and basic statistics of groundwater samples collected from the study area

Symbol	Variable	Method	Units	Detection Limit	DRY SEASON				RAINY SEASON			
					Min	Max	Mean	SD	Min	Max	Mean	SD
PH	PH	Potentiometry	pH	-	4.14	5.96	5.040	0.609	4.0	5.01	4.45	0.494
EC	Electrical conductivity	Electrolytic	$\mu\text{mhos/cm}$	-	21.3	106.0	39.570	32.816	18.8	107.1	38.13	34.134
TH	Total Hardness (as CaCO_3)	EDTA titrimetric	Mg/l	5	3.0	28.0	10.330	13.692	BDL	30.0	6.33	11.827
Ca	Calcium	EDTA titrimetric	Mg/l	2	BDL	9.2	3.000	3.096	BDL	7.9	1.8	3.047
Mg	Magnesium	By difference	Mg/l	1	9.6	4.5	0.850	1.794	BDL	4.83	1.24	1.923
Na	Sodium	Flame photometry	Mg/l	1	BDL	22.8	15.100	7.238	3.55	21.97	12.44	7.563
K	Potassium	Flame photometry	Mg/l	1	24.9	222.3	42.090	89.109	1.67	11.0	4.39	3.509
HCO ₃	Bicarbonate	Titrimetry	Mg/l	6	9.21	95.7	50.430	30.256	BDL	70.0	28.68	26.352
CL	Chloride	Argentometry	Mg/l	4	47.26	35.45	16.190	9.777	3.0	28.0	8.51	9.694
SO ₄	Sulfate	Nephelometry	Mg/l	5	BDL	129.19	78.380	29.626	18.75	75.95	36.6	20.014
NO ₃	Nitrate	Spectrophotometry	Mg/l	0.05	BDL	0.25	0.130	0.082	BDL	0.15	0.085	0.061

SD= standard deviation; BDL= below detection level; Min= Minimum value, Max- maximum value

4. Results and Interpretation

4.1. Graphical Methods

An important task in groundwater investigation is the compilation and presentation of chemical data in a convenient manner for visual inspection. For this purpose, several commonly used graphical methods are available.

The simplest of these is the pie chart, which represents the major ion compositions in equivalents per cubic meter or million equivalents per litre as percentages of total equivalents. The results of the water analysis (Appendix A) in this study are shown in pie charts in Figure 3 and Figure 4. Other representations are shown in Figures 4-9.

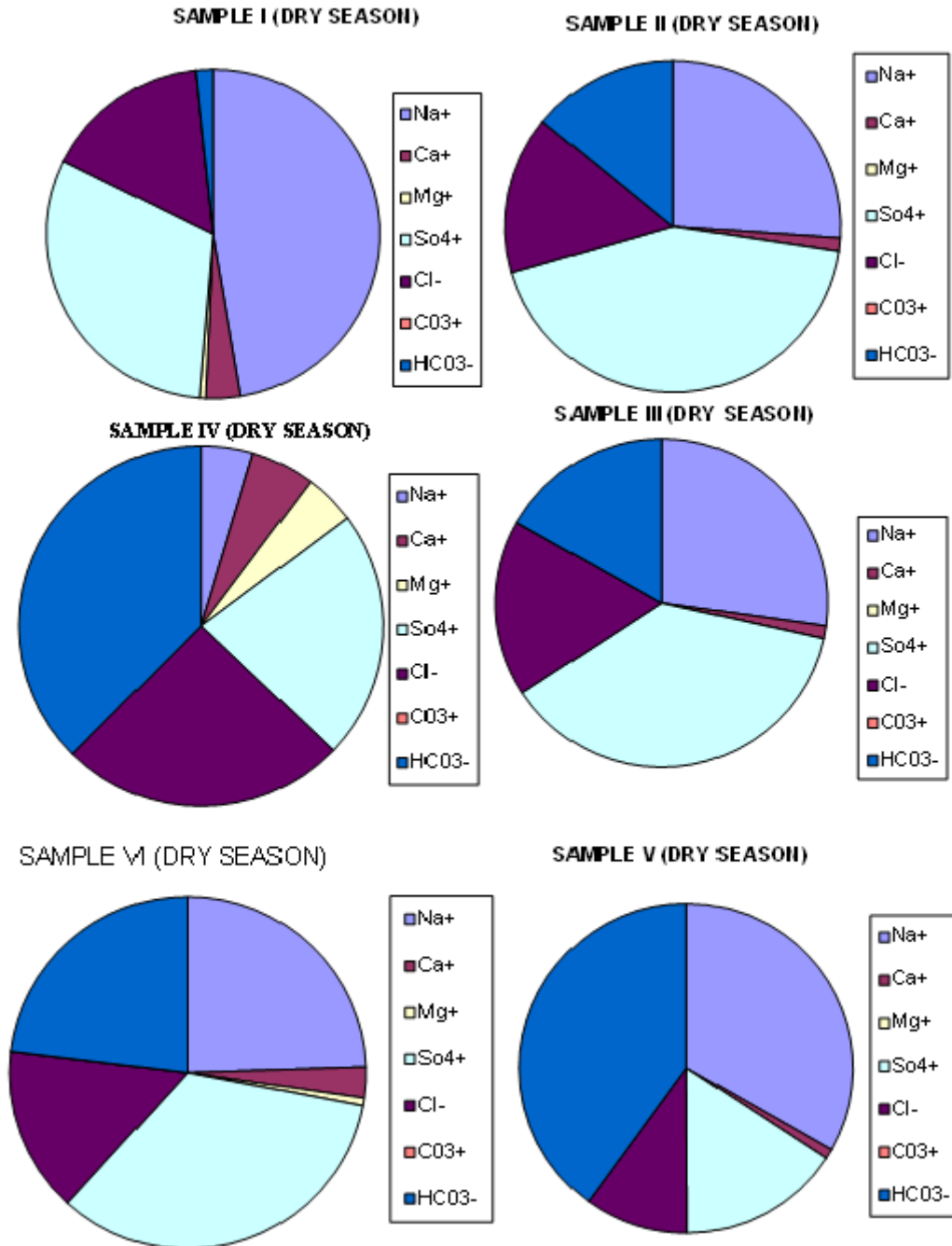


Fig. 3: Water samples for dry season.

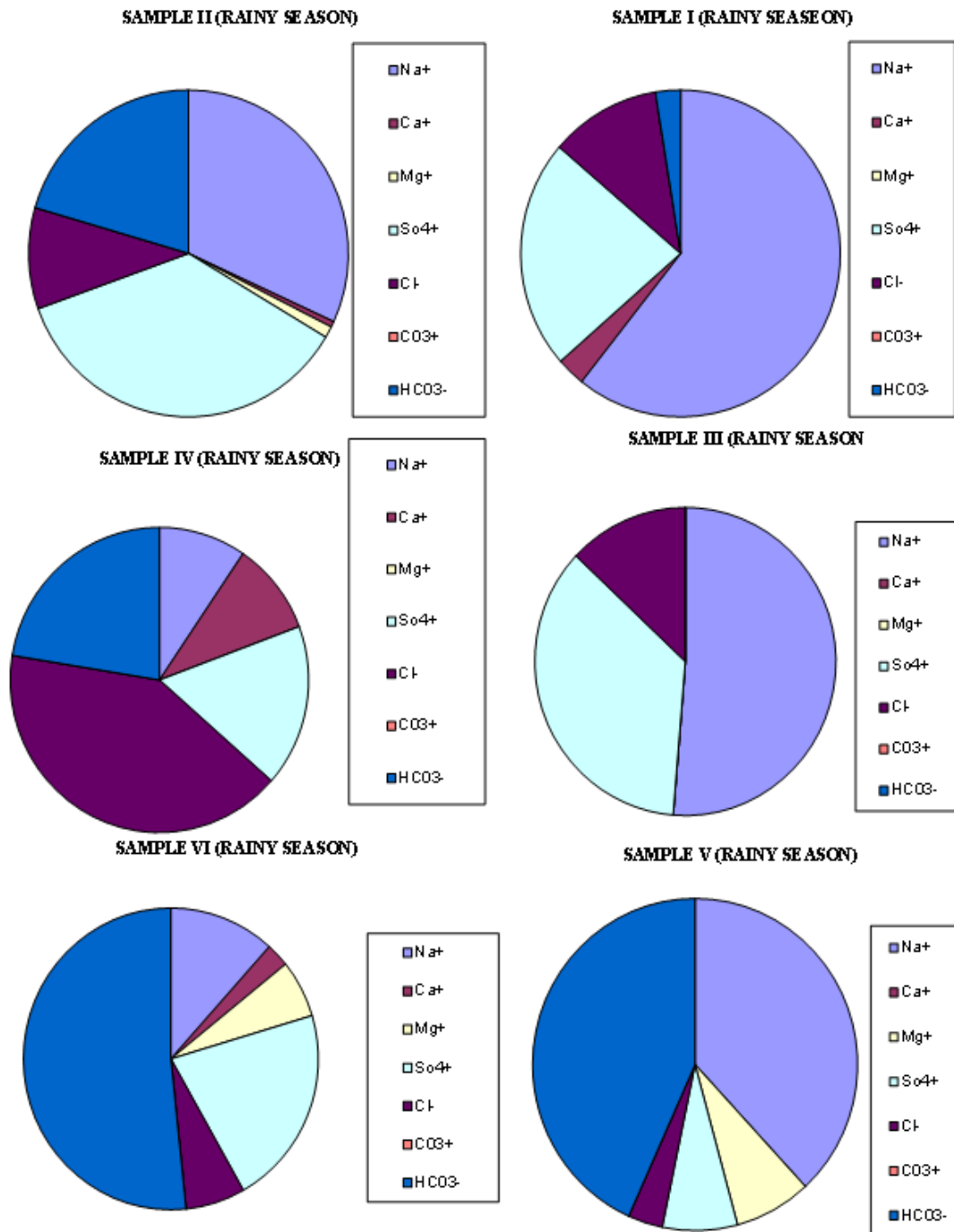


Fig. 4: Water samples for Rainy season

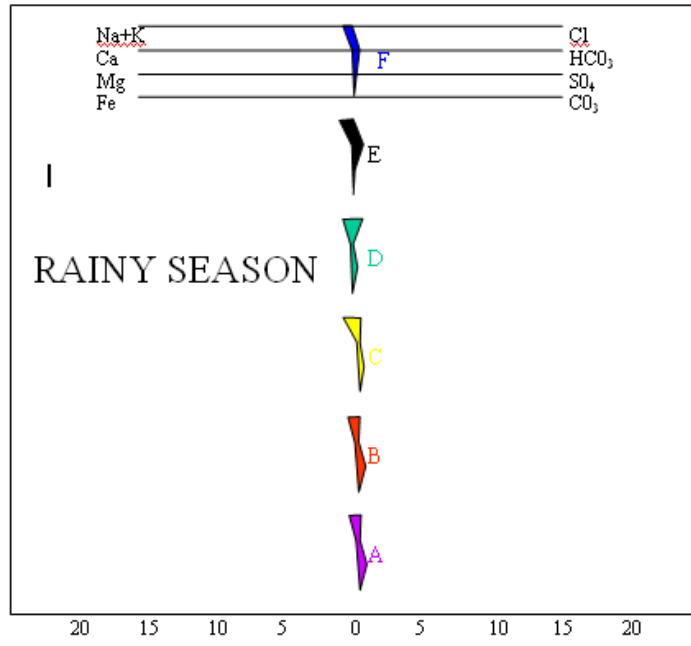


Fig. 5: Pattern diagrams for water Samples A, B, C, D, E & F (After Hem, 1989)

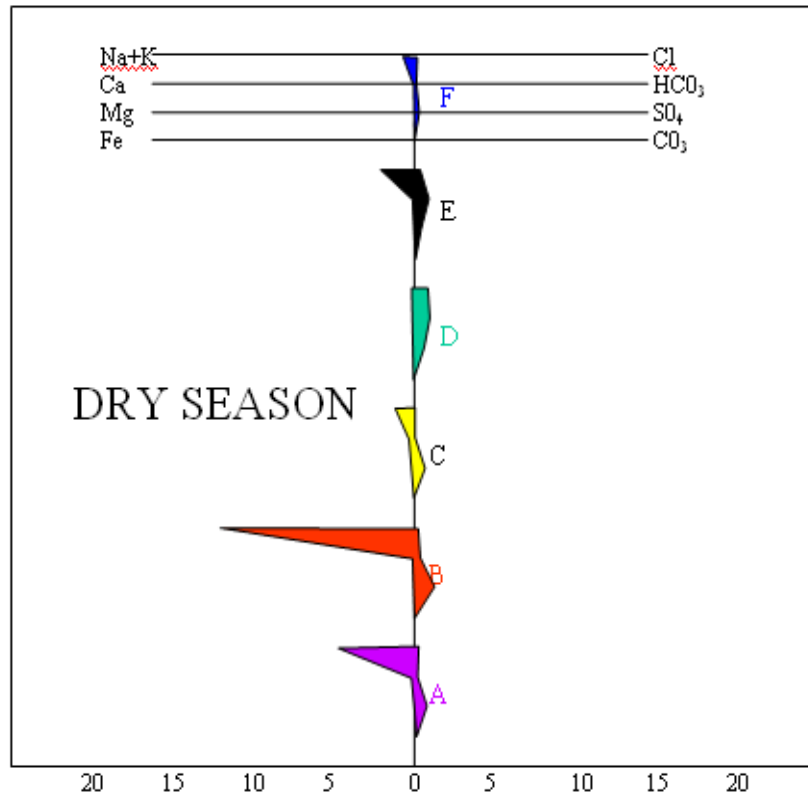


Fig. 6: Pattern diagrams for representing analysis of groundwater quality (After Hem, 1989)

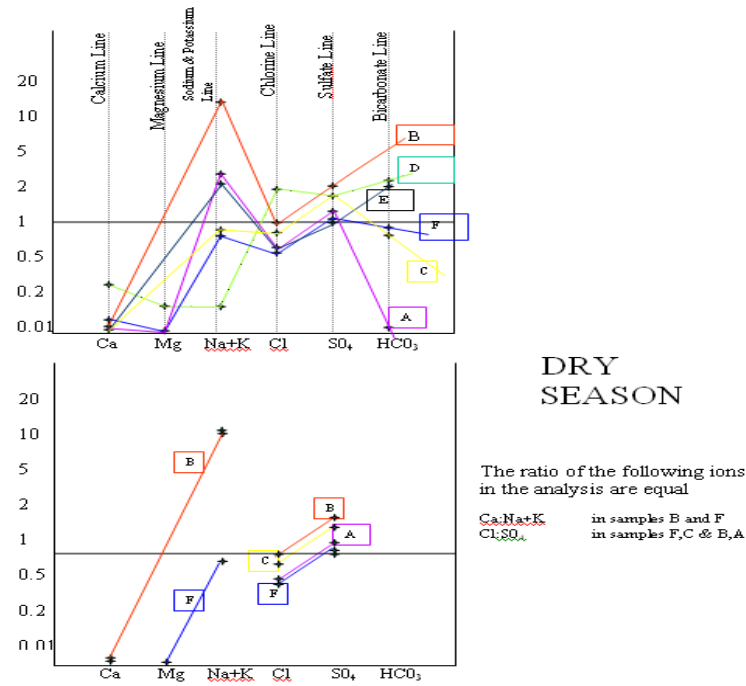


Fig. 7. Schoeller semilogarithmic diagram for representing analysis of groundwater quality (After Schoeller, 1962)

Fig. 7: Schoeller semilogarithmic diagram for representing analysis of groundwater quality for dry season water samples A,B,C & F (After

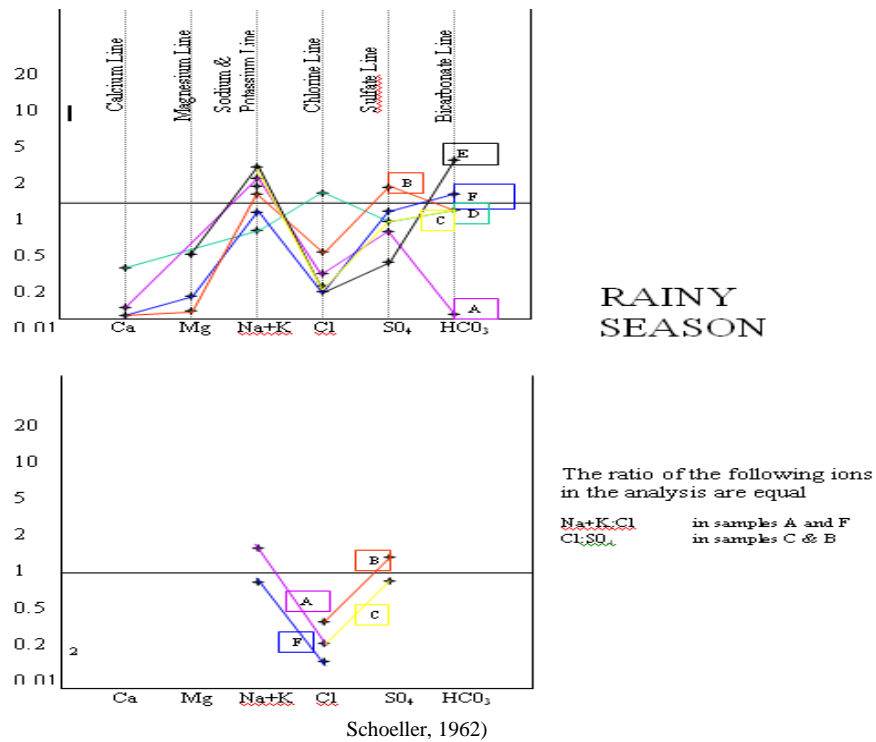


Fig. 8: Schoeller semilogarithmic diagram for representing analysis of groundwater quality for rainy season water samples (A, B, C & F) (After Schoeller, 1962)

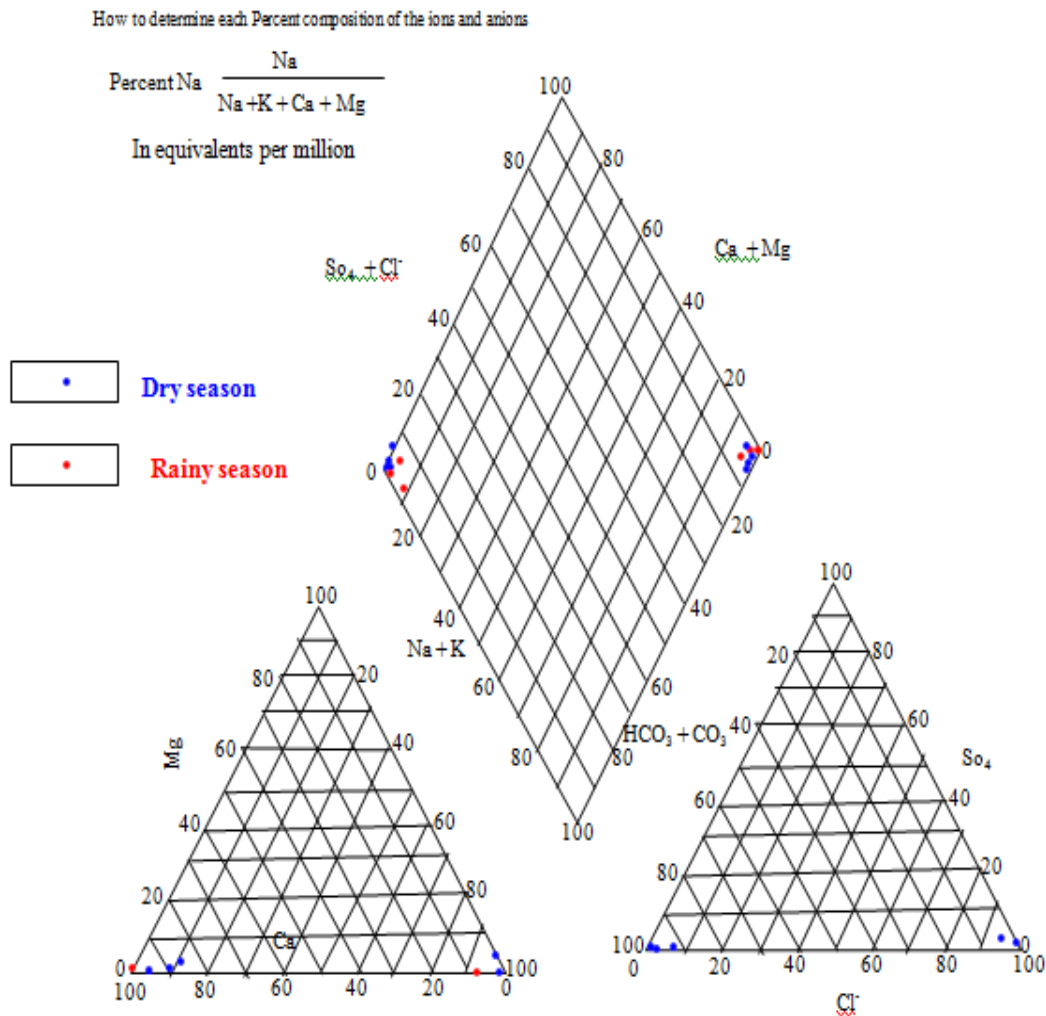


Fig. 9: Chemical analysis of water represented as percentages of total equivalents per litre on the diagram developed by Hill (1940) and Piper (1944).

4.2. Factor analysis (FA)

The Bartlett's sphericity test carried out on the correlation matrix shows calculated $\chi^2 = 1950.5$ and 2000 for the dry and rainy seasons respectively, which are greater than the critical value of $\chi^2 = 387.3$ ($P = 0.0005$ and 300 degrees of freedom), thus proving that the Principal Component (PC) extraction can achieve a significant reduction of the dimensionality of the original dataset. Factor Analysis (FA) was applied separately to the hydrochemical dataset pertaining to dry and rainy seasons. Table 4 summarizes the sorted FA results, including the variable loadings, and variance explained by each factor for the two seasons. The factor loadings were sorted according to the criteria of Liu *et al.* (2003), into strong, moderate and weak, corresponding to absolute loading values of >0.75 , $0.75-0.50$ and $0.50-0.30$ respectively. Loading values <0.30 are insignificant. During the Dry season, Factor 1 explains 56.65% of the variance and is characterized by strong positive loadings (>0.90) of TH, EC, TDS, Cl, HCO_3 , NO_3 and Ca, and strong loadings by TH, EC, TDS, Cl, HCO_3 , NO_3 , Ca; while SO_4 shows weak loadings. Others show moderate loadings. Factor 2 explains 28.62% of the variance and has strong loadings of

Mg, K, SO_4 and P^{H} ; TH, Ca, EC, TDS, Pb, Mn, Cl, NO_3 , Cl, HCO_3 and acidity are insignificant, while Fe shows weak loadings. Considerable overlapping of variables (TH, EC, Mg, K, SO_4 , TDS, Cl, HCO_3 , NO_3 and Ca) is observed. Hence, the underlying processes explaining these two Factors are mixed. Further, major ionic constituents that are highly correlated to EC, TH, P^{H} and TDS mainly contribute to Factor 1. Hence, Factor 1 may be termed as the 'major ion pollution factor'.

Factor 1 could represent as the Ama Brewery pollution factor and the zone of water mixing at the bank of the Ajali River. The sources of major ionic constituents are the poor industrial waste system; hence, Factors 1 and 2 could be collectively called pollution factors. Factors 3 and 4 account for 14.73% of the variance of the dataset; however, the variable loadings of Factors 3 & 4 are not clearly describable. Hence the possible sources associated with these factors could not be explained. Factor 1 (major ion pollution factor) explains 59.14% of the variance and has strong loadings of EC, Ca, TH, TDS, Fe and Cl. Similar to the dry season, SO_4 showed weak loadings.

Factor 2 explains 10.78% of variance and has strong loadings of Mg, K and NO_3 ; all the rest of the ions are considered insignificant (i.e. <0.30). The variance

explained by the two factors (i.e. Factor 1 & Factor 2) accounts for 69.92% of the total variance. Similar to dry season, overlapping of variables is observed. Also, the variable loadings of Factors 3 and 4 are not clear, though they account for 30.08% of the total variance. Comparison of FA for the two seasons shows the effect of groundwater recharge caused by downpour on the two processes associated with the two factors. It appears that the major ion pollution factor shows little change during the rainy season; but there is considerable reduction in pollution load caused by the Ama pollution factor. This is evidenced by the substantial reduction in the concentration of certain metals, notably, HCO_3 and major ionic constituents, such as EC, TH, Ca, TDS, and Cl during the rainy season. The loading pattern of Factors 3 and 4 during the dry season and during the rainy season is not clear and indicates the

absence of correlation with other variables. The factor score plots of the first two factors for the dry and rainy seasons are shown in Figure 10. Comparison of the factor score plots for the two seasons shows the effect of dilution on the hydrochemical variables caused by recharge. The score plots for the two seasons show almost the same grouping of samples. The samples affected by the two factors (factor score >1) are well identified for the two seasons. During the dry season, few of the samples are clustered around the origin, indicating contamination by the two processes to an average extent. Most of the samples were not affected by the two processes and have high negative scores (<-1). The clustering of samples around the origin is less pronounced during the two seasons, indicating the effect of dilution caused by rainfall.

Table 4: R-mode varimax rotated factor loadings of groundwater parameters for dry and rainy seasons in the study area

Variables	Factor 1	Factor 2	Factor 3	Factor 4		Variables	Factor 1	Factor 2	Factor 3	Factor 4	
PH	-1.48	-0.11	-0.53	1.51		PH	-1.01	-0.71	-0.91	0.34	
EC	2.02	-0.20	-0.34	-0.41		EC	2.02	-0.18	-0.31	-0.51	
TH	2.02	-0.46	-0.54	-0.17		TH	2.00	0.00	0.00	-0.03	
Ca	2.00	-0.45	-0.58	-0.06		Ca	2.00	0.00	-0.43	-0.07	
Mg	0.00	2.03	-0.31	-0.31		Mg	0.40	1.87	-0.33	0.00	
Na	-1.51	0.26	-0.11	0.92		Na	-1.09	-0.20	0.40	0.81	
K	0.00	2.02	0.00	-0.13		K	-0.09	1.88	-0.78	-0.49	
HCO_3	1.50	-0.76	-0.87	0.06		HCO_3	0.00	-0.03	-0.03	-1.01	
CL	1.97	0.01	-0.21	-0.50		CL	2.01	-0.44	-0.10	-0.33	
SO_4	0.34	1.72	0.24	-0.55		SO_4	-0.16	-0.16	1.97	-0.32	
NO_3	1.47	-0.37	0.24	0.24		NO_3	0.24	1.06	0.24	0.24	
Mn	0.00	0.00	0.00	0.00		Mn	0.00	0.00	0.00	0.00	
Pb	0.00	0.00	0.00	0.00		Pb	0.00	0.00	0.00	0.00	
TDS	2.02	-0.18	-0.33	-0.41		TDS	2.02	-0.18	-0.31	-0.51	
ACIDITY	0.00	0.00	0.00	0.00		ACIDITY	0.00	0.00	0.00	0.00	
Fe	-0.40	0.40	0.40	0.00		Fe	1.34	-0.80	0.27	0.80	
% Variance	56.65	28.62	4.37	10.36			59.14	10.78	19.30	10.78	
Cummulative %	56.65	85.27	89.64	100			59.14	69.92	89.22	100.00	

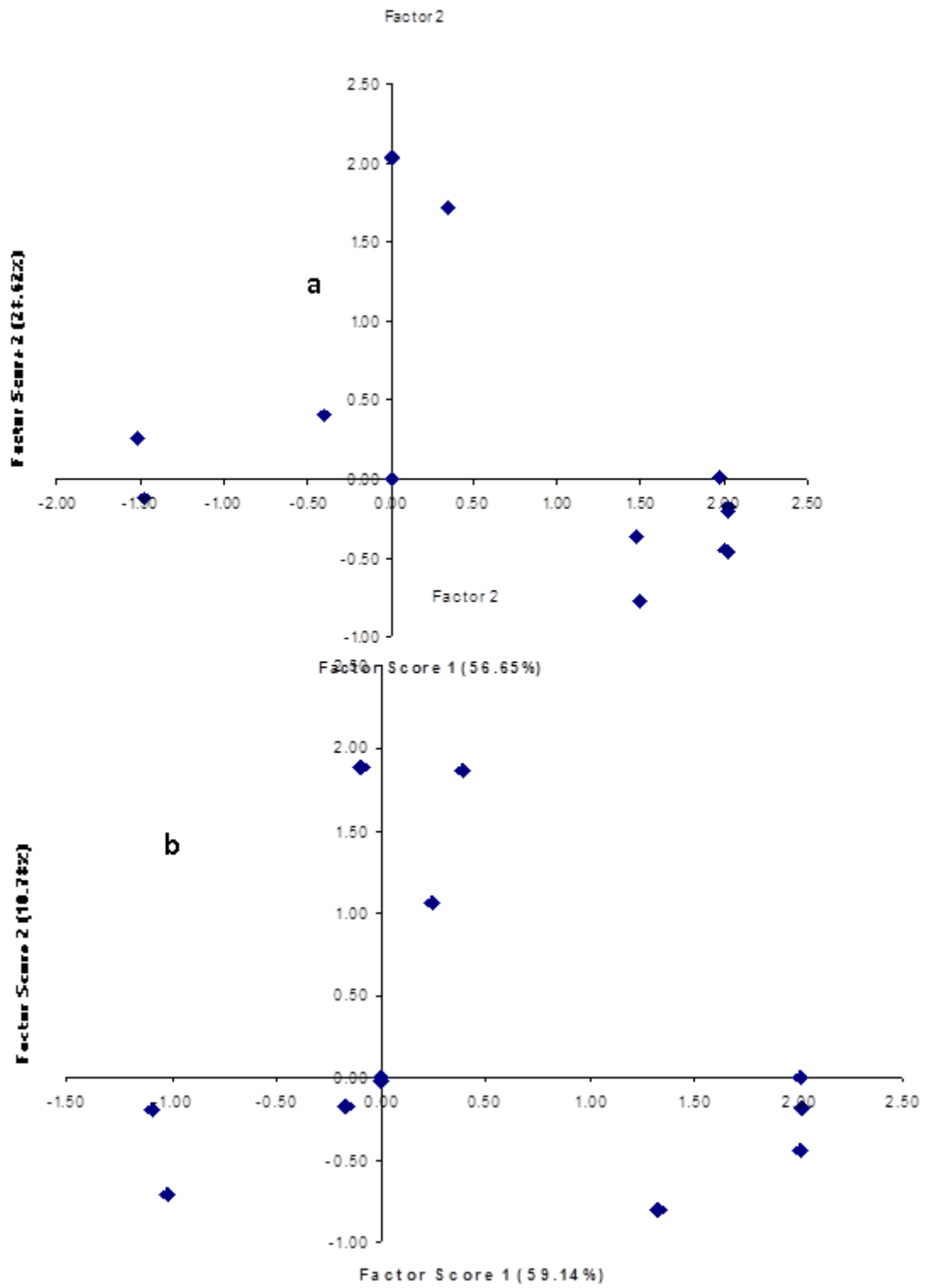


Fig. 10: Factor score plot of Factors 1 and 2 for (a) Dry season and (b) Rainy season

4.3. Water Quality Index (WQI)

The evaluation of water quality index in this study was based on the calculation proposed by Pesce and Wunderlin (2000). Water quality rating was assessed by considering the following ranges:

WQI < 40 = fit for human consumption.

WQI 40-70 = moderately polluted

WQI 70-100 = excessively polluted

WQI > 100 = severely polluted

A critical study of the WQI reveals the status of pollution of groundwater in the study area. WQI values for all the sampling sites A, B, C, D, E and F are below 40 WQI (Figure 11).

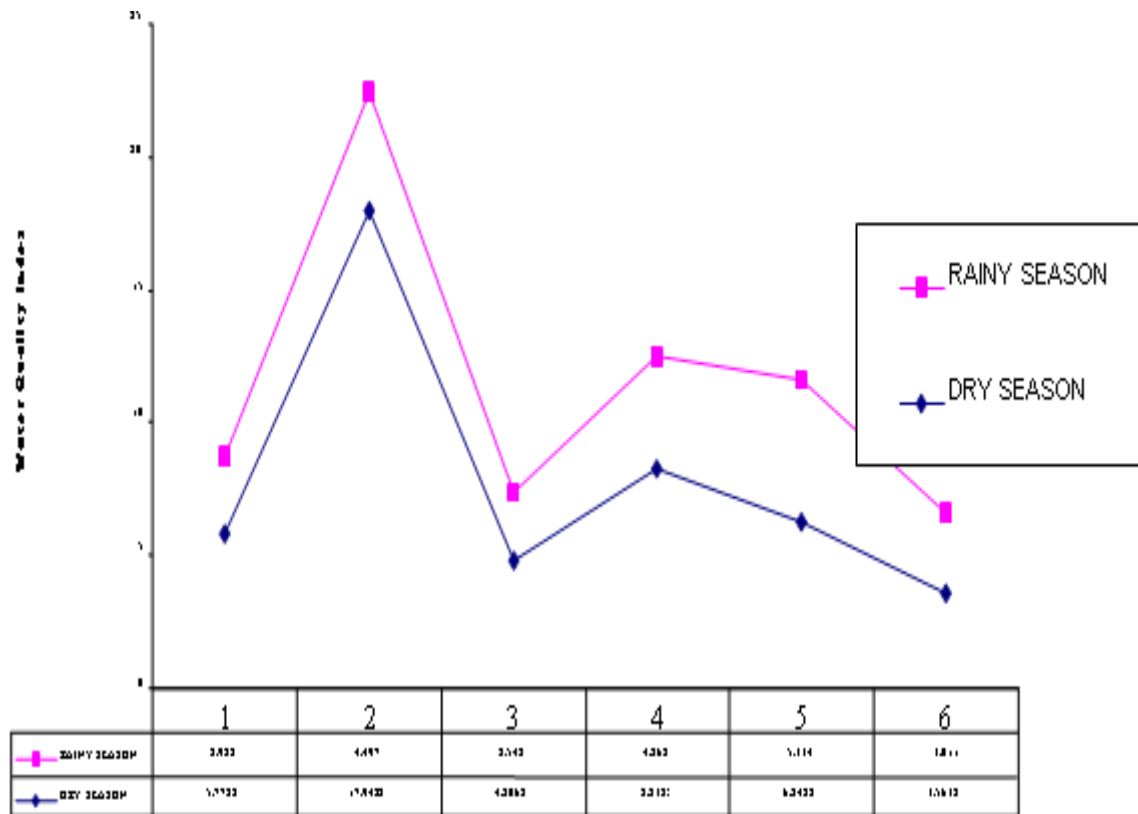


Figure 11: Variation in Water Quality Index (WQI) in the study area.

5. Summary and Conclusion

This paper demonstrates the effectiveness of factor analysis in sorting out otherwise ambiguous hydrogeochemical processes and in showing the spatial influence of such processes. Graphical methods, which include piper diagrams, stiff or shape diagrams, ionic concentration diagram and scattered diagram, were used to facilitate the presentation and interpretation of chemical analysis of groundwater in Udi, southeastern Nigeria. Virtually all diagrams were calculated in terms of equivalents per million or milliequivalents, which express the concentration of ions in solution in terms of their chemical equivalents. The application of the multivariate statistical analysis provided an insight into the underlying controlling hydrochemical processes in the area. Factors 1 and 2 represent ions with dominant concentrations and therefore the main contributors to the groundwater

pollution. Factor analysis (FA) identified two polluting processes, namely a zone of mixing of the two water types especially close to the bank of Ajali River pollution factor and Ama pollution factor, responsible for groundwater pollution in the area. The polluting processes associated with factors 3 and 4 during the rainy and dry seasons could not be identified because variable loadings of these factors were not clear. FA predicted that temporal changes in water quality are due to anthropogenic activities, as caused by the Ama pollution factor. However, it could not differentiate between the unpolluted and moderately polluted stations clearly. The findings of the study indicate the need for proper industrial planning and the safe disposal of industrial and urban wastes, which otherwise would lead to severe environmental degradation. Though several 'pump and treat' techniques could be used to make the water fit for its intended use, aquifer remediation techniques may be suitable for this type of small area.

References

- [1] APHA–AWWA–WEF, 1998. Standard methods for the examination of water and wastewater. Washington DC,
- [2] Ezeigbo, H. I., 1987. Quality of water resources in Anambra state, Nigeria. *Jour. Min. Geol.*, vol. 23 (1), pp. 97-103.
- [3] Helena, B., Pardo, R., Vega M., Barrado, E., Fernandez, J.M., and Fernandez, L., 2000. Temporal evolution of groundwater composition in an alluvial aquifer (Pisuerga River, Spain) by principal component analysis. *Wat. Res.*, vol.34, No.3, pp.807-816.
- [4] Hem, J. D., 1989. The study and interpretation of the chemical characteristics of natural water (3ed). USGS Water Supply Paper 2254.
- [5] Hill, R.A., 1940. Geochemical patterns in Coachella Valley. *Trans.Ame.Geophysics Union*, Part 1, pp. 46-49.
- [6] Kennel, P. R., Seockheon, P., Kanel, S. R. and Khan, S. P., 2007. Chemometric application in classification and assessment of monitoring locations of an urban river system. *Anal. Chim. Acta*, 2007, vol. 582, pp.390–399.
- [7] Kogbe, C. A., 1976. The cretaceous and paleogene sediments of southern Nigeria. *In* Kogbe, C.A. (ed.), *Geology of Nigeria*. Elizabethan publishing co., Lagos, pp. 325-334.
- [8] Ladipo, K. O., 1987. A depositional framework for the Anambra basin, southeastern Nigeria. *Bull. Centres Rech. Explor – Prod. Elf – Aquitaine*, vol. 11, pp. 166-167.
- [9] Liu, C.W., Lin, K.H. and Kuo, Y.M., 2003. Application of factor analysis in the assessment of groundwater quality in a blackfoot disease area in Taiwan. *Sci. Total Environ.*, vol.313, pp.77–89.
- [10] Nwajide, C. S. and Reijers, T. J. A., 1996. The geology of the southern Anambra basin. *In* Reijers, T. J. A., *Selected chapters on geology*. SPDC, Nigeria, pp. 131-148.
- [11] Offodile, M.E., 2002. Ground water study & development in Nigeria (2ed.). Mecon geology &engineering services ltd, Jos, Nigeria, 453p.
- [12] Ouyang, Y., Nkedi-Kizza, P., Wu, Q. T., Shinde, D. and Huang, C. H., 2006. Assessment of seasonal variations in surface water quality. *Water Res.*, vol.40, pp. 3800–3810.
- [13] Pesce S.F., and Wunderlin, D. A., 2000. Use of water quality indices to verify the impact of Cordoba city (Argentina) on Suquia river. *Water Res.*, vol.34, issue 11, pp. 2915-2926.
- [14] Piper, A. M., 1944. A graphic procedure in the geochemical interpretation of water analysis. *Trans. Am. Geophys. Union*, vol. 25, pp. 914-923.
- [15] Reghunath R., Murthy T.R.S. Raghavan, B.R., 2002. The utility of multivariate statistics techniques in hydrogeochemical studies: an example from Karnataka, India. *Water Res.*, vol.36, pp. 2437-2442.
- [16] Reyment, R. A., 1965. Aspects of the geology of Nigeria: the stratigraphy of the cretaceous and cenozoic deposits. University of Ibadan Press, 145p.
- [17] Ruiz, F., Gomis, V. and Blasco, P., 1990. Application of factor analysis to the hydrogeochemical study of a coastal aquifer. *J. Hydrol.* , vol.119, issues 1-4, pp. 169–177.
- [18] Schoeller, H., 1962. *Les eaux Souterraines*. Masson & Cie, Paris, 642p.
- [19] Uma, K. O., Egboka, B.C.E. and Onuoha, K.M., 1989. New statistical grain-size method for evaluating the hydraulic conductivity of sandy aquifers. *Jour. Hydrology*, vol. 108, pp 343-366.
- [20] Whiteman, A. 1982. Nigeria: its petroleum geology, resources and potential. Graham & Trotham, London, UK.

Appendix

ANALYSIS RESULTS

Sample Description:

Analysis Required: Physical, Chemical, and Microbiological

Data Collected: 19/08/09 Lab. Sample No.:

1	PARAMETER	UNIT	WHO std.	VALUES					
				A	B	C	D	E	F
	PHYSICAL ANALYSIS								
	Odour			-ve	-ve	-ve	-ve	-ve	-ve
	Turbidity	NTU	-	1.50	1.0	2.5	2.0	1.0	NIL
	PH value		6.5-9.0	4.62	4.00	4.10	3.95	5.0	5.01
	Conductivity	Microhms/cm	100						
2	CHEMICAL ANALYSIS								
	Acidity	Mg/L CaCO ₃	-	-	-	-	-	-	-
	Alkalinity	Mg/L CaCO ₃	30-500	-	3.00	-	-	10.10	9.10
	Total Solids	Mg/L	-	11.62	15.50	18.01	59.96	10.55	12.65
	Dissolved Solids	Mg/L	500	11.60	15.40	18.00	59.95	10.53	12.63
	Suspended Solids	Mg/L	-	0.10	0.04	0.005	0.005	0.008	0.035
	Calcium	Mg/L	75	1.60	.05	0.0	7.9	0	0.8
	Magnesium	Mg/L	Not >30	NIL	0.6	NIL	NIL	4.83	2.00
	Total Hardness	Mg/L CaCO ₃	100-200	6.00	NIL	NIL	30.0	NIL	2.0
	Calcium Hardness	Mg/L	200	7.00	2.50	2.0	18.0	2.0	4.0
	Magnesium Hardness	Mg/L	12	NIL	1.0	NIL	NIL	10.0	2.0
	Iron	Mg/L	0.3	0.40	0.3	0.1	NIL	0.5	0.2
	Manganese	Mg/L	0.1-0.5	NIL	NIL	NIL	NIL	NIL	NIL
	Lead	Mg/L	0.01	NIL	NIL	NIL	NIL	NIL	NIL
	Chloride	Mg/L	250	5.33	7.50	4.25	28.0	3.0	3.0
	Sulphate	Mg/L	250	30.11	75.95	33.33	33.35	18.75	28.09
	Nitrate	Mg/L	50	0.1	NIL	NIL	0.1	0.15	0.1
	Potassium	Mg/L		2.67	1.67	11.0	4.67	1.67	4.67
	Carbonate	Mg/L		NIL	NIL	NIL	NIL	NIL	NIL
	Bicarbonate	Mg/L		2.10	2.80	0.0	28.0	70.0	44.0
	Sodium	Mg/L		18.53	15.43	10.95	4.20	21.97	3.55
3	MICROBIAL ANALYSIS								
	E-Coli/100ml	Per 100ml	NIL	NIL	NIL	NIL	NIL	NIL	NIL
	Coliform/100ml	Per 100ml	3	180	140	99.0	120	75	200
	Total Plate Count @ 35°C after 24hrs	Per ml	100	100.0	87.20	99.0	120.0	180.0	30.0

Comments: Results of the samples are not consistent with the WHO maximum permissible level for potable water

ANALYSIS RESULTS

Sample Description:**Analysis Required:** Physical, Chemical, and Microbiological

Data Collected: 02/04/09

Lab. Sample No.:

1	PARAMETER	UNIT	WHO std.	VALUES					
				A	B	C	D	E	F
	PHYSICAL ANALYSIS								
	Odour			-ve	-ve	-ve	-ve	-ve	-ve
	Turbidity	NTU	-	2.0	1.0	1.0	2.0	1.0	Nil
	PH value		6.5-9.0	5.96	4.97	4.72	4.14	5.33	5.12
	Conductivity	Microhms/cm	100	26	33.0	28.5	106.0	21.3	22.6
	CHEMICAL ANALYSIS								
	Acidity	Mg/l CaCO ₃	-	-	-	-	-	-	-
	Alkalinity	Mg/l CaCO ₃	30-500	15.0	15.0	20.1	10.0	20.0	25.0
	Total Solids	Mg/l	-	14.59	18.50	16.02	59.40	12.0	12.69
	Dissolved Solids	Mg/l	500	14.56	18.48	16.02	59.36	11.93	12.66
	Suspended Solids	Mg/l	-	0.03	0.02	0.004	0.10	0.082	0.033
	Calcium	Mg/l	75	2.8	1.6	1.2	9.2	1.2	2.0
	Magnesium	Mg/l	Not >30	0.3	Nil	NIL	4.5	Nil	0.3
	Total Hardness	Mg/l CaCO ₃	100-200	8.0	4.0	3.0	38.0	3.0	6.0
	Calcium Hardness	Mg/l	200	7.00	4.0	3.0	23.0	3.0	5.0
	Magnesium Hardness	Mg/l	12	1.0	Nil	NIL	15.0	Nil	1.0
	Iron	Mg/l	0.3	0.08	0.1	0.1	0.06	0.15	Nil
	Manganese	Mg/l	0.1-0.5	NIL	NIL	NIL	NIL	NIL	NIL
	Lead	Mg/l	0.01	NIL	NIL	NIL	NIL	NIL	NIL
	Chloride	Mg/l	250	11.34	16.31	14.18	35.45	10.64	9.22
	Sulphate	Mg/l	250	62.19	129.19	85.55	88.33	47.26	57.75
	Nitrate	Mg/l	50	0.15	0.1	NIL	0.15	0.25	0.15
	Potassium	Mg/l		30.24	222.3	Nil	Nil	Nil	Nil
	Carbonate	Mg/l		0.0002	0.0002	0.0002	0.0002	0.0002	0.0002
	Bicarbonate	Mg/l		52.20	27.30	24.90	95.70	77.10	25.40
	Sodium	Mg/l		21.78	17.91	14.32	4.18	22.80	9.60
	MICROBIAL ANALYSIS								
	E-Coli/100ml	Per 100ml	NIL	NIL	NIL	NIL	NIL	NIL	NIL
	Coliform/100ml	Per 100ml	3	27.0	26.0	33.0	17.0	13.0	49.0
	Total Plate Count @ 35°C after 24hrs	Per ml	100	107.0	87.0	112.0	138.0	102.0	59.0

Comments: Results of the samples are not consistent with the WHO maximum permissible level for potable water

Sedimentology and Morphology of Quaternary Alluvial Fans in Wadi Araba, Southwest Jordan

Issa M. Makhoulouf^{a,*}, Belal S. Amireh^b, Abdulkader M. Abed^b

^a Department of Earth and Envir. Sci., Hashemite University, P.O. Box 330028 Zarqa 13133, Jordan.

^b Department of Environmental and Applied Geology, Jordan University, Amman, Jordan

Abstract

The eastern rim of Wadi Araba in southwest Jordan displays distinct alluvial fans, which were developed since the time of formation of the Dead Sea Transform (DST), initiated in Mid Miocene times. The DST fault system controlled the development of the alluvial fans and their stacking pattern. Siliciclastic sediments were supplied from the east, and dispersed radially forming a stream-flow dominated alluvial fan system. The continuous uplift of the eastern granitic basement and overlying Phanerozoic sedimentary succession, and the active intramontane valleys, whose outlets at the mountain front were elevated continuously above the piedmont plains, resulted in deposition of alluvial fans that coalesced to produce a huge bajada complex comprising several generations of overlapping and superimposed lobes consisting mostly of granitic gravels. Eight lithofacies are identified, comprising three lithofacies associations: proximal fan; medial fan and distal fan. These were deposited in environments ranging from proximal shallow stream and sheet floods, channelized non-cohesive debris flows, medial heterolithic deposits, distal muds and sabkha evaporites.

© 2010 Jordan Journal of Earth and Environmental Sciences. All rights reserved

Keywords: Alluvial fans, Wadi Araba, Dead Sea, Jordan.

1. Introduction

Alluvial fans are defined by geomorphological features rather than by a characteristic fluvial style. The most distinctive lithofacies components have been considered to be debris-flow deposits, although some fans are sandy (Miall, 1978; Rust, 1978, Harvey *et al.*, 2005). Other characteristics of alluvial fans are radiating distributaries and cone-shaped architecture.

This study aims to provide a better understanding of the alluvial fans in southwest Jordan, and the controls on their architecture and the spatial variability of sedimentary associations during their development. Little previous sedimentological study has been carried on the alluvial fans of Wadi Araba. A general description of the alluvial fans has appeared in the bulletins of the Natural Resources Authority (Rabba, 1991; Tarawneh, 1992) and in Bender (1974) and Abed (2000). Galli (1999) discussed the tectonic control on the development of Wadi Araba alluvial fans. Frostick and Reid (1989) studied the alluvial fans exposed at the western side of the Dead Sea.

Owing to the paucity of data concerning the sedimentary record of the alluvial fans in Jordan, the present study provides characterization of the gravel-dominated alluvial fans based on lithofacies analysis, bed

architecture and palaeocurrent directions measured in three-dimensional exposures. Wadi Araba alluvial fans are an important local source of groundwater in the prevailing arid region. For instance, the villages of Wadi Rahma and Qatar in Wadi Araba obtain their water supply from wells sunk in distal alluvial fans. The alluvial fans also provide a local source of aggregate. Wadi Araba alluvial fans are a valuable record of neotectonic seismic (earthquake) activities along Wadi Araba- Dead Sea Transform (DST) initiated in middle Miocene (Garfunkel *et al.*, 1981), and can be used as indicators of the Dead Sea Transform fault evolution and climatic changes (Atallah and Al-Taj, 2004).

Wadi Araba (Fig. 1) is oriented NNE-SSW, and in the study area is 10-17 km wide in an E-W direction. The elevation of Wadi Araba in the study area, about 45 km north of Aqaba, ranges from zero m above sea level (ASL) in its southern part to about 75 m ASL in its northern part. The southern Wadi Araba is a hot, arid region. Average air temperature range is 17.7^oC-30.8^oC (Jordan Climatological Handbook, 2000). The daily maximum temperature can reach 48^oC during the summer. Annual rainfall averages 30.4 mm. The eastern mountain range receives up to 200 mm/year rain fall; flood water flows westwards via numerous wadis to Taba Sabkha. The western mountains receive only about 50 mm/year. Annual mean wind speed at the Aqaba airport, south of the study area, is 8.6 knots and 70% of the prevailing winds are northerly and 8% are southerly (Jordan Climatological Handbook, 2000).

* Corresponding author. makhoulouf11@yahoo.com

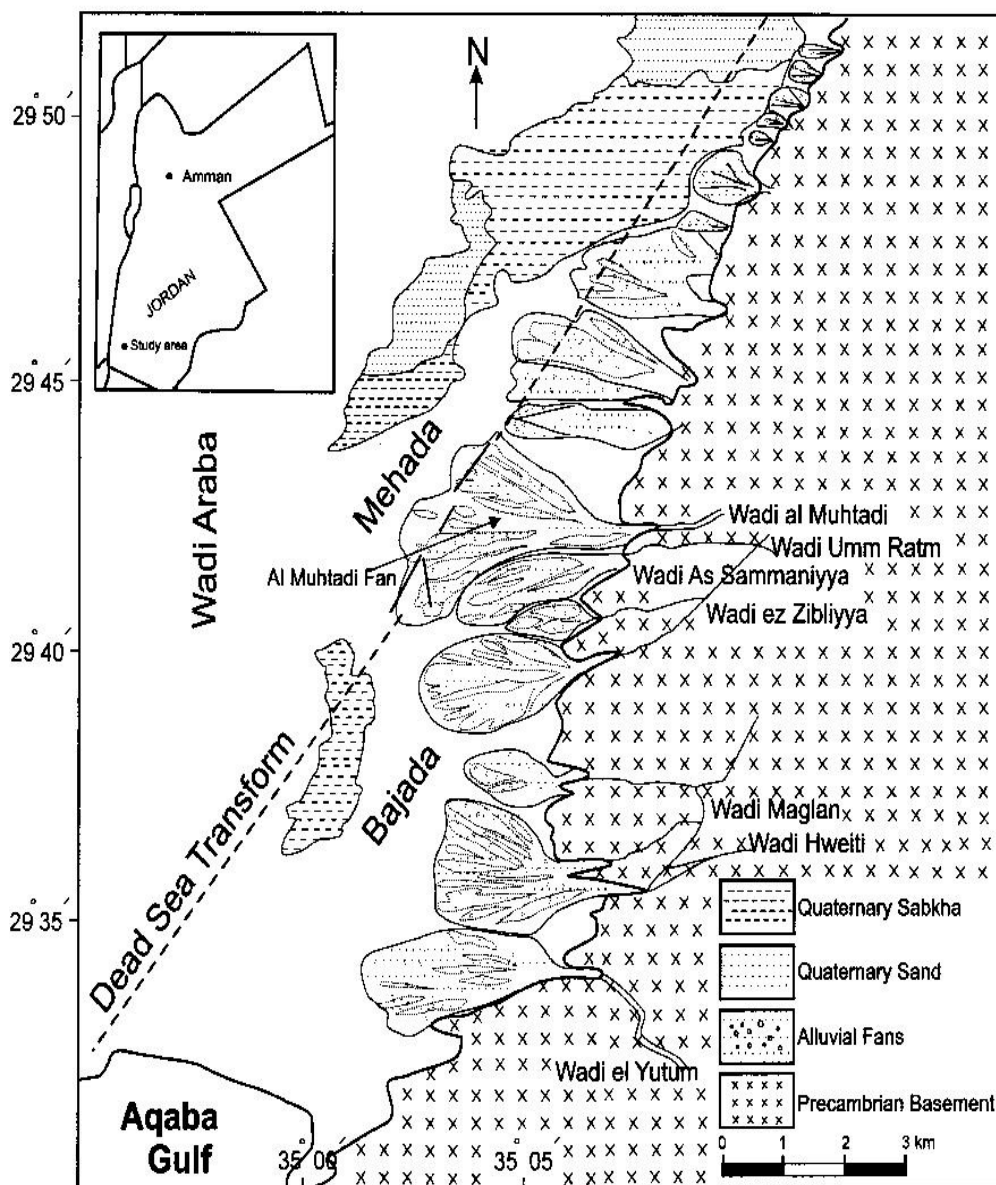


Fig. 1. Location map of the study area showing Wadi Araba, Precambrian Granitoid Basement, Dead Sea Transform (DST), multiple fans and palaeopidmont line. The map is based on satellite image.

2. Geological Setting

The alluvial fans in the study area are situated along the southernmost part of Wadi Araba, at the flanks of its eastern side. They form a series of alluvial fans extending from Aqaba, in the south, up till 45 km to the north (Fig. 1). Wadi Araba forms an important segment of the 1100 km long Red Sea - Dead Sea Transform (DST). The DST started to form in Mid-Miocene times as a plate boundary connecting the spreading regime of the Red Sea in the south with the collision regime in Anatolia in the north (Quennell, 1956; Atallah and Al-Taj, 2004). Jordan, including the eastern margin of the rift (Arabian Plate), is moving NNE along the DST with an average displacement of 5 mm/year, a total displacement, since the Miocene, of

107 km (Quennell, 1956; Amireh, 1997; Abed, 2000; Atallah and Al-Taj, 2004). Since its formation, the floor of the DST has been subsiding while the mountain ranges on both sides are rising. The net difference in elevation, at present, between the eastern mountains and the floor of the DST is in excess of 1000 m. This epirogenic movement (uplift and subsidence) created several interconnected basins along the DST including Wadi Araba in the south, the Dead Sea basin in Central Jordan and Jordan Valley in northern part of Jordan. These subsiding basins have a huge accommodation space, and they will continue to have it as long as the DST tectonics are active.

The main DST fault runs obliquely in Wadi Araba and it cuts through the lower reaches (medial fan) of the investigated fans. Throughout most of its length the main transform fault is buried by superficial alluvial deposits

and its position can only be inferred. However, at the Muhtadi medial fan, the trace of the fault splits into two faults producing a sag pond in between (Galli, 1999). Further north of the same fan a fault escarpment is also clear exposing some 10 m thick of the medial fan material (Fig. 1). The eastern mountain range consists entirely of the granitoids and later dyke rocks of the Aqaba Complex of late Neoproterozoic age (600-630 Ma) (Rashdan, 1988; McCourt, 1990; Ibrahim, 1991). Consequently, the clasts of the fans, at the surface, are almost entirely of igneous origin, although earlier buried fan deposits must include Phanerozoic cover sediments, now eroded. Due to the elevation difference between Wadi Araba and the eastern mountain range, many wadis dissect these mountains and discharge into Wadi Araba as ephemeral flow. The investigated fans are located at the mouth of these wadis; the largest is the Muhtadi Fan at the mouth of Wadi Al Muhtadi, located 25 km north of Aqaba. The coalesced fan complexes at Wadi Araba comprise generations of stacked lithofacies associations of different stages, including older debris flow deposits (some probably Pleistocene in age), and more recent stream flow deposits. Fans become finer-grained in composition towards the medial part of Wadi Araba where three inland sabkhas, separated by mudflats and minor sand dune fields are present. Together, they

form the distal part of the alluvial fan complex in the area. The largest of these sabkhas is the Taba Sabkha, located about 35 km north of Aqaba (Fig. 1). It is about 50 km² in area, and consists essentially of clay, silt and evaporite deposits with minor aeolian sand horizons (Abed, 1998).

3. Methods

Wadi Al Muhtadi fan was chosen for a detailed sedimentary logging as it is one of the largest alluvial fans in the area, and is well exposed (Fig. 2). Measurements of maximum particle size and bed thickness were made for specific lithofacies. Maximum particle size was calculated as an average of the long axis of the 10 largest clasts in a bed. The orientation of the a-b planes of a representative selection of clasts ranges from 10 to 15 readings. Palaeocurrents were measured from clast imbrication and occasional cross-beds.

Stratigraphic sections were measured from the main exposures in Wadi Al Muhtadi. Lithofacies associations are laterally distributed in the order of FP, FM and FD from east to west. Five sections were measured along the axial length of Al Muhtadi fan, from the fan apex eastward to the fan toe westward (Fig. 2).

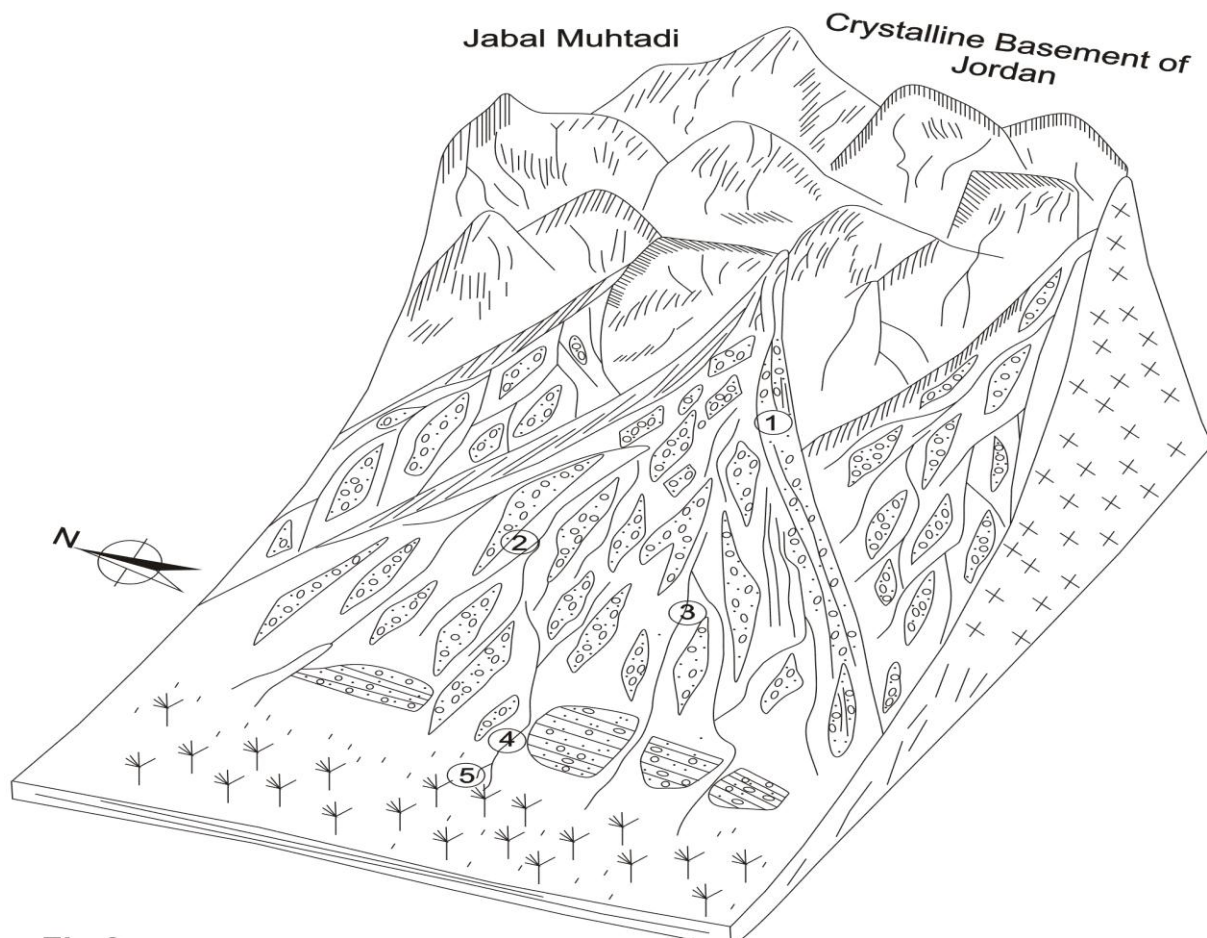


Fig. 2. Schematic block diagram showing the depositional system of the Muhtadi Fan and its section locations: (1) proximal fan, (2, 3, and 4) midfan, (5) distal fan.

4. Morphological Description

The spatial extent of the Al Muhtadi fan can be estimated based on distribution of lithofacies associations. The axial length of the fan is about 5 km displaying thin alluvial sheet appearance in the distal area, passing westward into a flat lowland sabkha area. The fan surface has a low gradient to the west (260°N) (Fig. 3A). Numerous alluvial fans have been recognized at palaeo-piedmont zones in front of the Wadi Araba-Dead Sea Transform fault escarpment (Fig. 1). The overlapping pattern of adjacent alluvial fans forms a proximal bajada along the southern part of Wadi Araba (Figs. 1, 3B). The

fan system is related to palaeo-piedmont lines, which are inferred from the basin-margin faults (Fig. 1). The fan system in this study area is rich in gravel-size clasts as they are derived from granitoid source areas located nearby (Fig. 3C, D).

The intermontane valleys are V-shaped (Fig. 3E) with maximum widths of around 200 m (Fig. 3F). The apical parts of the fans are at altitudes of 100- 200 m ASL. They have been affected by subsequent braided fluvial processes that reworked abandoned fan sectors, and deposited recent alluvium (Fig. 3F). Fan-head segments slope at 13° from the horizontal and decrease to 5° - 8° at about 800 m westward from the apex (Fig. 3A).

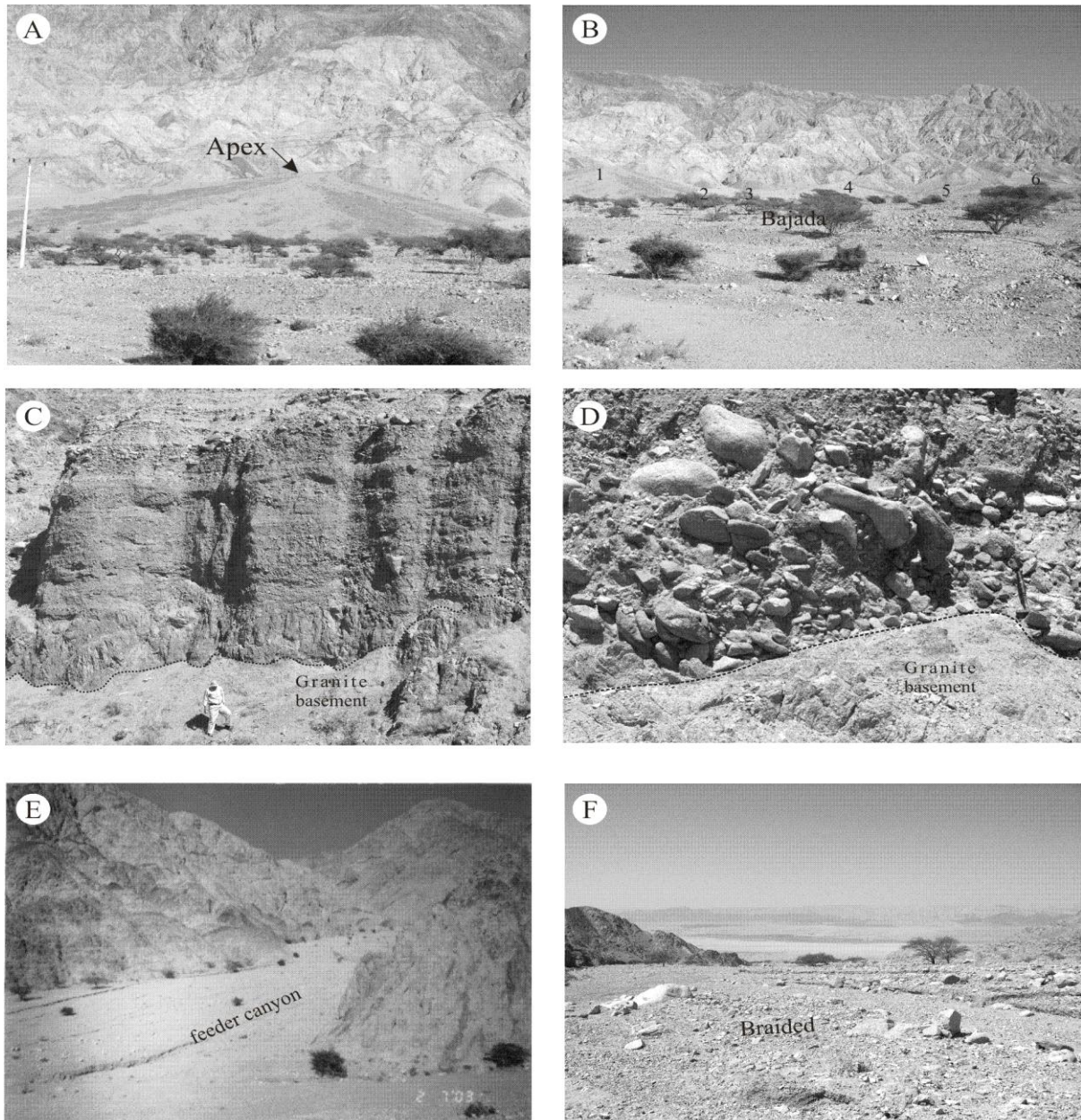


Fig. 3. Field photographs of the alluvial fans in Wadi Araba showing: (A) general view of Al Muhtadi alluvial fan, Wadi Araba, showing its apex, proximal and medial parts; the active lobe is modified by surface flow; (B) adjacent distal fans at the piedmont of the mountains producing a bajada; (C) the fan deposits resting unconformably on the basement granitic rocks.; (D) close-up of C to showing details of the boundary; note the eastward imbricated cobbles; (E) general view showing the fan apex and feeder canyon in the proximal part of Al Muhtadi alluvial fan; (F) braided channel displaying longitudinal bars at the fan-head trench.

Close to the apex of Al Muhtadi fan an abandoned ancient tributary fan trending NE-SW overrides the primary fan, building a huge cone of gravels including boulders and blocks, made of granitic and other igneous clasts (Figs. 4, 5A). This fan is 100 m wide and more than 10 m thick and is superimposed by a small more recent fan (Fig. 5B). It is truncated by the present braided channel which is trending westward (260°N).

Small scale colluvial fans are well developed along the recent valley margin faces incising the pre-existing fans (first generation), some of which are coalesced and others are solitary (Fig 5C). Clastic sediments are supplied to the colluvial fans as rock-fall and dry debris flow. Some

colluvial fans were developed along the truncated face of the abandoned fan (Fig. 5D).

5. Facies, Lithofacies and Facies Associations

Wadi Al Muhtadi fan is described in terms of three lithofacies associations comprised of eight lithofacies (Table 1), which were identified on the basis of sediment texture, clast fabric, matrix type, lithology and clast composition. Three representative lithofacies have been recognised in proximal fan (FP), three lithofacies in the medial fan (FM) and two lithofacies in the distal fan (FD). This subdivision serves as the basis for the interpretation of depositional processes.

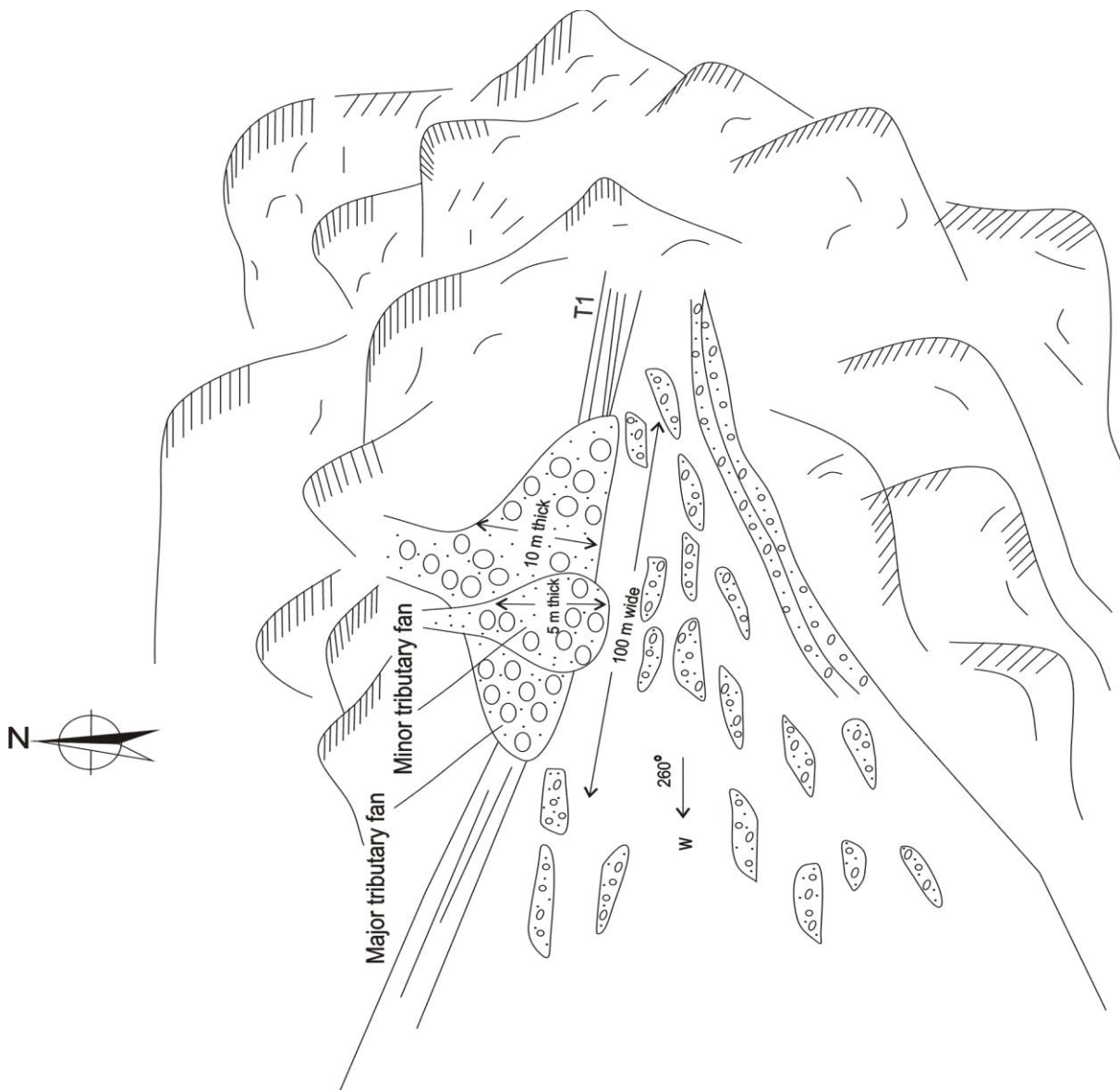


Fig. 4. Sketch showing an ancient abandoned alluvial fan overriding the primary fan, which in turn, is truncated by the present braided channel. The abandoned fan is superimposed by a small recent fan (T1 refers to channel terrace).

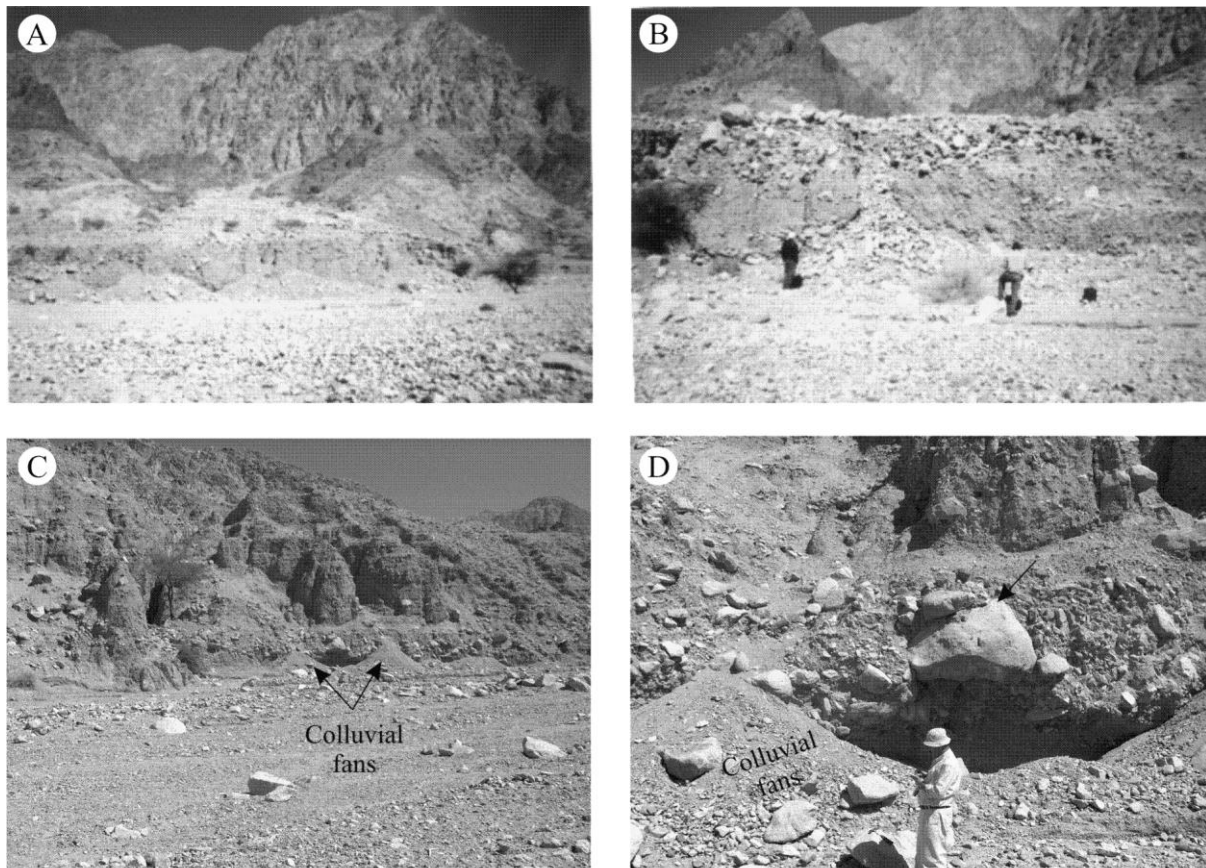


Fig. 5. Field photographs showing the channels at the apex: (A) abandoned tributary alluvial fan overridden by the primary fan and truncated by the present braided channel; (B) the abandoned fan is superimposed by a small recent fan; (C) small colluvial fans perpendicular to the present course of the channel, developed along the truncated face of the abandoned fan; (D) close-up of a colluvial fan overriding the ancient fan; note the large boulder.

Tabel 1. Lithofacies associations of Al Muhtadi fan.

Alluvial Fan Facies		
Proximal Fan Lithofacies (FP)	Medial Fan Lithofacies (FM)	Distal Fan Lithofacies (FD)
Lithofacies Associations	Lithofacies Associations	Lithofacies Associations
<p>1. <i>Clast-supported, disorganized conglomerate lithofacies (Gcd).</i></p> <p>2. <i>Clast-supported, organized conglomerate lithofacies (Gco).</i></p> <p>3. <i>Matrix-supported, disorganized conglomerate lithofacies (Gmd).</i></p>	<p><i>Trough-filling conglomerate lithofacies (Gt).</i></p> <p><i>Horizontally stratified conglomerate lithofacies (Gh).</i></p> <p><i>Heterolithic lithofacies (Htr).</i></p>	<p><i>Massive mudstone lithofacies (Mm).</i></p> <p><i>Evaporite lithofacies (Ev).</i></p> <p><i>Gypsum-Anhydrite sublithofacies (Evgyp).</i></p> <p><i>Halite sublithofacies (Evhal)</i></p>

5.1. Lithofacies Associations of Proximal fan (FP)

Not far from the apex of Al Muhtadi fan; two vertical sections were measured at the proximal part of the fan (Figs. 6, 7). The bedding is poorly developed in the upper settings and becomes more pronounced down-channel (Fig. 8A, B). Lithofacies association (FP) comprises poorly sorted boulder beds, horizontally stratified pebble to block beds (Fig. 8C) and clast-supported conglomerates (Fig. 3C). Boulders are subrounded to subangular, and are occasionally imbricated (Fig. 3D). Several huge fallen boulders of granitoid basement (up to 150 cm) were identified (Fig. 5D).

Well defined imbrication is present to some degree in most of the beds of the gravelly lithofacies (Fig. 8D). It appears as general inclination of the clasts (a-b planes dipping upstream) relative to bedding as shown in Fig. 8D. Imbrication is best developed in the finer grained, stratified conglomerates where clast long axes (a) are orientated transverse to flow (Fig. 8D). In the more poorly sorted, coarser grained deposits, there is no preferred orientation of clast long axes (Fig. 8A). Clast imbrication was used to determine palaeocurrent orientation (Fig. 9) which is unidirectional to the west (250°N).

Most of the beds show sheet-like geometries without apparent basal scour, although a few beds show irregular erosional bases with variable relief (about tens of centimetres) (Fig. 8A, B). Sharp bounding surfaces separating boulder beds from the underlying pebble-rich beds indicate distinct ephemeral flow (Fig. 8B). Some bedding planes are fairly distinct and locally show scour and fill features. Clast-size grading is obvious at different levels of bedding (Fig. 8C). Bed thicknesses vary between 0.2 m and 1m (average 0.6 m). The conglomerates have a loose to moderately tight packing and commonly comprise normally graded, cobble- to pebble-size clasts (Fig. 8A, B). Matrix (up to granule grade) is abundant in most of the units (Fig. 8C). The conglomerates are commonly capped by medium- to coarse-grained sandstones up to 0.30 m thick, which drape the irregular topography of the underlying clasts (Fig. 8B). They are usually parallel laminated or display low angle (5°) bedding planes. Planar cross-stratification often parallel to the fabric in the conglomerates, and faint medium-scale trough cross-bedding is present. Two types of upward-fining cycles are present; firstly from cobble-pebble size to sand size fraction; and secondly from boulder size to pebble size fraction.

5.1.1. Clast-supported, disorganized conglomerate lithofacies (Gcd)

This lithofacies reveals erosional surfaces in the form of two troughs truncating the underlying matrix-supported gravel lithofacies, and is characterized by planar, wedging cross-bedding directed westwards. Bedding is gently undulating, and appears as troughs of low amplitude. The first trough is filled with clast-supported, ungraded, disorganized, and very poorly sorted gravel. The lithofacies comprises subrounded to rounded, granule-, pebble-, cobble- to small boulder-gravels. The mean size

of the ten largest clasts is 0.45 m. The second trough is filled with a clast-supported, ungraded, disorganized, poorly sorted, subangular to subrounded, sandy, granular, pebbly coarse cobble lithofacies (Fig. 8A, B). Laterally eastward, a channel of 20 m width, and a maximum height of 1.85 m occurs, filled with boulder-sized clasts that are randomly oriented. This channel-fill lithofacies is characterized by a clast-supported fabric, and a random orientation for the large clasts, and faint imbrication for the smaller clasts. The mean size of the ten largest clasts is 65.5 cm. This lithofacies represents deposits of gravel sheets or low-relief longitudinal bars (Boothroyd and Ashley, 1975; Hein and Walker, 1977; Nemeč and Postma, 1993), emplaced by high-velocity flood flows (Allen, 1981; Todd, 1989; Maizels, 1993).

5.1.2. Clast-supported, organized conglomerate lithofacies (Gco)

This lithofacies is a thickly bedded, clast-supported, ungraded, organized, horizontally orientated, well stratified (Figs. 8C, 9), very poorly sorted, subrounded, sandy, granule, pebble, cobble and boulder-gravel lithofacies. Excluding one outsized clast of 0.95 m, the mean size of the ten largest clasts is 0.21 m. This unit is characterized by remarkable lateral variation, and imbrication (Fig. 8C). The clast size increases vertically, and the mean size of the ten largest clasts is 0.70 m. This lithofacies occurs as deposits of sheet bars/longitudinal bars or diffuse gravel sheets (Boothroyd and Ashley, 1975; Hein and Walker, 1977), formed by grain-by-grain bedload sedimentation (Harms et al., 1982).

5.1.3. Matrix-supported, disorganized conglomerate lithofacies (Gmd)

This lithofacies is thickly bedded, very poorly sorted, matrix-supported, muddy, sandy ungraded, very poorly sorted, pebble to cobble gravels. Large clasts are occasionally present randomly floating in the mud matrix. Clasts are subrounded to rounded. The mean size of the ten largest clasts is 0.20 m (Fig. 8A). The interparticle matrix consists mostly of very small pebbles and granules similar in composition to the larger clasts. The shape of clasts is mainly spherical to discoidal, with rare prolate and tabular clasts. Clasts are mainly granite with less common basalt and rare rhyolite. The larger clasts commonly occur in local concentrations or small clusters, but are scattered without apparent order throughout the beds (Brayshaw, 1984; Went, 2005). Deposition of this lithofacies took place from visco-plastic debris flows (Shultz, 1984; Costa, 1988).

5.2. Lithofacies Associations of Medial fan (FM)

Part of the medial fan outcrops about 3km westward of the fan-head, and very close to Aqaba-Amman highway at the eastern side (Fig. 10). The exposed scarp is produced due to uplift, which took place along the Wadi Araba-Dead Sea Transform. The section strikes north-south, which is normal to the general dispersal of the fan deposits. The fan fault scarp is exposed due vertical displacement along the fault.

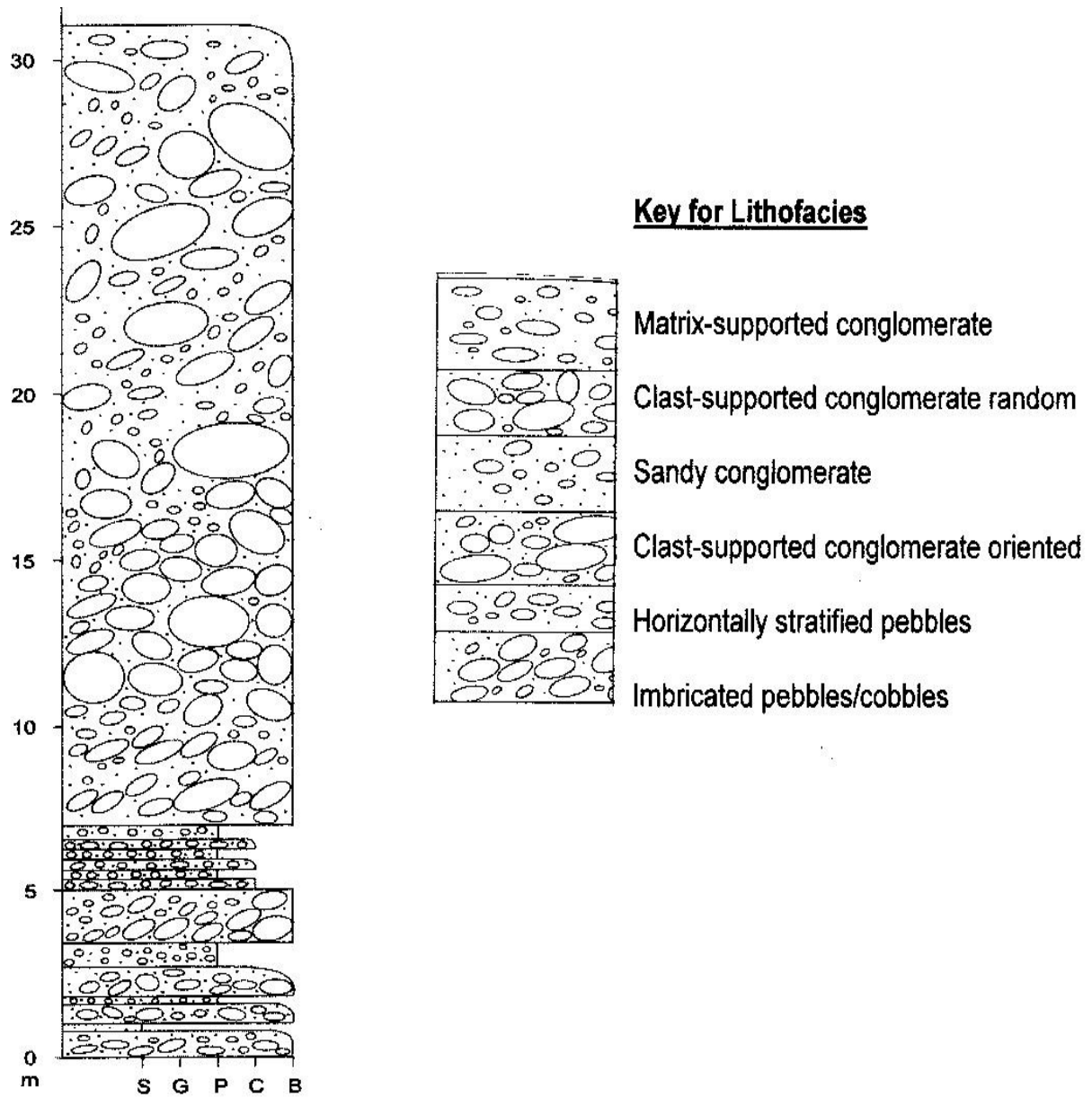


Fig. 6. Columnar section showing the thickness and lithofacies distribution at the southern side of the proximal part of Al Muhtadi alluvial fan (section 1, see Fig. 2 for location). Ancient fan deposits eroded by the stream.

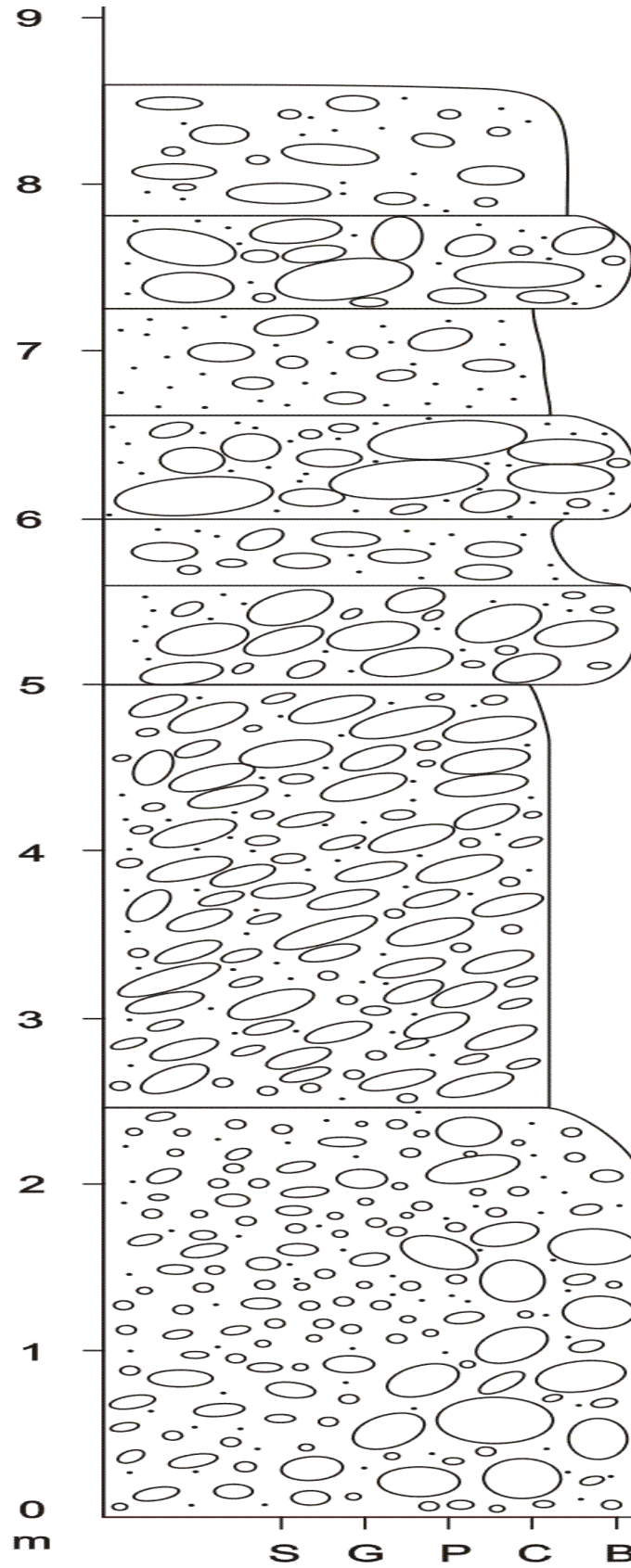


Fig. 7. Columnar section showing the thickness and lithofacies distribution at the northern side of the proximal to midfan part of Al Muhtadi alluvial fan (section 2; see Fig. 2 for location, and Fig. 6 for lithofacies key).

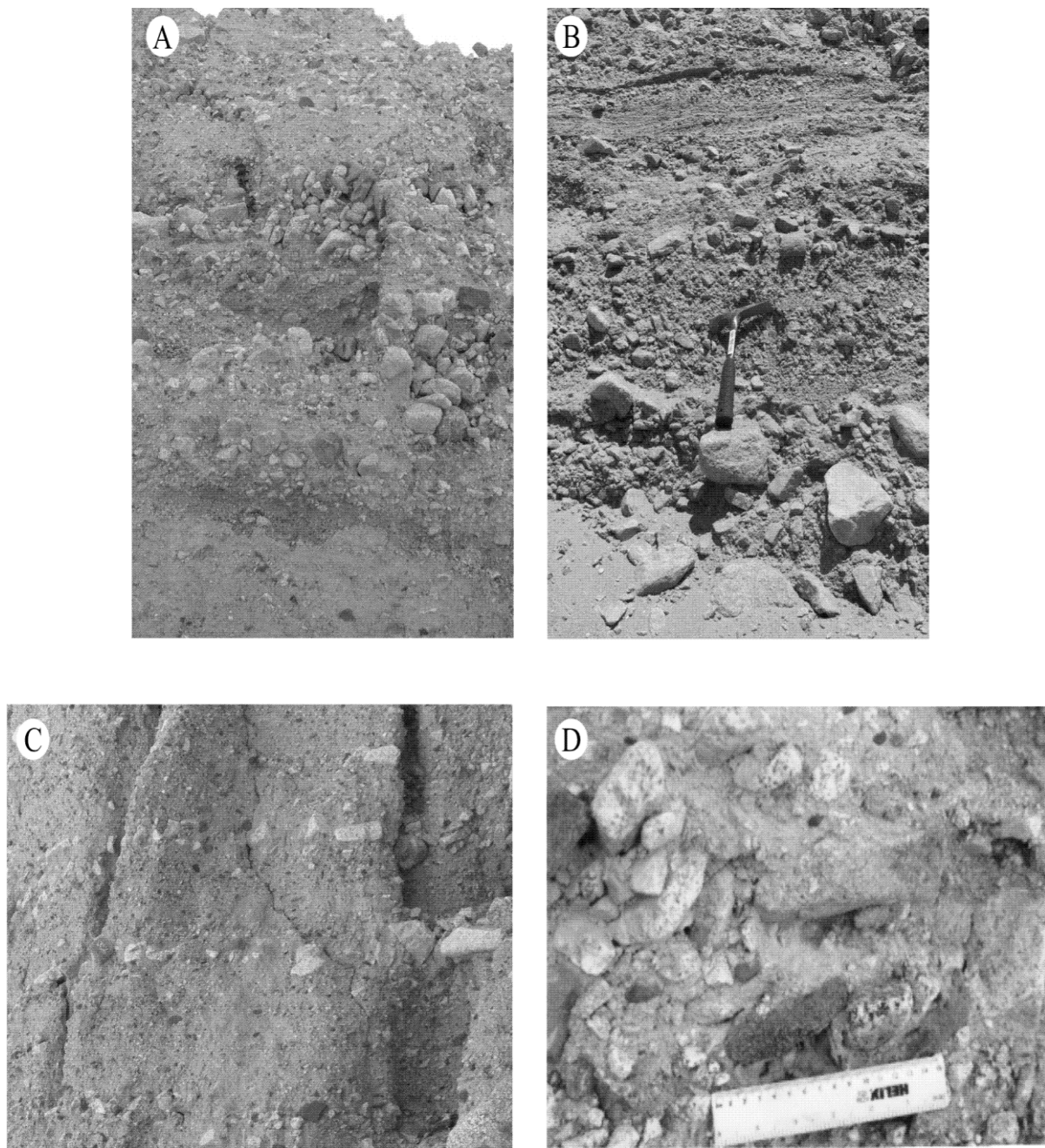


Fig. 8. Field photographs showing the proximal lithofacies associations: (A) lithofacies association (FP) comprises poorly-sorted, clast-supported boulder beds with horizontally stratified pebble- to boulder-size clasts, some showing clusters (Gcd); (B) fining upward cycle starting with disorganized boulders and terminating with thinly bedded sandstones (Gcd), which drape the irregular topography of the underlying clasts. (C) graded beds with matrix (up to granule size are abundant in most of the units supporting clasts; here arranged as multiple cycles of horizontally bedded conglomerates (Gco) commonly capped by granular sandstones; (D) boulders are subrounded to subangular, and are well imbricated (Gco).

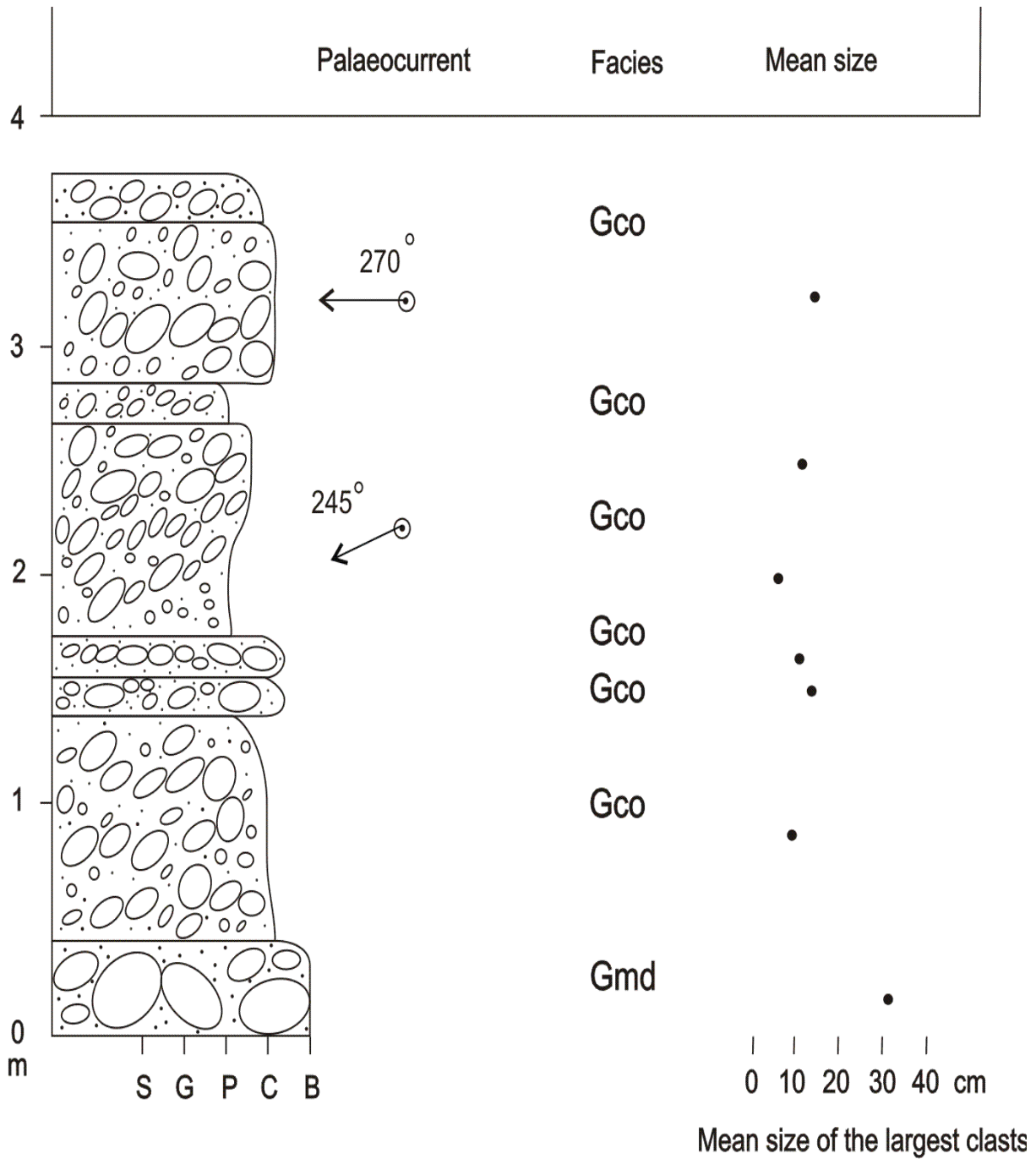


Fig. 9. Columnar section showing the thickness and lithofacies distribution at the southern side of the proximal to midfan part of Al Muhtadi alluvial fan (section 3, see Fig. 2 for location, and Fig. 6 for lithofacies key).

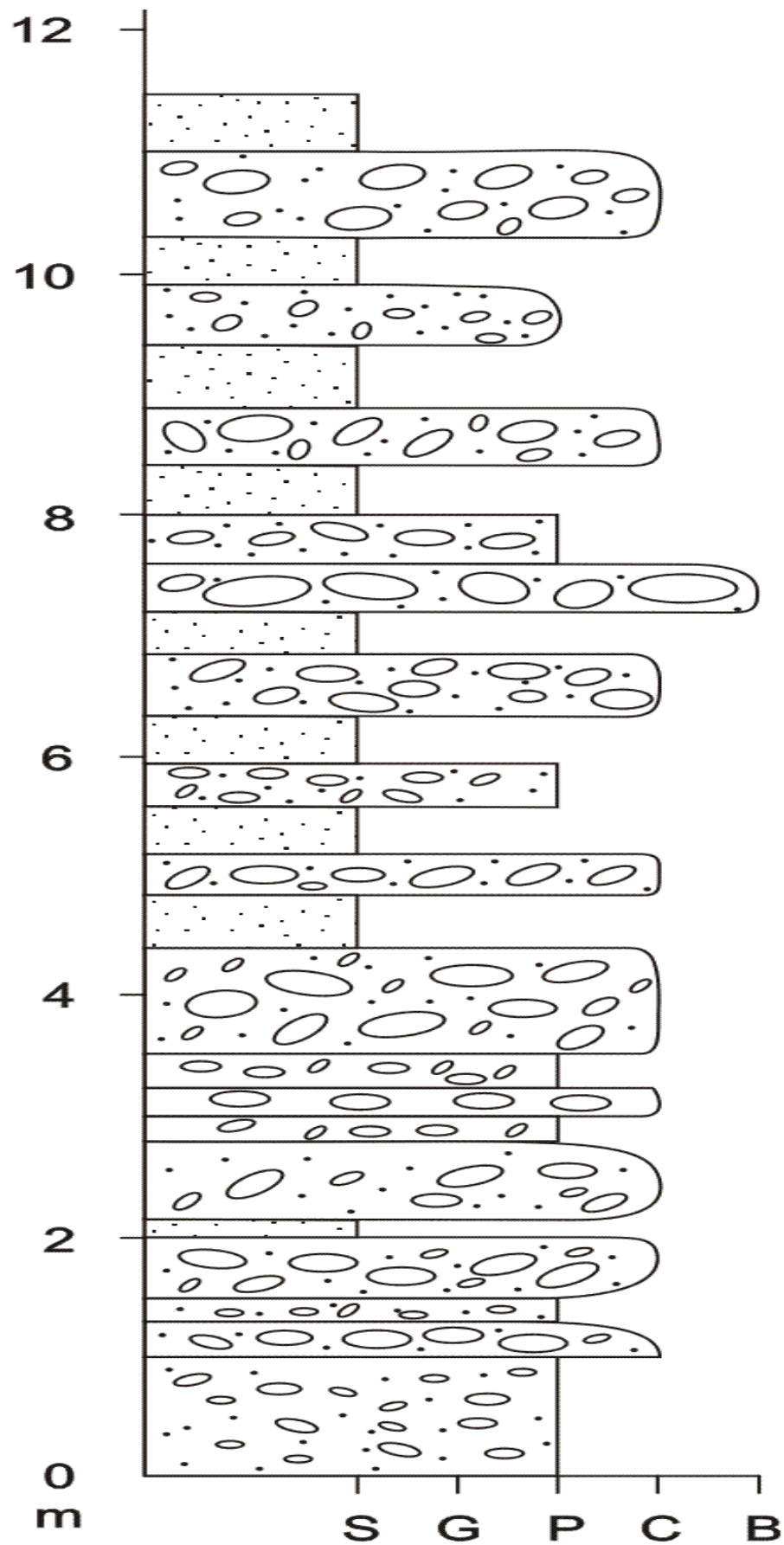


Fig. 10. Columnar section showing the thickness and lithofacies distribution of the midfan of Al Muhtadi alluvial fan (section 4, see Fig. 2 for location, and Fig. 6 for lithofacies key).

The measured section at the fault escarpment facing west attains a thickness of 12 m (Fig. 11A-D). The medial fan lithology consists of fine cobbles, pebbles and large amounts of sand arranged in several fining-upward cycles (Fig. 11A). Beds are inclined toward the upstream (eastward) as a result of fault tilting.

The lower reaches of the medial fan at about 300 m elevation, located to the west of the highway; the medial fan crops out due to the western fault scarp facing SE. The exposed fan lithofacies attains a thickness of 10 m, and is generally fine grained. Unfortunately, much of the outcrop is covered with talus. The gravel component decreases, and the beds become thin and laminated. Sedimentary structures are well pronounced (Fig. 12A, D). Parallel laminated granular sandstones alternate with pebbly horizons that pass upward into structureless granular sandstones (Fig. 12A-D). Small-scale cross-bedding, ripple marks and cross lamination are common. The following three lithofacies were recognized:

5.2.1. Trough-filling conglomerate lithofacies (Gt)

Two units of this lithofacies are encountered; the first one consists of horizontally bedded, clast-supported, ungraded, organized, imbricated to horizontally orientated, poorly sorted, muddy, sandy, granular, coarse pebble gravel. The mean size of the ten largest clasts is 0.57 m. The second unit is a thick bedded, clast-supported, ungraded, slightly to well-imbricated, subrounded to rounded, poorly sorted, clayey, pebbly, fine cobble conglomerate lithofacies. The mean size of the ten largest clasts is 0.88 m, disregarding two outsized clasts that attain a diameter of 0.29 and 0.34 m. The upper part of this unit is characterized by almost horizontal orientation of the clasts leading to horizontal stratification. This unit constitutes a bed of 1 m thickness that persists laterally for 12 m before dying out below base of the outcrop. This lithofacies was deposited as infills of minor channels, scours and channel pools (Miall, 1977).

5.2.2. Horizontally stratified conglomerate lithofacies (Gh)

This lithofacies consists of a horizontally bedded, matrix-supported, ungraded, organized, subrounded to subangular, poorly sorted, clayey, silty, sandy, coarse pebble gravel lithofacies. The mean size of the ten largest clasts is 0.27 m (Fig. 11D). The lithofacies constitutes the fine-grained component of the fining-upward cycles which start with lithofacies (Gt). Thicknesses of the upward-fining cycles vary from 0.10 to 0.12 m (Fig. 11A). The lower half to two thirds of each cycle is usually of gravel size. Cross-bedded sandstones are rarely present. Flame structures were observed at certain levels at the boundaries separating the sandstones from gravelly beds, where differential loading has taken place. Upper plane bed sedimentation was suggested for the deposition of this lithofacies (Boothroyd and Ashley, 1975; Allen, 1981; Harms *et al.*, 1982; Todd, 1989; Maizels, 1993).

5.2.3. Heterolithic lithofacies (Htr)

This is an assemblage of relatively fine grained sediments. The best exposures are at the western side of

the Aqaba Highway. This lithofacies consists of silty sandstones, granular sandstone and small-pebble conglomerate (Fig. 12A-D). The sandstones show parallel and wavy laminations alternating with pebbly horizons. Others are structureless granular sands. Some of them show fining upward cycles, graded bedding, ripple marks and cross lamination (Fig. 12B, C). Beds of laminated sandstones and intercalated mudstone show normal grading. Parts of the sand deposits are certainly aeolian, derived from the dune field located to the north (Fig. 13).

5.3. Lithofacies Associations of Distal fan (FD)

The distal fan (FD) forms a flat area "Mehada" (Fig. 13 B, C) trending north-south, a result of the coalescence of the distal part of adjacent and overlapping alluvial fans (the term Mehada in Arabic best expresses this definition). An inland sabkha, known as Taba Sabkha (Fig. 14A-C), also occurs to the north.

The Taba Sabkha represents part of the distal fan setting (FD), situated in the southern part of the Dead Sea - Wadi Araba rift, 32 km north of the Gulf of Aqaba. It occupies an area of about 55 square km west of the Precambrian granitic basement. It is drained by E-W wadis that have their alluvial fans on the eastern side of Wadi Araba. The surface inclination of the sabkha is only a few seconds to the west and south-west (Fig. 14 A-C). It forms the distal lithofacies of several alluvial fans emerging from the eastern basement mountains. The sabkha sediments are mainly the result of ephemeral deposition from these wadis. Twenty shallow pits (1-1.5 m deep) and 9 boreholes up to 17 m depth were drilled into the sabkha during detailed studies by Abed (1998). Samples and cores were obtained, and a few groundwater samples were collected during these earlier studies, which showed zonation in the sabkha reflected in both plant habitat and evaporite minerals as a function of increasing salinity of groundwater towards the centre. Brown clays dominate its centre, grading eastwards into more sandy lithofacies. The following lithofacies are recognized:

5.3.1. Massive mudstone lithofacies (Mm)

These massive mudstones occur at the distal part of the fan composing the centre of the sabkha (Fig. 14 A-C). Petrographic study (Abed, 1998) has shown that the detrital minerals include quartz, feldspar, chlorite, mica, kaolinite, illite, smectite and illite / smectite mixed layers. Calcite, though partly authigenic, is dominantly detrital and aeolian in origin. Bedding surfaces show desiccation cracks up to 1 m in diameter (Fig. 14 B, C) and rain prints.

5.3.2. Evaporite lithofacies (Ev)

The barren interior of the sabkha consists of two colours: (a) whitish involving the relatively low areas with a salt crust and desiccation cracks (Fig. 14 B, C), and (b) brownish, a little higher in elevation, with older desiccation cracks (Abed, 1998). The former areas are the currently active areas of sedimentation. Geochemical analyses (Abed, 1998) indicate that the main evaporite minerals are gypsum, anhydrite and halite.

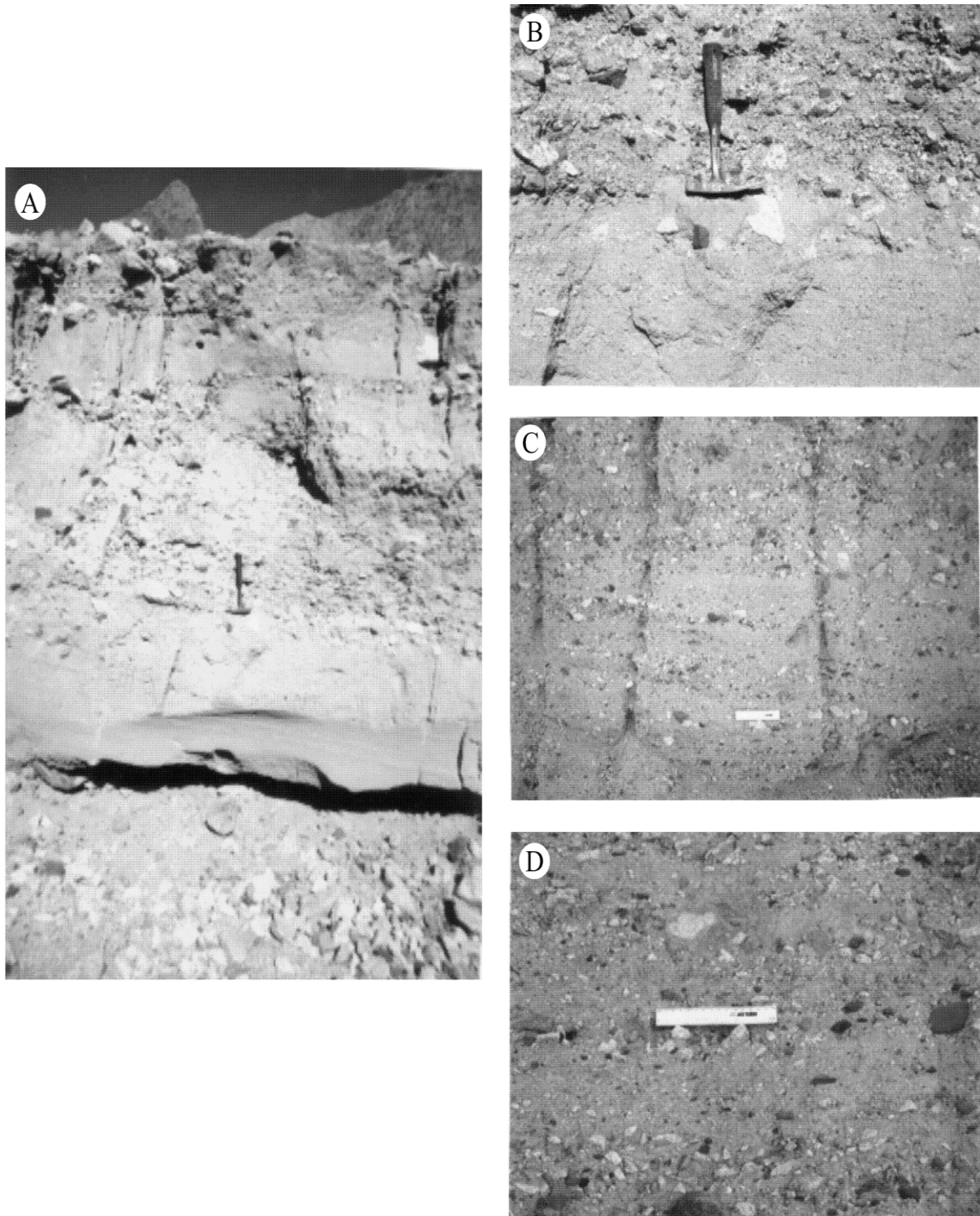


Fig. 11. Field photographs showing lithofacies associations of the medial fan (FM): (A) graded beds comprising three thick upward fining cycles terminated by thick bedded sandstones (Sh); (B) sharp bounding surfaces separating cobbly beds (Gt) from the underlying granular sandstone beds (Sh) indicate abrupt termination; (C) faint medium-scale trough cross-bedded conglomerates (Gt); (D) thin multiple cycles of conglomerates (Gt) (up to 30cm thick each) commonly capped by coarse-grained sandstones (Sh) which drape the irregular topography of the underlying conglomerates.

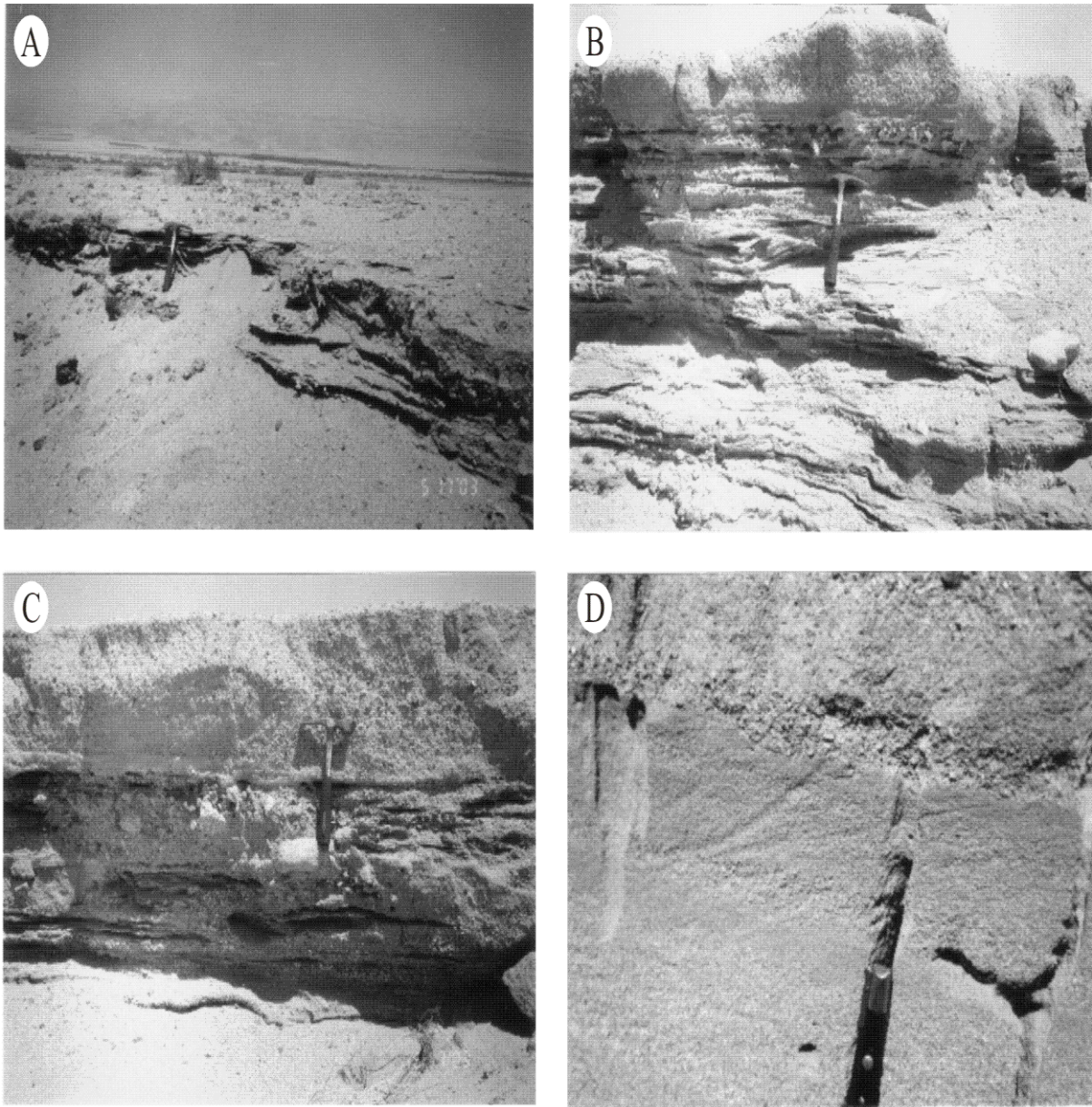


Fig. 12. Field photographs of the lowermost reaches of Al-Muhtadi medial fan facing west and passing gradually to the distal fan (Htr): (A) laterally persistent, thin bedded, pebbly sandstones; ripple marks and small scale cross-bedding are present; (B) the medial fan (FM) consists of trough cross-bedded, rippled and cross-laminated granular sandstone passing upward into coarser structureless granular sandstone; (C) the medial fan (FM) displaying parallel lamination of granular sandstone with occasional pebbly horizons passing upward into a structureless bed; (D) planar and trough cross-stratification often parallel to the fabric in the conglomerates.

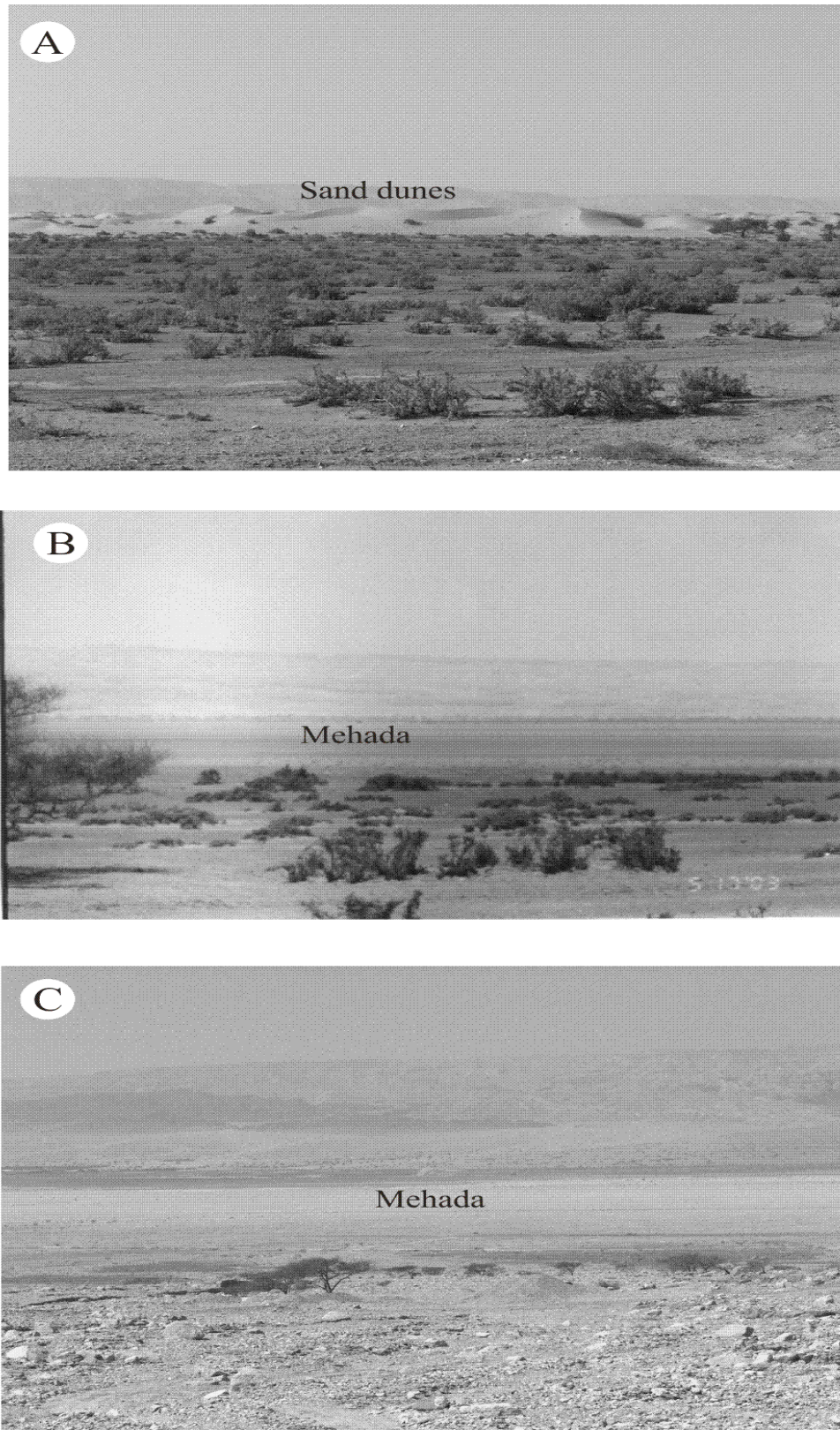


Fig. 13. (A) aeolian sand dunes advancing from the north and covering parts of the medial and distal fan zones; (B) lower reaches of the medial fan (FM) grading into the distal fan (FD); (C) the toe of the fan appears as a flat strip trending north-south as a result of coalescence of the distal part of adjacent and overlapping alluvial fans. Sabkha is also present locally.

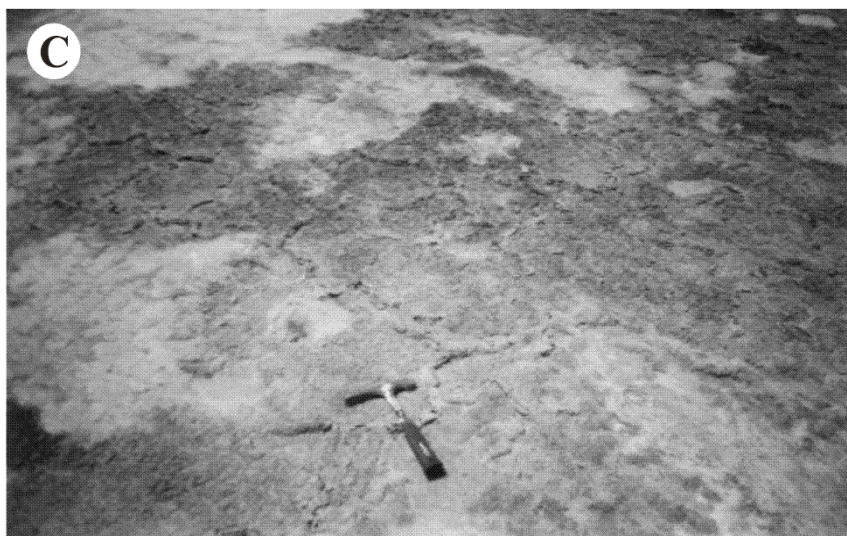
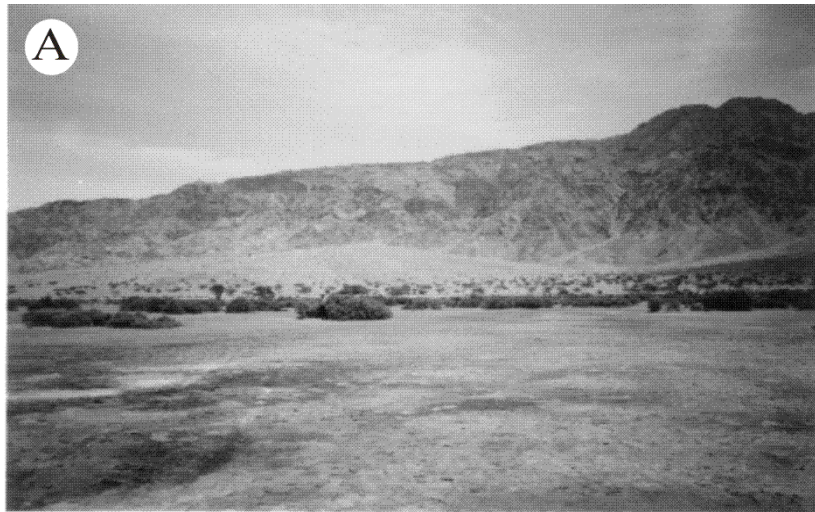


Fig. 14. Field photographs of the Taba Sabkha (looking eastward) located at the northern part of the distal fan (FD): (A) general view of the fan and sabkha; (B) bedding surface of the sabkha showing polygonal desiccation cracks; (C) close up view of B to show the large-scale polygons, up to 1 m in diameter.

i) Gypsum-Anhydrite sublithofacies (Evgyp)

Gypsum (sometimes present as the hydrated salts anhydrite and/or basanite in summer) is found in two settings: (a) at the surface or near surface, as concretionary and powdery deposits, especially around the plants. This type is due to direct precipitation from the groundwater and (b) at a deeper horizon, overlain by halite, towards the centre of the sabkha (Abed, 1998). This type is precipitated by the rising groundwater due to capillary action. The presence of overlying halite supports this interpretation (Schreiber and El-Tabakh, 2000).

ii) Halite sublithofacies (Evhal)

Halite predominates towards the inner parts of the sabkha and is also present in two settings: (a) as a desiccated whitish crust, about 0.01m thick, precipitated from the highly saline surface water noted above. In the older, reddish parts of the sabkha "salt-rich cakes" are found underlying "dissolution holes" at the centre of the shrinkage polygons indicating downward movement of the surface salt, and (b) as a subsurface horizon 0.15-0.40 m thick, several centimetres below the surface and underlain by gypsum in the centre of the sabkha. It is composed of discrete crystals, a few mm in diameter, scattered within the red clay matrix. This type has a similar origin like the underlying gypsum (Abed, 1998).

1. Interpretation

Lithofacies Gcd and Gco largely show characteristics of streamflow deposits that are similar to those of gravel-bed streams in alluvial fans and outwash fans (Boothroyd and Ashley, 1975). The poor sorting of lithofacies may be due to clast interactions in flood flows that were hyperconcentrated to some degree (Costa, 1988; Went, 2005, Harvey *et al.*, 2005), deposited in deep, high velocity, sediment-concentrated floods, either within the fan head trench, at the mouth of the fan head trench or in other major fan channels (Went, 2005). The absence of the finer sand and gravel components indicates that they were winnowed from between many of the larger clasts. The Gcd and Gco lithofacies are interpreted as cobble- and boulder-clogged stream channels and surface lags, such as those commonly found on the surface of modern fans (Blair, 1999; Went, 2005, Harvey *et al.*, 2005).

Lithofacies Gcd and Gco are interpreted as waterlain deposits, resulting from sheet flood, stream flood and stream flow processes. Palaeocurrents indicate unidirectional flow. Moderately organized textures and fabrics, including clast imbrication and horizontal stratification, point to the selective deposition of clasts, from an energetic flashy or bedload-dominated braided fluvial system (Went, 2005). The locally preserved undulating surfaces and locally cross-cutting strata are interpreted as channel-forms. The lack of any foreset beds indicates that they were not generated from migration of gravelly dune bed-forms. They may be produced by rapidly shifting narrow channels. The lenticular beds of cobble and boulder conglomerates are interpreted as stream channel deposits (Fig. 11C).

The erosive base to many of the deposits might suggest an earlier phase of more turbulent flow. The imbrication of clasts with a-b planes dipping upstream is typical of water

lain gravels. Clasts where the long axis (a) is perpendicular to flow suggest rolling of the clast along the stream bed. The heterolithic lithofacies of sandstones and small pebble conglomerate is interpreted as representing the deposits of relatively low energy streams (Fig. 12A-D). The occurrence of ripple cross-lamination grading into wavy lamination suggests deposition by low energy bedload and suspended processes. The finer conglomerate layers are consistent with deposition from stream flows.

The mudcracks and rain prints of the massive mudstone lithofacies (Mm) confirm periodic exposure. These features point to streams that were of much lower velocity than any other streamflow operating on the fan surface. The fine-grained sediments are possibly the products of low energy stream reworking of an abandoned fan sector at the distal fan setting. The thicker intervals of structureless, clay-dominated mudstone suggest prolonged periods of deposition from suspension in a standing body of water at the toe of the fan, when the abandoned sector of the fan was inundated by a marginal playa lake (sabkha). The presence of the evaporite lithofacies (Ev), including the Gypsum-Anhydrite (Evgyp) and the Halite sublithofacies (Evhal), strongly support the existence of the playa lake at the marginal toe of the fan.

2. Discussion and Conclusions

The fan system in this study fully illustrates the criteria for piedmont alluvial fans given by McPherson and Blair (1993), Blair and McPherson (1994) and Harvey *et al.* (2005), such as the large amount of gravelly debris flow deposits and high slope gradient. The poorly sorted boulder beds are interpreted as the deposits of debris flows, as suggested by their extreme large size (up to 150 cm), clast shape (angular to sub-angular), scarce erosional surfaces, and abrupt lateral termination of beds. The cross-bedded, pebbly sandstone beds were produced by the bed load transportation by streams. The abundance of angular clasts in these gravel beds indicates the proximal setting in relation to the granitoid basement rocks to the east, which supplied the clasts (Figs. 2, 3A). Clast compositions and fabric clearly indicates that they were derived chiefly from *in situ* weathered and fractured granitic basement rocks as large blocks (up to 1.50 m).

Interpretation of lithofacies associations and other sedimentological characteristics indicate the depositional processes of the alluvial system in the area. Lithofacies association FP (large-scale debris flow) represents proximal fan deposits. MF (mixed pebble, sand) corresponds to medial-fan deposits, and FD (sand, silt, clay) corresponds to distal fan deposits. Faulting processes and the associated subsidence of the floor of Wadi Araba, and the uplift of the adjacent mountains in the study area took place prior to the deposition of alluvial fans which were likely formed on palaeo-piedmont fronts.

The upward-coarsening sequences are interpreted as representing episodes of alluvial fan progradation, probably formed under a tectonic control (Heward, 1978). Perhaps, during periods of source area uplift and basin floor subsidence, the fan would have abandoned its former position to fill the newly created space adjacent to the mountain front.

Acknowledgements

The authors would like to thank the University of Jordan and the Hashemite University for funding this research project. The authors would like to thank Prof. John Powell of British Geological Survey and an anonymous reviewer for their constructive comments on this paper.

References

- Abed, A.M., 1998. The geology and mineral genesis of the Taba inland sabkha, southern Dead Sea Transform, SW Jordan. In: Quaternary Deserts and Climatic Changes Ed. By A. AL-Sharhan, K. Glennie, & C. Kendall. Balkema, p. 71-87.
- Abed, A.M., 2000. Geology of Jordan, it's Environment and Water. Scientific Series 1. Publications of Association of Jordanian Geologists, (in Arabic) 571p. Jordan.
- Allen, P.A., 1981. Sediments and processes on a small streamflow dominated, Devonian alluvial fan, Shetland Islands. *Sedimentary Geology* 29, 31-66.
- Atallah, M., Al-Taj, M., 2004. Active surface ruptures of the Dead Sea Transform in Wadi Araba, Jordan. *Dirasat* 31, 59-80.
- Bender, F., 1974. Geology of Jordan. Borntraeger, 196p.
- Blair, T.C., 1999. Sedimentary processes and facies of the waterlaid Anvil Spring Canyon alluvial fan. Death Valley, California. *Sedimentology* 46, 913-940.
- Blair, T.C., McPherson, J.G., 1994. Alluvial fans and their natural distinction from rivers based on morphology, hydraulic processes, sedimentary processes, and facies assemblages. *Sedimentary Research*, A64, 450-489.
- Boothroyd, J.C., Ashley, G.M., 1975. Processes, bar morphology, and sedimentary structures on braided outwash fans, northeastern Gulf of Alaska. In: Jopling, A.V. and MacDonald, B.C. (Eds.), *Glaciofluvial and Glaciolacustrine Sedimentation*, Society Economic Palaeontology Mineralogy, Special Publication 23, pp.193-222.
- Costa, J.E., 1988. Rheologic, geomorphic and sedimentologic differentiation of water floods, hyperconcentrated flows, and debris flows, In: Baker, V.R., Kochel R.C. and Patton, P.C. (Eds.), *Flood Geomorphology*. Wiley, New York, pp. 113-122.
- Frostick, L.E. and Reid, A.N., 1989. Climatic versus tectonic controls of fan sequences: lessons from the Dead Sea, Israel. *Geological Society* 146 / 3, 527-538. UK.
- Galli, P., 1999. Active tectonics along Wadi Araba-Jordan Valley Transform fault. *Geophysical Research* 104, 2777-2796.
- Garfunkel, Z., Zak, I., Freund, R., 1981. Active faulting in the Dead Sea Rift. *Tectonophysics* 80, 1-26.
- Harms, J.C., Southard, J.B., Spearing, D.R., Walker, R.G., 1982. Depositional environments as interpreted from primary sedimentary structures and stratification sequences. Lecture Notes, Society Economic Palaeontology Mineralogy, Short Course 2, Dallas, 161pp.
- Harvey, A.M., Mather, A.E. and Stokes, M. 2005. Alluvial fans: Geomorphology, Sedimentology, Dynamics (Eds.). Geological Society of London, Special Publication 251. UK. pp. 248.
- Hein, F.J., Walker, R.G. 1977. Bar evolution and development of stratification in the gravelly, braided Kicking Horse River, British Columbia. *Can. Journal Earth Sciences* 14, 562-570.
- Heward, A.P., 1978. Alluvial fan sequence and megasequence models: with examples from Westphalian D-Stephanian B coal fields, northern Spain. In: Miall, A.D. (Ed.), *Fluvial Sedimentology*, Canadian Society of Petroleum Geologists, Memoir 5, 669-702.
- Ibrahim, K. M., 1991. The Geology of the Wadi Rahma. Map sheet no. 3049 IV. Natural Resources Authority of Jordan, Geological Mapping Division Bulletin 15.
- Jo, H.R., Rhee, C.W., Chough, S.K., 1997. Distinctive characteristics of a streamflow-dominated alluvial fan deposits: Shagori area, Kyongsang Basin (Early Cretaceous), southeastern Korea. *Sedimentary Geology* 110, 51-79.
- Jordan Climatological Handbook, 2000. Jordan Meteorological Department, Amman, Jordan.
- Maizels, J., 1993. Lithofacies variations within sandur deposits: the role of runoff regime, flow dynamics and sediment supply characteristics. *Sedimentary Geology* 85, 299-325.
- McCourt, W.J., 1990. The geology, geochemistry, and tectonic setting of the granitic rocks of southwest Jordan. *Natural Resources Authority of Jordan, Geological Mapping Division Bulletin* 10.
- McPherson, J.G., Blair, T.C., 1993. Alluvial fans. Fluvial or not? Keynote Address, 5th International Conference on Fluvial sedimentology, Brisbane, pp. K33-K41.
- Miall, A.D., 1977. A review of the braided river depositional environment. *Earth Science Review* 13, 1-62.
- Miall, A.D., 1978. Lithofacies types and vertical profile models in braided river deposits: a summary. In: Miall, A.D. (Ed.), *Fluvial Sedimentology*, Memoir Canadian Society of Petroleum Geologists, Calgary, 5, 597-604.
- Nemec, W., Postma, G., 1993. Quaternary alluvial fans in southeastern Crete: sedimentation processes and geomorphic evolution. In: Marzo, M. and Puigdefabregas, C. (Eds.), *Alluvial sedimentation*, International Association of Sedimentologists Spec. Publ. 17, 235-276.
- Quennell, A.M., 1956. Tectonics of the Dead Sea Rift. 20th International Geological Congress, Mexico. P. 385-403.
- Rabba, I., 1991. The geology of the Al Quwayra area. Map sheet 3049 I. Natural Resources Authority of Jordan, Geological Mapping Division, Bulletin 16.
- Rashdan, M. 1988. The regional geology of the Aqaba-Wadi Araba area. Map sheets 3049 III, 2949 II. Natural Resources Authority of Jordan, Geological Mapping Division, Bulletin 7.
- Rust, B.R., 1978. A classification of alluvial channel systems. In: Miall, A.D. (Ed.), *Fluvial Sedimentology*, Memoir Canadian Society of Petroleum Geologists, Calgary, 5, 187-198.
- Schreiber, B.C., El Tabakh, M., 2000. Deposition and early alteration of evaporites. *Sedimentology* 47, 215-238.
- Shultz, A.W., 1984. Subaerial debris-flow deposition in the Upper Paleozoic Cutler Formation, Western Colorado. *Journal of Sedimentary Petrology* 54, 759-772.
- Tarawneh, B., 1992. The geology of the Fifa area. Map sheet 3051 I. Natural Resources Authority of Jordan, Geological Mapping Division, Bulletin 20.
- Todd, S.P., 1989. Stream-driven, high-density gravelly traction carpets: possible deposits in the Trabeg Conglomerate Formation, SW Ireland and theoretical considerations of their origin. *Sedimentology* 36, 513-530.
- Went, D.J., 2005. Pre-vegetation alluvial fan facies and processes: an example from the Cambro-Ordovician Rozel Conglomerate Formation, Jersey, Channel Islands. *Sedimentology* 52, 693-713.

Geology and Mineralogy of Jabal Kabid Phosphorite Deposits, Southeastern Jordan

Saeb Al-Shereideh ^{a,*}, Khaled Tarawneh ^b, Hani Nawafleh ^b, Nazem El-Radaideh ^a and Khaled Moumani ^c

^aYarmouk University, Faculty of Science, Department of Earth and Environmental Science. P. O. Box 566

^bAl-Hussein Bin Talal University, Faculty Of Engineering, P.O. Box 20, Ma'an-Jordan.

^cNatural Resources Authority, Geology Directorate, Geological Mapping Division, P.O. Box. 7, Amman-Jordan

Abstract

The phosphorites of *Jabal Kabid* (Campanian-Maastrichtian), crops out along the southeastern extension of Ras En Naqab - Batn Al Ghul escarpments, are up to 20 m thick and unconformably overlie the Upper Cretaceous-Batn Al Ghul Group. The phosphorite sequence in the study area shows lateral variations in lithology, thickness and distribution of the phosphorite beds. Generally, phosphates at these localities form approximately 50% of the sequence and occur as beds, up to 1.4 m thick. The petrographic studies indicate the presence of phosphate pellets, bone fragments, fish teeth, and phosphate intraclasts. The main phosphate mineral is francolite. Chemical results indicate that P₂O₅ content of the phosphate beds increases upwards in the sequence from 8.0 to 26.42 %. The SEM-EDS results indicate that the P₂O₅ content ranges between 36.98-41.67%. The phosphorites, in the study area, were deposited in a marginal marine environment close to the shore line.

© 2010 Jordan Journal of Earth and Environmental Sciences. All rights reserved

Keywords: Jordan, phosphorite, genesis of phosphates, francolite.

1. Introduction

Economic phosphorite deposits are present in Jordan in Rusiefa, Qatrana, Al Abyad, Al Hasa, and Ash-Shidiya areas (Fig. 1). The phosphorites in Jordan are found in the phosphorite member of Bender (1974), the topmost of Amman Formation of Masri (1963), and Maastrichtian in age according to Burdon (1959). The term Al Hisa Phosphorite Formation (AHP) (Campanian-Maastrichtian) is adopted by the National Geological Mapping Project (Natural Resources Authority).

New deposits were discovered in northwest Jordan (Mikbel and Abed, 1985). The phosphate of Jordan is part of the Upper Cretaceous-Eocene Tethyn Phosphorite Belt stretching from Morocco to Turkey, Syria, Iraq, Saudi Arabia, and Palestine (Klemme, 1958; Sheldon, 1964; Notholt *et al.*, 1989). The belt belongs to South Tethyn Phosphogenic Province (STPP); a carbonate-dominated phosphorite giant that is composed of greatest accumulation of known sedimentary phosphorites and hosts 66% of the world's phosphate reserve base and accounts for approximately 30% of global phosphate rock production (Pufahl *et al.*, 2003). The Jordanian phosphorites were deposited in the transitional zone between a stable shelf in the south and the Tethys Sea in the north Jordan due to the upwelling currents (Bender,

1974). Details on the geology, petrology, mineralogy, chemistry and genesis of phosphate deposits are found in Reeves and Saadi (1971), Khalid (1980), Khalid and Abed (1982), Abed and Khalid (1985), Al-Agha (1985), Mikbel and Abed (1985), Abed and Ashour (1987), Abed and Al-Agha (1989), Abed and Fakhouri (1990, 1996), Abed *et al.* (1992), Tarawneh (1997), Pufahl *et al.* (2003), Tarawneh and Moumani (2006), Tarawneh (2006), and Abed *et al.* (2007).

The following work is the first detailed study of the phosphorite deposits along the southeastern part of Batn Al Ghul Escarpment (Jabal Kabid/Naqab Etaiq area) in southeast Jordan (Fig. 1). The aim of this research is to investigate the petrology, mineralogy, chemistry and genesis of phosphates at this locality.

2. Geological Setting

The phosphorite deposits crops out in the southeastern part of Jordan along the southeastern extension of Batn Al Ghul Escarpment (Jabal Kabid /Naqb Etaiq area). The area is situated to the southeast of Ash Shidiya Phosphate Mine; close to the Saudi Arabia border (Fig. 1).

The phosphorite deposits (20m thick) rest unconformably on the Upper Cretaceous of Batn Al Ghul Group (Fig. 2).

The phosphorite sequence shows lateral and vertical variations in lithology, thickness and distribution of the phosphorite beds (up to 1.4m thick). The phosphorite beds occur at several levels, increase upward and intercalate

* Corresponding author. shereideh@yahoo.com, Saeb@yu.edu.jo

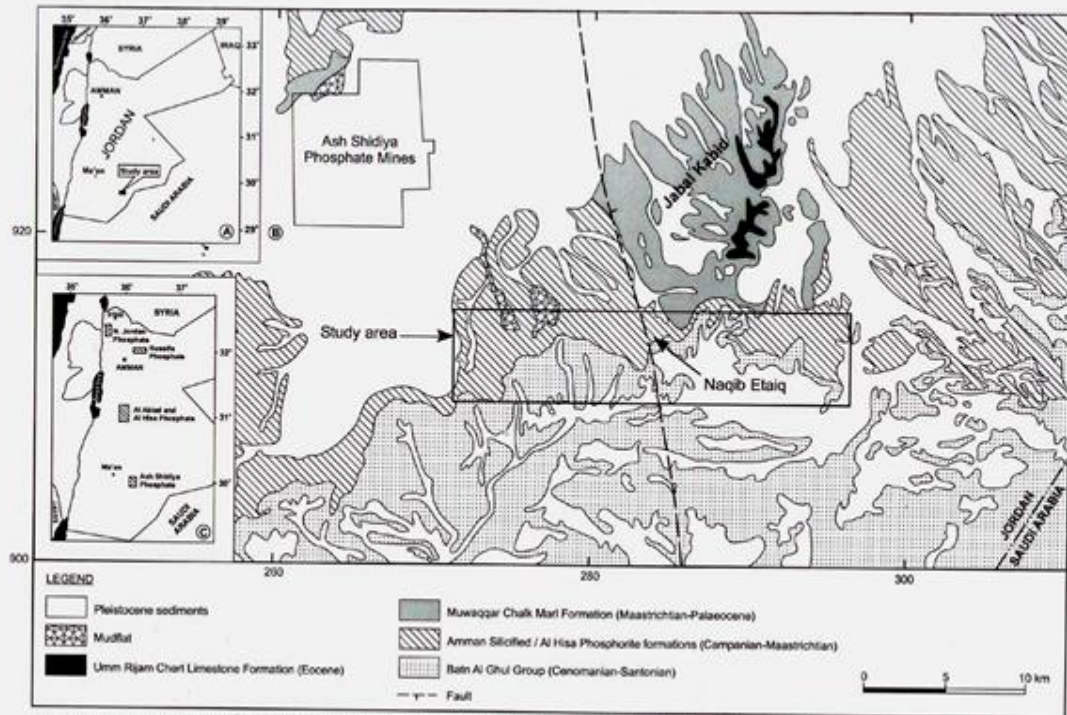


Fig. 1: A) Location map, B) Simplified geological map of the study area, C) Distribution of the phosphate deposits in Jordan.

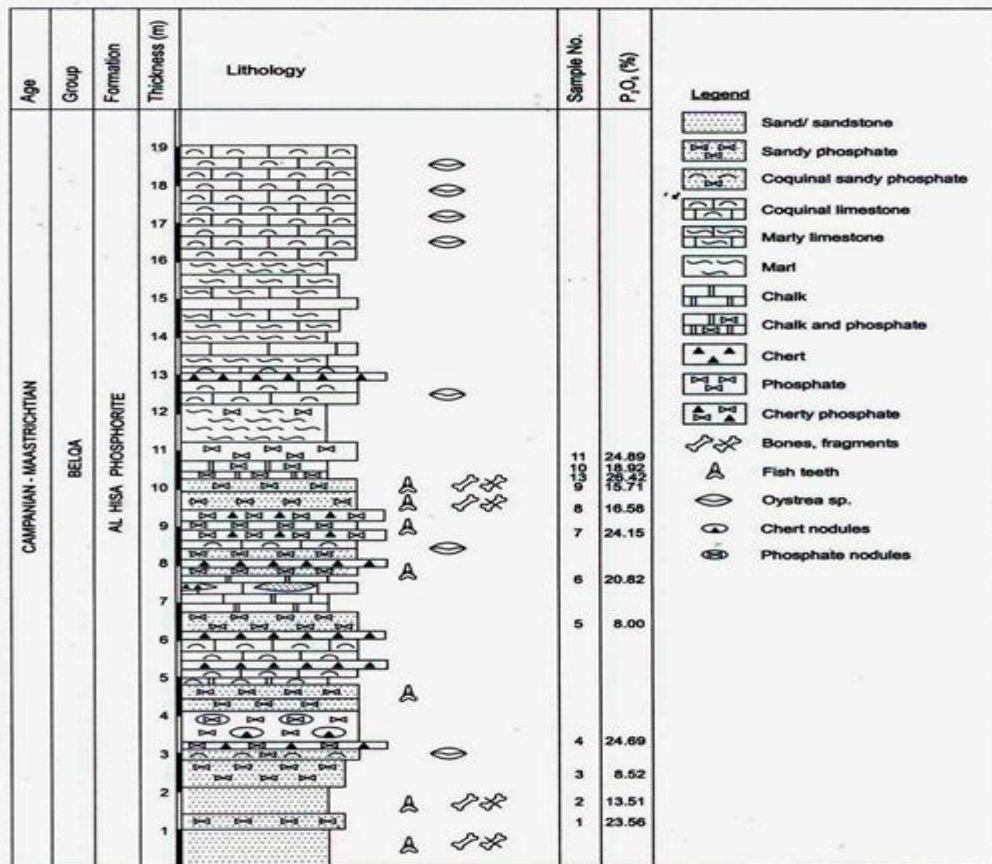


Fig. 2: Graphic log of Al Hisa Phosphorite Formation in Naqib Etaiq area.

with fine to medium-grained sand and sandstone, limestone, coquina, chert, cherty phosphate, marl and chalky limestone with macrofossils in the basal and upper parts of the phosphate sequence. The coarse-grained granular sandy phosphate occurs in the basal and in middle parts of the formation. This bed is characterized by enrichment of fish teeth and bones. Generally, the contact between the phosphate beds and the interbedded lithologies are usually gradational. The P_2O_5 content is variable and increases upward in the sequence (Fig. 2). Generally, phosphates form more than 50% of the formation. Field observations indicate the presence of different phosphate fragments, as well as, bone fragments, reptile carapaces, and different types of fish teeth intensively occur in the friable sandy phosphate of the lower part of the geological section.

3. Field Work and Analytical Methods

The results presented in this work are based on detailed measurements of the phosphate sequence and sampling from typical localities in the study area. Petrographic studies were performed by using polarizing optical microscope type (Leica- DMLP). Thin and polished sections were prepared for detailed petrographic studies. X-ray fluorescence (XRF), X-ray diffraction (XRD) using Philips 1370 X-ray diffractometer, and Scanning Electron Microscope (SEM/EDS) using Jeol 6060 instrument were used to characterize the collected samples. Selected areas of the phosphates in thin and polish sections were investigated. The later utilized a Jeol 6060 instrument-high vacuum, equipped with a link 10000 Energy Dispersive Spectrometry (EDS) system. SEM coupled with back-scattered electron (BSE), and secondary electron image (SEI) microanalyses.

4. Results and Discussion Petrography

Petrographic examination has revealed that the phosphate grains, as peloids (pellets), constitute most of the phosphatic particles., particularly in the high-grade phosphorite beds. The pellets are structureless, sometimes oval in shape and uniform in size with smooth boundaries, dark in color with 0.060-0.5 mm in diameter grains (Fig. 3). Pellets are part of peloids which might be fecal in origin (Abed and Fakhouri, 1996). Through burial processes, peloids will become cemented and preserved (Bogg, 2006).

Intraclasts are also common in the studied phosphorites. They have irregular shape (up to 1cm in diameter) with internal microstructure. Some of these intraclasts are composed noncrystalline apatite or amorphous phosphate (Fig. 4). Skeletal fragments include bones and teeth of various sizes up to 1 mm in diameter. They made an important component of the phosphorite grains and concentrated mostly in the lowermost part of the sandy phosphate beds and in the friable quartzarenites in the basal part of the phosphate beds. Petrographically, the internal part of the phosphate particles is made of microcrystalline translucent apatite to noncrystalline (amorphous) type (Fig. 5). Many pellets show a relict structure of organic material. Some of the skeletal

fragments are replaced by microcrystalline quartz, indicating silicification. Coated grains of phosphate and microaggregates are present. They are generally larger than 0.25 mm, and are made of translucent apatite at the center and at the rim of these grains (Fig. 5).

Detrital quartz is abundant in the studied samples. The grains are rounded, subrounded to subangular with various sizes. It occurs as siliceous matrix, usually fine to medium grains. Silicification of some phosphate particles can be noticed in cherty phosphate horizon (Fig. 6). The cement is siliceous and is locally calcareous as a result of diagenetic silicification and partial calcitization. Silicification of phosphate particles has previously been reported by Kolodny (1969) from the northern Negev phosphorites. Cryptocrystalline dolomite and calcite (sparite) are present as cement, whereas secondary gypsum occurs in some micro-veins in thin sections.

In general, Jordanian phosphates are made up of four types of phosphatic particles; as peloids (pellets), intraclasts, skeletal fragments and coated grains (Abed and Al Agha, 1989; Khalid and Abed, 1982; Abed and Fakhouri, 1996; Pufahl, 2003; Tarawneh, 2006; Abed *et al.*, 2007). The composition of the phosphate in this study is similar to other Jordanian phosphates, with small differences in the amount of phosphatic particles in some parts of the phosphate beds.

5. Mineralogy and Chemistry

XRD results indicate that the major phosphate mineral is francolite (carbonate fluorapatite). The Calcite, quartz, dolomite are detected and trace of gypsum has been indicated (Fig. 7).

In general, the phosphate beds in the study area compared with the Upper Cretaceous phosphorite horizons in central and northern parts of Jordan. The beds are richer in SiO_2 and poorer in CaO, whereas the P_2O_5 content has a relatively wide range.

The P_2O_5 content ranges from 8.0 to 26.42%. This wide range of P_2O_5 content, in the studied samples, is mainly due to the admixture of non-phosphatic minerals such as quartz, calcite and dolomite. That is the reason of the weak relationship between the P_2O_5 and most of the oxides associated phosphatic facies. Most of the relationships are randomly oriented (Fig. 8). The positive relationships have been noticed between P_2O_5 with CaO and F, ($r=0.46$ and 0.32), respectively, whereas the negative relationships have been seen between P_2O_5 with CO_2 , SiO_2 , SO_3 and F/P_2O_5 ($r= -0.11, -0.51, -0.08, -0.71$), respectively.

The average content of SiO_2 in the study area is 29.91% and is mainly detrital quartz. In some cases, microcrystalline silica appears in the form of chalcedony filling some shells or as cement. According to Cathcart and Gulbrandsen (1973), silicon could replace phosphorous in the apatite lattice.

The CaO content ranges between 12.74-41.76%. Chemical analyses and microscopic investigations indicate that the major part of the carbonate materials is made of sparite and microsparitic calcite.

The MgO content in the studied samples ranges between 0.13 to 2.34%. Dolomite is only present in a few samples in the dolomitic sandy phosphate.

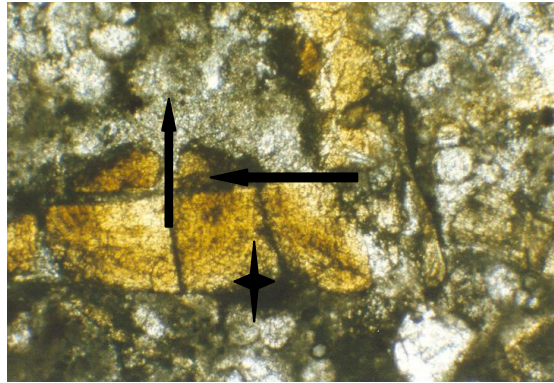


Fig. (3): Phosphate intraclast filling with translucent and amorphous phosphate (V-shape showing with an arrow) in sparitic to microsparitic cement and subrounded grains of quartz showing in stars, and fine-grained dolomite (PPL, X150).

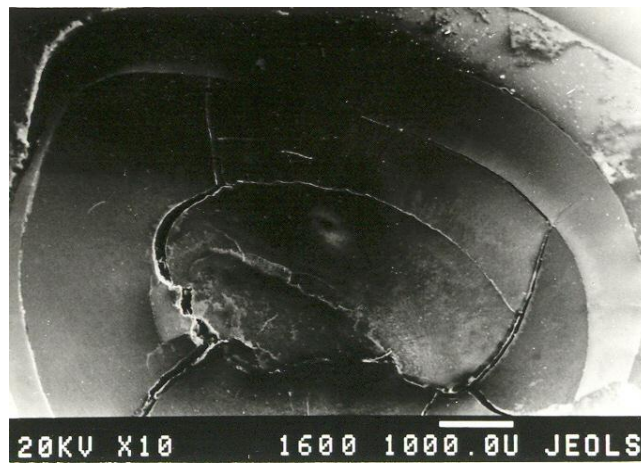


Fig. (4): Fish teeth with rounded smooth boundaries, filling with translucent anisotropic phosphate.

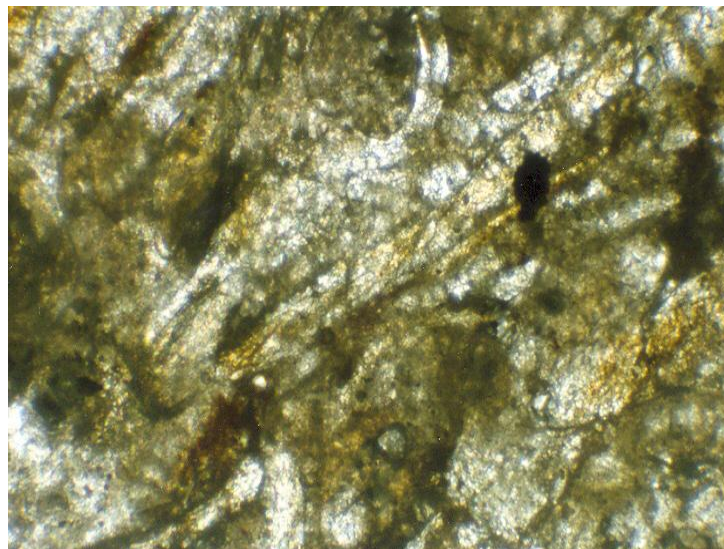


Fig. 5: microcrystalline to translucent apatite at the center and at the rim of skeletal fragments and noncrystalline phosphate (amorphous) filling them (PPL, 50X).

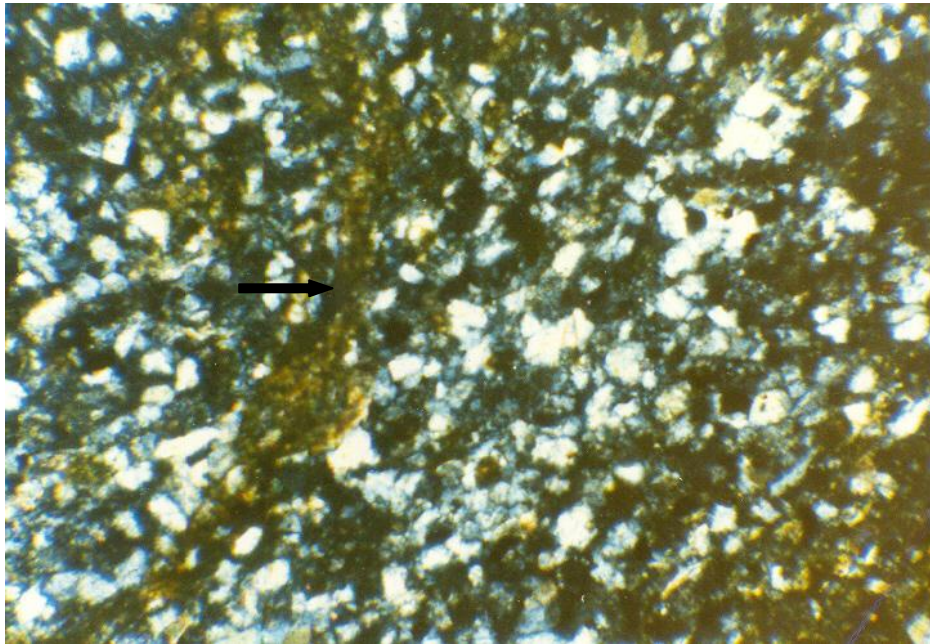


Fig. (6): Noncrystalline apatite (amorphous) filling the cavities (showing with arrow), surrounded with detrital quartz and chalcedony (.XPL,50X).

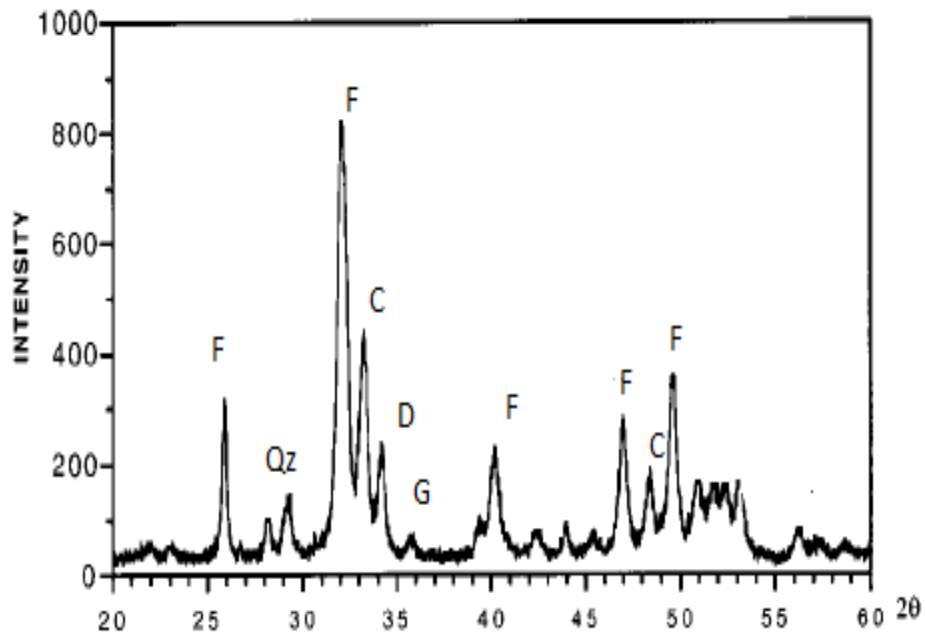


Fig. (7): XRD showing francolite (F), quartz (Qz), calcite (C), dolomite and gypsum (G) minerals.

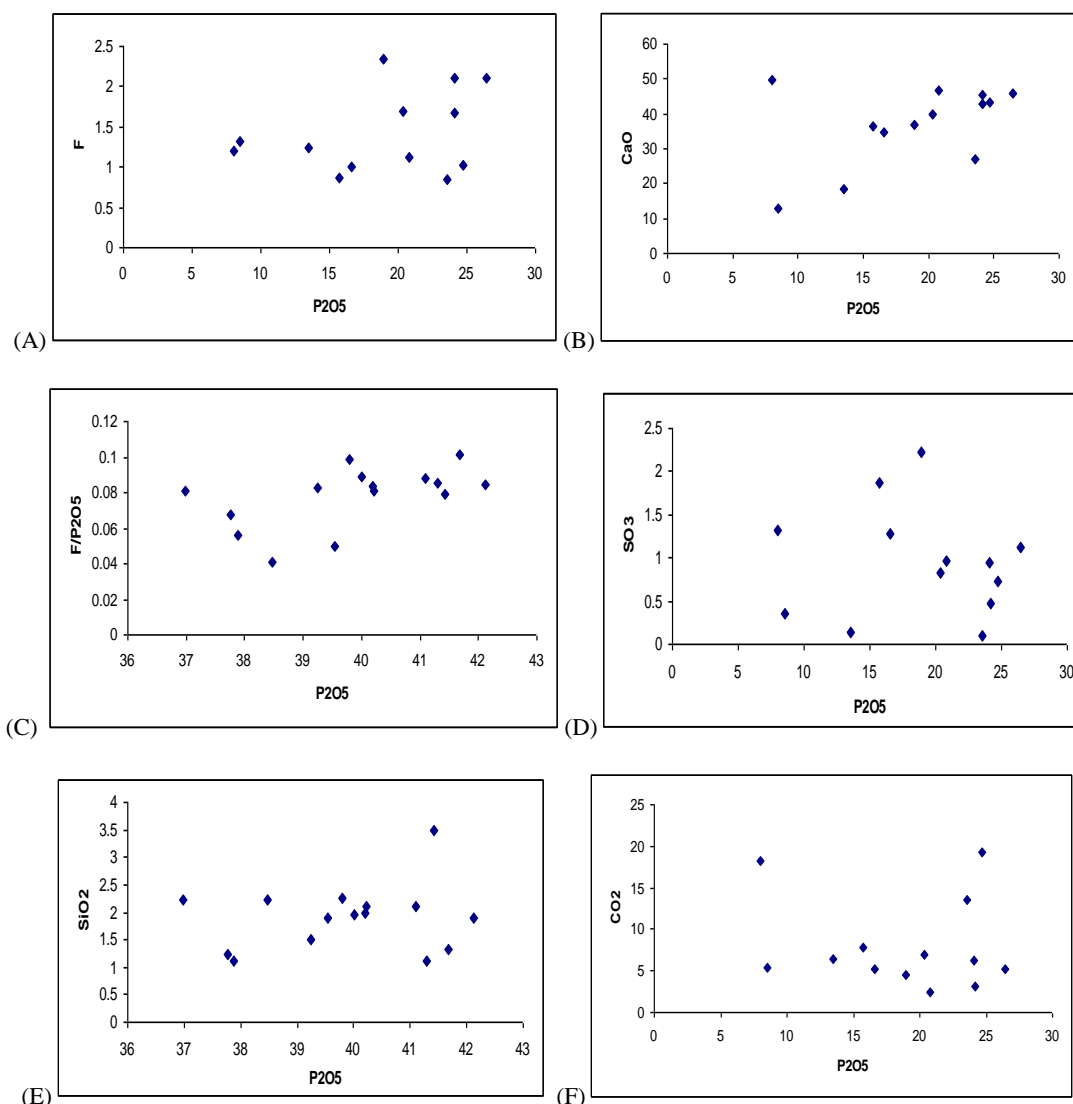


Fig.(8): Graphical representation demonstrating the relationships between: (A):P₂O₅:F; (B):P₂O₅:CaO; (C):P₂O₅:F/P₂O₅; (D):P₂O₅:SO₃; (E): P₂O₅:SiO₂; (F): P₂O₅:CO₂

Mg can replace Ca in apatite and calcite lattice (McClellan, 1980). The content of TiO₂, K₂O, Na₂O and Fe₂O₃ oxides is very low. The greatest amount of these oxides may be referred to the sandy facies.

The CO₂ content ranges between 1.28-18.29%. McConnell (1973) considered that the carbonate anionic group partly substitutes for PO₄ group. In the studied samples, CO₂ is mainly present in the carbonate and phosphate (francolite) facies.

The SO₃ content ranges between 0.10-1.87%. Sulphur may occur in the apatite structure as a normal constituent of phosphate lattice or in gypsum that was detected by X-ray diffraction as trace mineral. The (PO₄) group in the apatite can be also replaced by SO₄ (Stowasser, 1975).

The fluorine content ranges between 0.85-2.34%. Fluorine is present in the lattice and it occurs free or associated with (OH) and O-ions (McConnel, 1973).

The chlorine content in the studied samples varies from 0.04 to 1.31%. In the phosphates, chlorine may be present in the apatite lattice where it may replace F or OH group (Blatt *et al.*, 1972). The Cl may be associated with clay minerals, or partly incorporated in the apatite structure replacing F. The apatite PO₄-group may be partly replaced by OH-group (McConnell, 1965). Phosphorous may be partly replaced by the following elements As, V, Si, S, C and Cr (Cathcart and Gulbrandsen, 1973), whereas calcium can be partly replaced by Na, Sr, Ba, Cd, Rb, Re, Th and U (McConnell, 1973).

The EDS results for the *major* and minor elements are given in Table 2. These results indicate that the

groundmass of the studied phosphates consists of microcrystalline apatite, pellets, fish teeth, bone fragments and other unidentified phosphorite fragments. Apatite

occurs as dark envelops surrounding light cores of these components (Figs. 9, 10).

Table (1): XRF results in (wt %) of the phosphate samples collected from the study area

P ₂ O ₅	CO ₂	Fe ₂ O ₃	CaO	SO ₃	SiO ₂	Al ₂ O ₃	MgO	Cl	F
23.56	13.56	0.33	27.18	0.1	33.23	0.05	0.76	0.08	0.85
13.51	6.5	0.23	18.24	0.13	59.03	0.01	0.45	0.09	1.25
8.52	5.32	0.44	12.74	0.36	69.94	0.07	0.32	0.65	1.32
24.69	19.26	0.19	43.22	0.72	8.07	0.02	1.26	0.04	1.02
8.22	18.23	0	49.55	1.31	6.98	0.05	14.75	0.40	1.21
20.82	2.35	0.88	46.88	0.97	23.14	0.21	1.86	0.89	1.12
24.15	3.21	0.89	42.94	0.48	24.23	0.97	0.58	0.82	1.68
16.58	5.25	0.33	34.56	1.28	39.4	0.01	0.7	1.30	1.01
15.71	7.75	0.26	36.31	1.87	33.85	0	2.34	0.04	0.87
18.92	4.54	0.89	36.65	2.23	33.25	0.07	0.61	0.70	2.34
24.09	6.23	0.5	45.3	0.95	18.66	0.11	0.9	1.31	2.11
20.35	6.89	0.26	39.88	0.83	29.08	0	0.13	0.87	1.7
26.42	5.23	0.71	45.67	1.12	15.5	0	1.89	1.01	2.1

Table (2): Chemical analyses in (wt %) of the various types of phosphate particles using SEM-EDS method

Object of study	CaO	P ₂ O ₅	SiO ₂	Na ₂ O	F	Cl	F/P ₂ O ₅	CaO/P ₂ O ₅
Cement	51.1	41.7	1.32	0.88	4.2	0.8	0.1	1.22
Pellet core	48.5	40.1	1.93	1.04	3.6	1.1	0.08	1.2
Pellet rim	49.4	41.4	3.52	0.89	3.3	1.1	0.07	1.19
Skeletal material	52.3	40.2	2.22	1.18	3.4	0.9	0.08	1.3
Bone	51.1	41.3	1.12	1.12	3.5	1.3	0.08	1.23
Fish teeth	54.2	39.3	1.51	1.21	3.3	0.5	0.08	1.38
Intraclast	50.7	41.1	2.11	1.17	3.6	1.3	0.08	1.23
Bone	49.8	39.8	2.25	1.97	3.9	1.2	0.09	1.25
Isotropic phosphate	51.95	40.01	1.95	1.65	3.6	0.8	0.08	1.29
Anisotropic phosphate	48.5	37.8	4.23	1.98	2.6	1.8	1.8	1.28
Shell fragment	49.23	36.98	5.23	1.23	2.98	1.95	0.08	1.33
Cement	49.3	39.6	4.89	1.88	2	1.3	0.05	1.24
Coprolite	47.9	37.9	6.11	1.94	2.1	1.9	0.05	1.26
Fish teeth	49.9	40.2	4.12	1.25	3.3	1	0.08	1.23



Fig. (9): Apatite (microcrystalline to amorphous) occurs as dark envelopes surrounding light cores of phosphate particles (pellets)

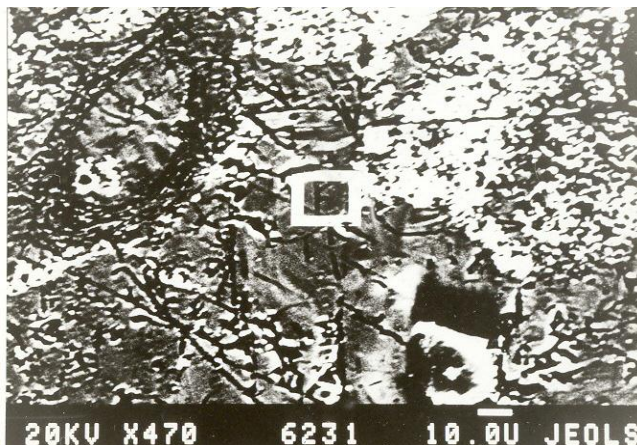


Fig. (10): Pellets are structureless, sometimes with oval forms and smooth boundaries.

SEM-EDS results of cement, core and rim of pellets, fish teeth, coprolite, and bone fragments indicate that the P_2O_5 content varies from 36.98 to 41.67 %. The content of other elements and oxides associated with the phosphorite facies is given in Table 2.

EDS results confirm that the phosphorite facies are mostly made up of P, Ca, F, Cl and partly of Si and Na, that could be involved in the apatite lattice (Fig. 11). Replacement of P by Si, Ca by Na and F by Cl, respectively, is more common in similar phosphates (Cheney *et al.*, 1979). Results of EDS indicates that the F/ P_2O_5 ratio ranges from 0.04 to 0.10, while CaO/ P_2O_5 value ranges from 1.23 to 1.38, which are similar to the values reported on the composition of francolite in other phosphate (Cheney *et al.*, 1979 and McClellan, 1980). Using the results of EDS, it can be assumed that positive relationships have been seen between P_2O_5 with CaO, F, SiO_2 and F/ P_2O_5 ($r=0.32, 0.65, 0.18, 0.54$), respectively.

6. Genesis

Field observations and experimental results have indicated that the phosphates of the study area are grain-supported type. Such type of phosphate in ancient strata are commonly viewed largely as a reworked product of symsedimentary phosphatized mud generated in low-

energy and organic rich marine environments (Riggs, 1979; Glenn and Arthur, 1990). The processing of washing and transport would concentrate the phosphorite bodies "Pellets" generated as phosphorite beds within tectonic troughs in near shore setting (Soudry, 1992). Therefore, such phosphates could be formed due to a series of successive processes providing a final concentration of phosphorus (Baturin and Bezrkovis, 1979). These processes include winnowing of light and fine non-phosphatic fractions and residual concentration of coarser material, including phosphorite grains (Soudry and Nathan, 1980). The granular phosphorites of both southeastern Jordan and Negev (Soudry, 1987; Soudry and Lewy, 1988) are essentially grainstones to packstones, which are extremely porous and are situated near-surface in an arid area. Deposition of phosphorite deposits in arid zones has been long recognized by Strakov (1962). Formation of pelletal or granular phosphorites in Jordan, particularly in southeast Jordan and Negev and elsewhere appears to be diagenetic (Soudry and Nathan, 1980). Khalid (1980) recognized that Ash-Shidiya phosphates, which are close to the study area, were deposited in syntectonic depressions with high rate of sedimentation. Reworking could liberate internal molds and produce well-rounded phosphate mud particles, which may be

erroneously, interpreted as fecal pellets (Abed and Fakhouri, 1996).

The environment of deposition and early diagenetic processes are apparently reflected in the fabrics and grain

composition in such phosphate. The bioturbation features commonly associated with the granular phosphorites, and the high energy of character of these rocks, point to

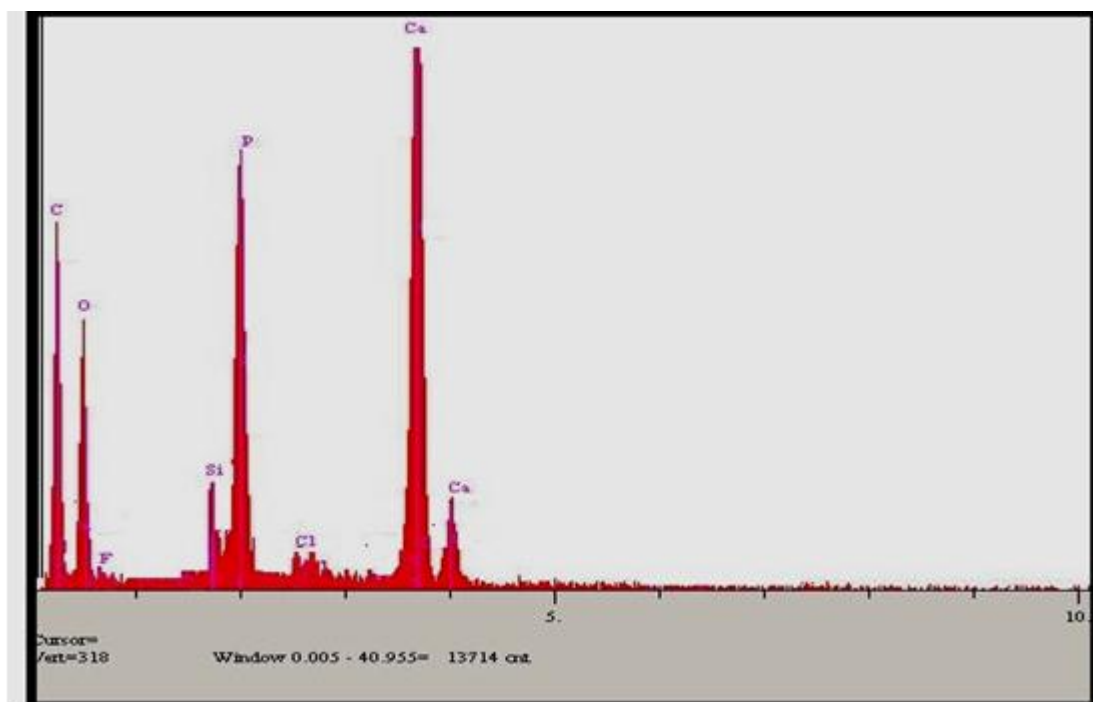


Fig. (11): EDS spectra of selected phosphate sample, showing the distribution of the major and minor elements associated in phosphatic facies.

deposition in arid environments with good mixing of waters that have chemical composition typical to sea-water (Nathan *et al.*, 1990). The abundance of bone fragments in the phosphate of this study is apparently related to onshore reworking of vertebrate remains from phosphatizing hemipelagic environment, as suggested by Anita and Whitaker (1978) and in Reif (1982). This model of deposition stands in contrast to the peloids of sandy phosphorites that are derived mainly from nearshore environments (Soudry, 1987). Pufahl *et al.* (2003) indicates that the southern Tethyan margin in Jordan was characterized by phosphogenesis in sedimentary environments spanning nearshore, mid-shelf, and distal shelf setting. Pufahl, *et al.* (2003) mentioned that the “phosphorite nursery” is a non-uniformitarian phenomenon reflecting phosphate precipitation across a broad paleoenvironmental spectrum. The former author described that the phosphogenesis on the Jordanian shelf was stimulated primarily by the microbial respiration of sedimentary organic matter. Phosphatic grainstones formed through the successive winnowing, transport and redeposition of phosphate grains and intraclasts derived from pristine phosphate facies via storm-generated currents as indicated by Pufahl *et al.* (2003). The relatively high abundance of biogenic forms may indicate high biogenic activity and accompanying phosphatization (Reisi, 1988; Tarwneh and Moumani, 2006). Abed *et al.* (2007) summarized that the deposition of Ashdiyya phosphorite platform in southern Jordan, near the study area, was deposited in open shelf conditions with

upwelling, shallow subtidal to inner shelf. He concluded that higher bioproductivity coupled with high rates of death and sedimentation; increase the P and Si concentration in the poor water of the sediments and lead to the authogenic formation of phosphorites, chert and porcellanite, as well as, mentioned by Birch (1980) and Burnett (1990).

From the previous discussion, it is concluded that the phosphates can be formed under a variety of depositional environments. However, it can be assumed that the presence of fauna and high abundance of biogenic forms as indicted in this study accompanying phosphatization process. The higher amounts of siliciclastics indicate that the phosphorites, in the study area, were probably deposited in a marginal marine environment; very close to the shore lines of the continent. It could be argued that the sedimentary structures, composition and thickness of the phosphorite deposits in the study area are closely controlled by the local palaeostructural relief.

7. Conclusions

This is the first detailed study to shed light on phosphorite deposits along the southeastern extension of Batn Al Ghul Escarpment (Jabal Kabid/Naqab Etaiq area) in southeast Jordan. The phosphorite deposits (~20m thick) overlie unconformably the Upper Cretaceous Batn Al Ghul Group. The composition of the phosphate in this study is similar to other Jordanian phosphates, with small differences in the amount of phosphatic particles in some

parts of the phosphate sequence. Petrographic examinations reveal that the phosphates are made up of four types of phosphatic particles; pellets, intraclasts, skeletal fragments and coated grains. The results of XRD indicate that the major phosphate mineral is francolite (carbonate fluorapatite). The XRF results of selected samples indicate that the P₂O₅ content ranges from 8.0 to 26.42%, whereas through SEM-EDS analyses, the P₂O₅ content ranges from 36.89 to 41.67%. It can be assumed that the presence of fauna, in addition to the higher amounts of siliciclasts indicate that the phosphorites in the study area were probably deposited in a marginal marine environment; very close to the shore lines of the continent.

Acknowledgements

The authors would like to thank to the anonymous reviewers for their constructive criticism of the manuscript. Thanks also extended to the Al Hussein Bin Talal University and to the Natural Resources Authority for facilitating and supporting this study. Thanks also extended to the General Director of the NRA and Geol. Basam Tarawneh, the Director of Geology/NRA. Thanks also for Geol. Mohamed Abdelghafour from NRA for his help in drawing of the figures.

References

- Abed, A. M, Zaid, K., Al Hawari, Z., Sadaqah, R., S and Abu Mirri, O. 1992. The red phosphorites of Esh Shidiya, SE Jordan. Geol. of Arab World, Cairo University.
- Abed, A., M. and Ashour, M., 1987. Petrography and age determination of the NW Jordan phosphorites, Dirasat. 14: 247-263.
- Abed, A., M. and Fakhouri, K., 1990. Role of microbial processes in the genesis of the Upper Cretaceous Phosphorites. Geol. Soc. London. 52: 193-203.
- Abed, A. M and Fakhouri, K., 1996. On the chemical variability of phosphatic particles from Jordanian phosphorite deposits. Chemical Geology. 131: 1-13.
- Abed, A. M. and Al Agha, M., 1989. Petrography, geochemistry and origin of the NW Jordan phosphorites. J. Geol. Soc. London. 146: 499-506.
- Abed, A. M. and Khalid, H., 1985. Distribution of uranium in the Jordanian phosphates. Dirasat. 12: 91-103.
- Abed, A. M., Sadaqah, R. and Al Jazi, M., 2007. Sequence stratigraphy and evolution of Eshidiya phosphorite platform, southern Jordan. Journal of Sedimentary Geology, 198, 209-219.
- Al Agha, M. 1985. Petrography, geochemistry and origin of the NW Jordan phosphorites. Unpubl. M. Sc. Thesis. University of Jordan.
- Anita, D. and Whitaker, H., 1978. Scanning Electron Microscope study of the genesis of the Upper Silurian ludlow bone bed, Geol. Abstracts, England, 119-134.
- Baturin, G. and Bezrkovis, P., 1979. Phosphorite of the sea floor and their origin. Marine Geology, 31: 317-332.
- Bender, F., 1974. Geology of Jordan, Gebruedre, Berlin. 196p.
- Birch, G. F., 1980. A model for penecontemporaneous phosphatization by diagenetic and authigenic mechanism from the western margin of south Africa. In: Bendor, Y (Edition Marine Phosphorites. SEPM special publications, 29, 70-100.
- Blatt, D., Middleton, G. and Murray, R. 1972. Origin of sedimentary rocks. Prentice-Hall, New Jersey.
- Boggs, S. 2006. Principles of sedimentology and stratigraphy: Fourth Edition, New Jersey, 165p.
- Burdon, D. J. 1959. Handbook of the geology of Jordan. Government of Jordan, Amman, 82p.
- Burnett, W. C., 1990. Phosphorite growth and sediments dynamics in the modern Peru shelf upwelling system. In: Burnett, W. C., Riggs, S. (Eds.), phosphorite deposits of the world. Neogene to Modern phosphorites, Vol. 3. Cambridge University Press, Cambridge, pp:62-74.
- Cathcart, J. and Gulbradsen, R., 1973. Phosphate deposits U. S. Geol. Surv., Profess. 820-515.
- Cheny, T., Mc Clellan and Montgomery, E., 1979. Sechura Phosphate deposits. Econ. Geol. 74; 2: 232-259.
- Glenn, C. and Arthur, M., 1990. Anatomy and origin of a Cretaceous phosphorite green sand gint, Egypt. Sedimentology, 37: 123.
- Khalid, H. and Abed, A. M., 1982. Petrography and geochemistry of Esh Shidiya phosphate. Dirasat 9: 81-101.
- Khalid, H. 1980. Petrography, geochemistry and origin of Esh Shidiya phosphorites. Unpubl. M.Sc. Thesis, University of Jordan, 147p.
- Klemme, H. D., 1985. Regional geology of Circum-Mediterranean region, Am. Assoc. Pet. Geol., 42: 477-512.
- Kolodny, Y., 1969. Petrology of the siliceous rocks in the Mishash Formation, Negev. J. Sed. Pet., 39: 165-175.
- Masri, M. 1963. Report on the geology of the Amman-Zerqa area. Unpub. report.
- McCConnell, D. 1973. Apatite, its crystal chemistry, mineralogy utilization and geologic and biologic occurrences, New York.
- McClellan, G., 1980. Mineralogy of carbonatefluorapatite. Journal Geol. Soc. London, 137, 657-681.
- McCConnell, D., 1965. Crystal chemistry of hydroxyapatite, its relation to bone mineral. Arch oralbiol, 10: 421-431.
- Mikbel, S. and Abed, A. M., 1985. Discovery of large phosphate deposits in NW Jordan, Dirasat XII, 2: 125-126.
- Nathan, Y., Soudry, D., and Avigour, A., 1990. Geological significance of carbonate substitution in apatites. Soc. Lond. Spec. Publ. 52: 179-191.
- Notholt, A., Sheldon, R. and Davidson, D., 1989. Phosphate deposits of the world, Vol. 2, phosphate rock resources, Cambridge Univ. Press.
- Pufahl, P., Grimm, K., Abed, A. M and Sadaqah, R., 2003. Upper Cretaceous (Campanian) phosphorites in Jordan: Implications for the formation of a south Tethyan phosphorite giant. Journal of Sedimentary Geology, 161:170-205.
- Reeves, M. and Saadi, T., 1971. Factors controlling the deposition of some phosphate bearing strata from Jordan, Econ. Geol. 66: 451-465.
- Reisi, Z., 1988. Assemblages from a Senonian high productivity sea. Rev. Palobiol 2: 323-332.
- Rief, W., 1982. Muchelkak keubar bone beds (Middle Triassic-SW Germany) storm conditions a regressive cycle. Rigges, S. R.,

1979. Petrology of the Tertiary phosphorite system of Florida. *Econ. Geol.* 74: 194-220.
- Sheldon, R.P., 1964. Palaeolatitudinal and paleogeographic distribution of phosphorite. *U.S. Geol. Surv.*, 501: 106-113.
- Soudry, D., 1987. Ultra-fine structures and genesis of the Campanian Negev high-grade phosphorites. *Sedimentology*, 34: 642-660.
- Soudry, D., 1992. Primary bedded phosphorites in the Campanian Mishash Formation, Negev, *Sed. Geol.* 80: 77-88.
- Soudry, D., and Lewy, Z., 1988. Microbially influenced formation of phosphate nodules and microfossil moulds. Negev. *Palaeogeography, Paleoclimatology and Palaeoecology*, 64:15-34.
- Soudry, D. and Nathan, Y., 1980. Phosphate periods from the Negev phosphorites, *Journal. Geol. Soc. London*, vol. 137: 749-755.
- Stowasser, W. 1975. Phosphate rocks. In: U.S. Bureau of mines, *Bulletin* 667.
- Strakov, N. 1962. Fundamentals and theory of lithogenesis, 3 *acad. science. UCCR*, 95.
- Tarawneh, K. 1997 Geological and mineralogical studies on the phosphorite horizon in the Azraq area-East Jordan. *Second Jordanian Mining Conference, Amman*, 1: 420-437.
- Tarawneh, K. 2006. Geological Map of Wadi Abu Mil. Map Sheet No 3249-IV. Natural Resources Authority. Geol. Dir., Geol. Map. Div., Amman-Jordan.
- Tarawneh, K. and Moumani, K. 2006. Petrography, chemistry and genesis of phosphorite concentrations in the Eocene Umm Rijam Chert Limestone Formation in Ma'an area/ southern Jordan. *Journal of Asian Earth Science.* 26: 627-635. New York, 180-188.

Eutrophication Process in the Mujib Dam

Sura T. Al-Harashsheh^{a,*}, Hani R. Al-Amoush^a

^a Institute of Earth and Environmental sciences, Al al-Byet University, Mafraq, 130040, Jordan

Abstract

This study aims at analyzing the physical, chemical, and biological components of the water stored in Mujib dam as related to eutrophication processes. Several seasonal water samplings starting from the year 2006 until summer 2010 were carried out, analyzed and interpreted. The results showed small variations in the pH and EC values of the Mujib dam water. The EC in winter time were low compared to summer time as a result of dilution process by floodwater. In addition, the concentration of major cations and anions were found to be higher in summer season due to evaporation. Moreover, it was found that the concentrations of NH_4^+ and heavy metals are lower than the permitted level in drinking water according to the Jordan standards for drinking purposes. The concentrations of chlorophyll "a" and the Plankton counts were very low. This study shows that factors like high nutrient concentration, high sun illuminations, suitable pH, high temperature, and the low velocity of water should lead to the eutrophication processes in the Mujib dam water, but, the eutrophication processes is very limited and do not reach to the level of algae blooms.

© 2010 Jordan Journal of Earth and Environmental Sciences. All rights reserved

Keywords: Eutrophication; Mujib Dam; Algal blooms; Nutrients; Organisms.

1. Introduction

The main problem seems to face the use of surface water for domestic purposes in semi-arid regions is eutrophication of surface waters bodies which results from direct or indirect result of anthropogenic activities (Salameh, 1985).

Nutrients, such as nitrogen, phosphorus and silicate Silica in lakes, reservoirs and some streams, rivers, and near shore marine water are prerequisites for life, and do not form an environmental problem. Nutrients are not pollutants but life givers (Carpenter *et al.*, 1998; Hornung *et al.*, 1995). They become a problem when too large inputs affect the original character, properties or functions of the ecosystem. When this occurs, it is referred to as eutrophication. Eutrophication is characterized by the presence of sufficient planktonic, algae and water weeds, which cause water quality impairments for use in domestic water supply.

The human factors affecting water quality are generally associated with the type and level of development activities within the catchments of a water body. The presence of human activity in a public water supply area is considered as a potential risk to water quality impairment. In addition, human activities can accelerate the rate at which nutrients enter ecosystem. Runoff from agriculture and development, pollution from septic systems and sewers and other human related activities increase the flux of both inorganic nutrients and organic substances into terrestrial, aquatic, and coastal marine ecosystems

(Anderson, 1994; Bartram *et al.*, 1999; Ongley, 1996). Beside nutrient inputs, some physical conditions support eutrophication development. Thermal stratification of water bodies, (such as lakes and reservoirs), temperature and light influence the development of aquatic algae (WHO, 2002; Schramm, 1999).

The aim of this work is studying the chemical parameters in Mujib dam water, which could lead to the Eutrophication processes such as PO_4^{3-} , NO_3^- , and SiO_2 . In addition to the other physical, chemical and biological water constituents of Mujib dam such as (EC, pH, Na^+ , K^+ , Ca^{2+} , Mg^{2+} , NH_4^+ , HCO_3^- , CO_3^{2-} , Cl^- , SO_4^{2-} , BOD5, COD, TOC, Chlorophyll "a", Plankton count, Total Coli forms and *Escherichia coli*).

Previous investigations had already studied the eutrophication process in Jordan especially in the upper Jordan River regions (Salameh, 1985; Al-Khory, 2005; Khalil and Jamal 2007; Hailat and Manasreh, 2008; Manasreh *et al.*, 2009; Al-Harashsheh, 2010; Al-Harashsheh and Salameh, 2010; and Sophia, 2010).

The Hashemite Kingdom of Jordan is located within the Eastern Mediterranean Basin between latitudes [-110000-255000] N and longitudes [121000-570000] E, according Palestine Grid 1924 (PG) coordinates system (Figure 1), covering a land area of approximately 88.500 km^2 (NWMP, 2004).

* Corresponding author. surah_h71@yahoo.com;

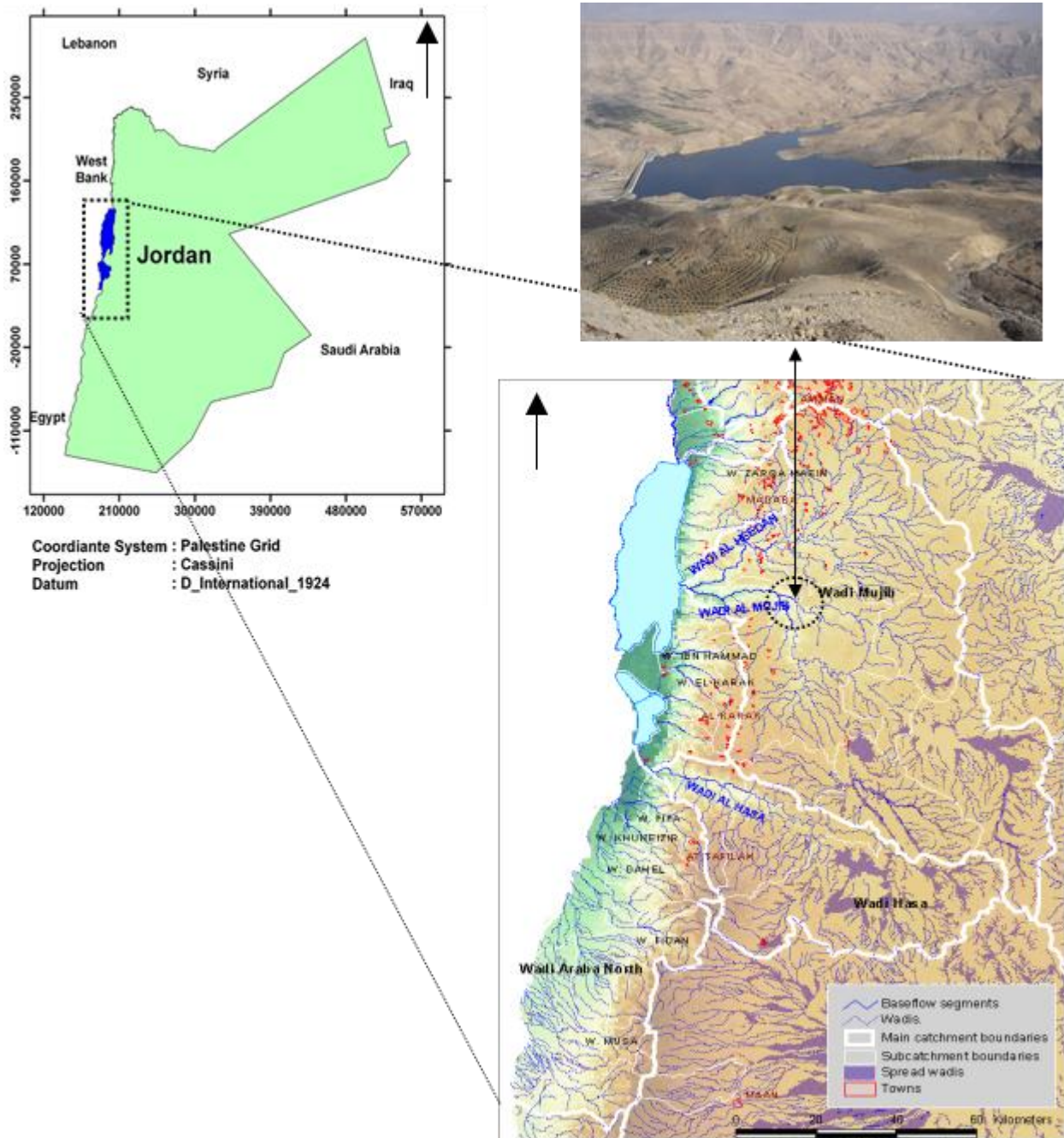


Figure 1. Location map of Mujib Dam (Photo) and its catchments area in Jordan.

Jordan has a limited amount of rain fall and, hence, limited surface and ground water resources. Jordan does not possess rivers in the World-Wide known scale, except the Jordan Rivers which used to discharge around 1400MCM/y into the Dead Sea before the development of the water resources in its catchments area (Al-Ansari and Salameh, 2006). Other surface water resources in Jordan are found in the Yarmouk and Zarqa Rivers and in wadis like Karak, Mujib, Hasa, Yabis and El-Arab, in addition to flood flow wadis in the different parts of the country (Al-Ansari and Salameh, 1999). Jordan built many dams to store flood water along the main rivers and wadis such as

King Talal Dam, Wadi El-Arab Dam, Wadi Ziglab Dam, Kafrein Dam, Wadi Shueib Dam, Al Karameh Dam, Wala Dam, Tannour Dam, Mujib Dam and many desert dams. Figure 3 shows the location of some of these dams.

The Mujib Wadi is located between latitudes [95393 - 137739]N, and longitudes [205442 - 244775]E. The Wadi Mujib system comprises the Wala, Swaqa, Heidan and Mujib, with total catchments area of about 6.700 km² (Al-Asa'd and Abdullah 2010; NWMP, 2004). On the other hand, Wadi Hasa catchments area is about 2,600 km², (NWMP, 2004) (Figure 1).

Perennial flow for both Wadi Mujib and Wadi Hasa is restricted to the downstream reaches, where ground surface elevation is below 400m BSL (below sea level). The base flow originates primarily from the continuous array of springs within the Dead Sea escarpment, and partly from the Ajloun Group and the lower sandy aquifer systems (Kurnub sandstone) (NWMP, 2004).

The average annual precipitation is 154 mm and ranges from 300 mm in the northwestern part of the watershed to 50 mm or less in the southeastern corner, and the average annual potential Evaporation is 2200 mm (DOM, Open files).

Wadi Mujib downstream of the confluence of wadi Heidan discharges an average amount of 83 MCM/y directly into the Dead Sea. Half of the river flow consists of base flow and the other half of flood flows (DOM, Open files).

The catchments area is sparsely inhabited, with moderate agricultural activity and almost no industry; therefore, industrial pollution is not a major issue in the Wadi Mujib area (Al-Ansari and Salameh 2006).

The Mujib dam aiming at exploiting floods flows to provide water to the Arab Potash company, the Dead Sea chemical complex, the tourist's area at the eastern shore of the Dead Sea and drinking water to Amman city (Mahasneh, 2001). Land uses/ land covers of Mujib catchments area are strongly influence the chemistry of lake water and its temporal variations. Of the major land uses of Al-Mujib catchments area and its lake the followings: Cultivated land and livestock farm, Gypsum

mines, Disposal of wastewater in cesspits, fishing in the lake (Margane *et al.*, 2008).

2. Methodology

Water samples were collected during the period 2006 to 2010 and analyzed in the laboratories of Water Authority of Jordan; In addition parallel samples were collected and analyzed in the laboratories of Institute of Earth and Environmental Science at Al-al Bayt University.

Samples were collected monthly from the lake surface in polyethylene bottles (1000 ml) for chemical analysis and in sterilized glass bottles for microbiological analysis and transported to the laboratory. In addition, pH and EC measurements were conducted in the field using portable meter.

The analysis of Na^+ , K^+ , Ca^{2+} , Mg^{2+} , NH_4^+ , HCO_3^- , CO_3^{2-} , Cl^- , SO_4^{2-} , PO_4^{3-} , NO_3^- , SiO_2 , B, Cd, Cr, Fe, Pb, Mn, Ni, Zn, dissolved non-specific organic compounds measured as BOD₅, COD, and TOC, chlorophyll "a", plankton count, total Coli forms and Escherichia Coli were analyzed according to the Standard Methods for Examination of Water and Wastewater. The total bacterial count was determined by incubating on a nutrient in agar plate at 28°C for 48 hour. Total Coliforms count and fecal Coliforms were determined using multiple tube fermentation. The total Coliforms numbers were estimated in a lauryl Tryptose broth and the tubes were incubated at 37°C for 24 to 48 hours. For fecal Coliforms count, *Escherichia Coli* were incubated at 44.5°C for 24 hours.

The analytical methods which have been used to analyze the water samples are listed in (Table 1).

Table 1. Analytical methods used for measuring hydrochemical and biological parameters of the water samples.

Parameter	Unit	Analytical Method
EC	µS/cm	Field EC probe
pH	Value	Field pH electrode
Na^+	mg/l	Flame Photometer
K^+	mg/l	Flame Photometer
Ca^{2+}	mg/l	Titration method
Mg^{2+} (TH- Ca^{2+})	mg/l	Titration method
Cl^-	mg/l	Ion Chromatographic system
HCO_3^-	mg/l	Ion Chromatographic system
CO_3^{2-}	mg/l	Ion Chromatographic system
NO_3^-	mg/l	Ion Chromatographic system
SO_4^{2-}	mg/l	Ion Chromatographic system
PO_4^{3-}	mg/l	Ion Chromatographic system
SiO_2	mg/l	Spectrophotometer
NH_4^+	mg/L	Ammonia Selective Electrode
BOD ₅	mg/L	5 day BOD Test (Ref. WW-BOD ₅ -R003)
COD	mg/L	Closed Relux Titration Method (Ref. WW-COD-R005)
TOC	mg/L	Per sulfate-Ultraviolet Oxidation
Heavy metals (B, Cd, Cr, Fe, Pb, Mn, Ni, Zn)	µg/l	ICP-OES (Coupled Plasma Optical Emission Spectroscopy)
Plankton Count	Unit/ml	Concentration by Sedimentation Technique
Chlorophyll "a"	ppb	Fluorometric Determination (Ref:MIC-CHA-R*003)
Total Coli forms	MPN/100 ml	Multiple Tube Fermentation (Ref:MIC-TFC-R*003)
Escherichia coli	MPN/100 ml	Multiple Tube Fermentation (Ref:MIC-TFC-R*003)

3. Result and Discussion

The concentration of the different parameters is affected by the different water source, large variations

input water flow, water velocity, human activity and the climatic variations between winter and summer seasons.

The seasonal average of some chemical laboratory analyses of water samples are listed in (Table 2).

Table 2. Seasonal average of chemical and biologic laboratory analyses of water samples.

Sampling Time	pH	EC ($\mu\text{S/cm}$)	Na^+ (mg/l)	K^+ (mg/l)	Ca^{+2} (mg/l)	Mg^{+2} (mg/l)	HCO_3^- (mg/l)	Cl^- (mg/l)	SO_4^{-2} (mg/l)	Chlorophyll (ppb)	Escherichia coli	Total coliform
W 2006	7.9	1754	201.7	15.6	119.2	50.9	182.3	375.2	305.5	0.86	2700	13000
Sp 2006	8.1	1790	180.7	11.7	135.8	56.0	130.0	335.4	480.4	1.08	7500	6800
Su 2006	8.2	1761	183.4	14.6	103.5	40.5	157.1	332.6	196.9	1.05	5169	4483
W 2007	8.2	1326	51.6	6.9	67.8	21.6	161.3	68.1	153.4	1.04	2305	4328
Sp 2007	8.2	1269	44.3	5.7	61.7	21.0	155.7	65.8	139.2	1.15	2760	13667
Su 2007	8.1	1483	65.1	5.8	70.7	25.3	168.5	90.8	161.9	1.2	2760	3160
W 2008	8.1	969	76.5	5.8	80.4	28.1	186.5	99.8	180.3	1.17	1453	3658
W 2009	8.2	1254	52.4	6.2	68.8	20.2	160.9	67	154.1	0.95	318	690
Sp 2009	8.2	1566	212.5	14.4	147	48.2	226.9	424.2	174.4	1.03	1083	1113
Su 2009	8.1	1289	113.2	12.9	83.8	31.2	143.8	191.8	170.2	1.12	800	255
W 2010	8.3	1360	236.2	15.9	118.2	47.8	154.9	434.7	238.2	1.04	1273	2530
Sp 2010	8.3	1683	240.3	14.3	112.2	44.7	134.2	425.6	240.3	1.08	1680	1500
Su2010	8.3	1820	252.1	16.0	125.6	50.9	163.5	453.4	244.3	1.16	2400	1360

3.1. Physical Parameters (pH, EC)

3.1.1. pH Value

The pH value for the Mujib Dam water shows small variations between summer and winter samples (Figure 2). The average pH value ranged between 7.93 in winter 2006 to 8.32 in summer 2010 and these values are considered suitable for drinking water (Figure 2).

Furthermore, a general trend of pH increasing during the period 2006 and 2010 is clearly shown (Figure 2), this could be attributed to the dissolution of basic minerals such as carbonates (limestone, dolomite, calcite,..) and clay minerals that found along the course of tributaries of Mujib catchments area, which eventually increases the water lake alkalinity and hence its acidity.

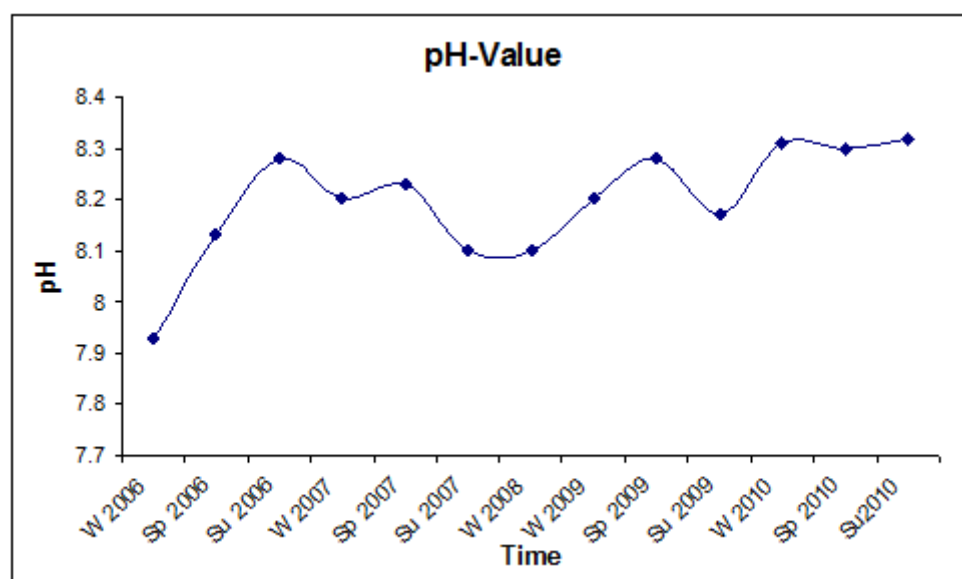


Figure 2. Temporal Variations of the average pH of the Mujib Dam water during the period (2006-2010), (W: Winter, Sp: Spring, Su: Summer)

3.1.2. Electric Conductivity (EC)

In general, the EC value is a good indicator for water salinity and hence its quality, the EC value in summer seasons was found to be higher than it in winter seasons due to dilution by floodwater during winter (Figure 3). The average EC value ranged between 969 $\mu\text{S}/\text{cm}$ in winter 2008 and 1820 $\mu\text{S}/\text{cm}$ in summer 2010. Furthermore, Figure (3) shows a gradual decrease in the EC values from

around 1800 $\mu\text{S}/\text{cm}$ in W2006 until it reaches 969 $\mu\text{S}/\text{cm}$ in W2008, then a gradual increase in the EC until it reaches around 1800 $\mu\text{S}/\text{cm}$ in 2010, these variations could be attributed to different interrelated factors such as: dissolution processes, rainfall, lake water level, evaporation (e.g. the higher evaporation rate, the higher concentration of ions and higher EC and salinity values).

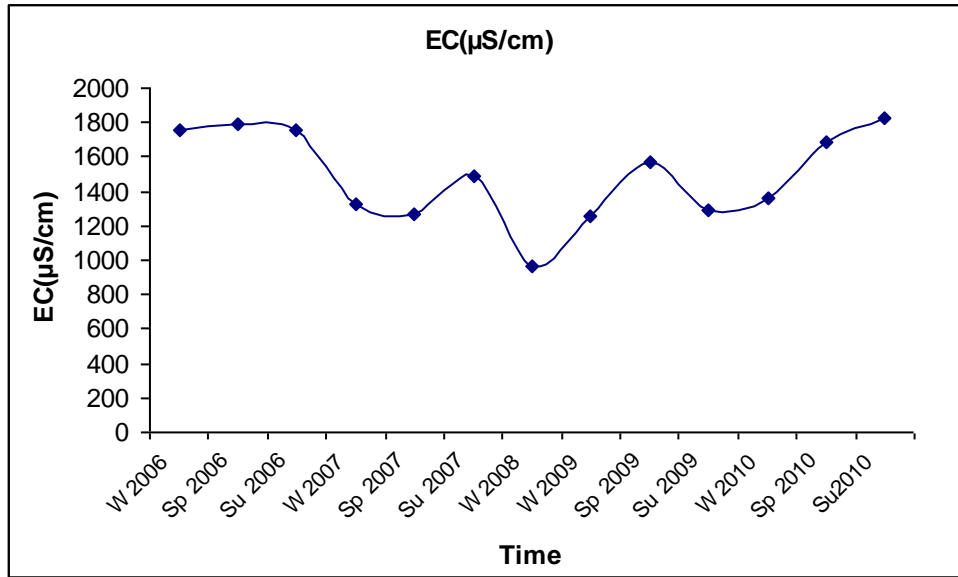


Figure 3. Temporal Variations of the average EC of the Mujib Dam water during the period (2006-2010)

3.2. Chemical Parameters

3.2.1. Cation concentration

The cations Na^+ , K^+ , Ca^{2+} , Mg^{2+} and NH_4^+ concentration ranged between 44.3, 5.87, 61.72 and 20.21 mg/l to 252.13, 16.03, 147.09 and 56.06 mg/l respectively.

The variations between cations concentration in 2006 and 2010 were found to be higher than 2007, 2008, and 2009 due to differences in the average. The average values of cation concentration during summer seasons are higher than winter seasons due to the high evaporation in the summer time except 2006 (Figure 4).

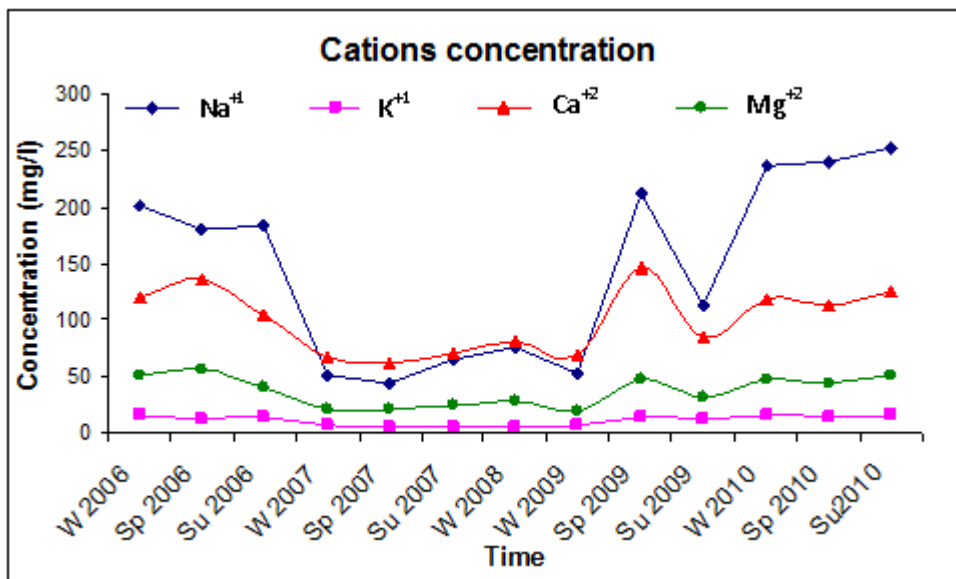


Figure 4. Temporal Variations of the average cations concentration of the Mujib Dam water

The result of the ammonium (NH₄⁺) analyses in all samples was found to be less than 0.1mg/l may be because no waste water recharge in these area which reflecting the sparsely inhabited catchments area.

3.2.2. Anions concentration

The anions HCO₃⁻, CO₃²⁻, Cl⁻ and SO₄²⁻ concentration ranged between 130.07, 0, 67 and 139.2 mg/l to 226.92, 12, 454.76 and 480.48 mg/l respectively. Most the average value of the anions concentration during summer seasons were higher than during winter seasons and this difference due to the evaporation in the summer

seasons with the exception of 2006. The Cl⁻ concentration in 2007 and 2008 was less than in 2006, 2009 and 2010 while the concentration of CO₃²⁻ equal zero except during the spring of 2009 and spring 2010. The cations Na⁺, Ca²⁺ and anions Cl⁻, SO₄²⁻ concentration are higher than another cations and anions in Mujib Dam due to dominated the halite and gypsum salt in the Mujib Dam catchments area (Figure 5). In addition to Gypsum mining activities, unsewered houses inside the catchments area could be considered another source of higher sulfate concentration (Figure 5).

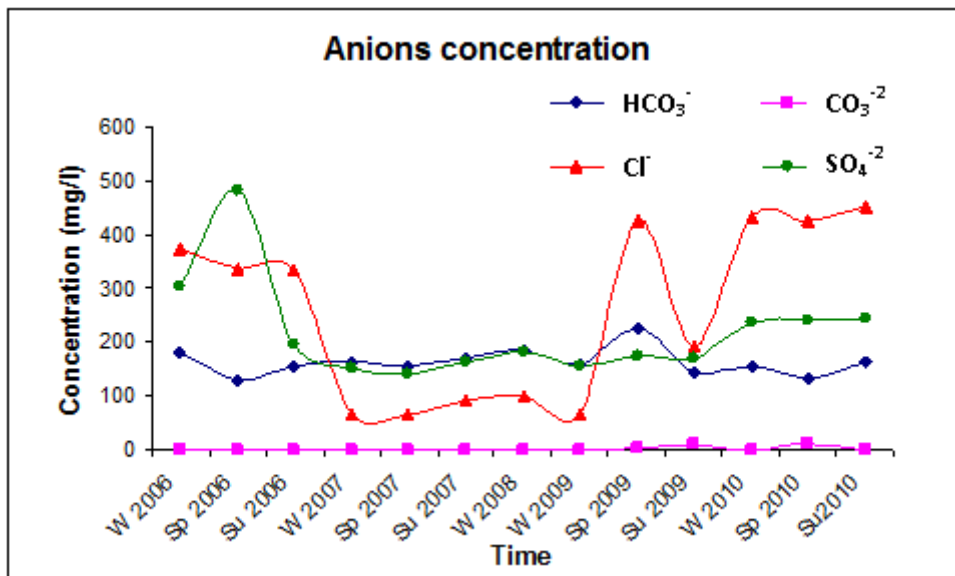


Figure 5. Temporal variations of the average anions concentrations of the Mujib Dam water

3.2.3. The Nutrients (PO₄³⁻, NO₃⁻, SiO₂)

The PO₄³⁻, NO₃⁻ and SiO₂ concentrations ranged between 0.01, 0.94 and 0.356 mg/l to 0.177, 3.98 and 15.55mg/l respectively. In general, the average value of (PO₄³⁻, NO₃⁻, SiO₂) concentrations in winter is higher than in the summer seasons except 2006 due the flushing of the soil by the run off (Figure 6). The concentrations of the nutrients are above the Eutrophication level, combined with high temperatures, high light intensity, when

eutrophication processes seems to be inevitable. The NO₃⁻ and PO₄³⁻ concentrations are necessary for the eutrophication process 0.2-0.3 and 0.01 mg/l respectively (Lee and Lee, 2005), (Figure 6). The main sources for nutrients are disposal wastewater in cesspits, chicken farms and cultivated lands inside Mujib dam catchments area. The higher values of silica contents could be attributed to the dissolution of sandstone of Kurnub Formation or clay deposits in the study area.

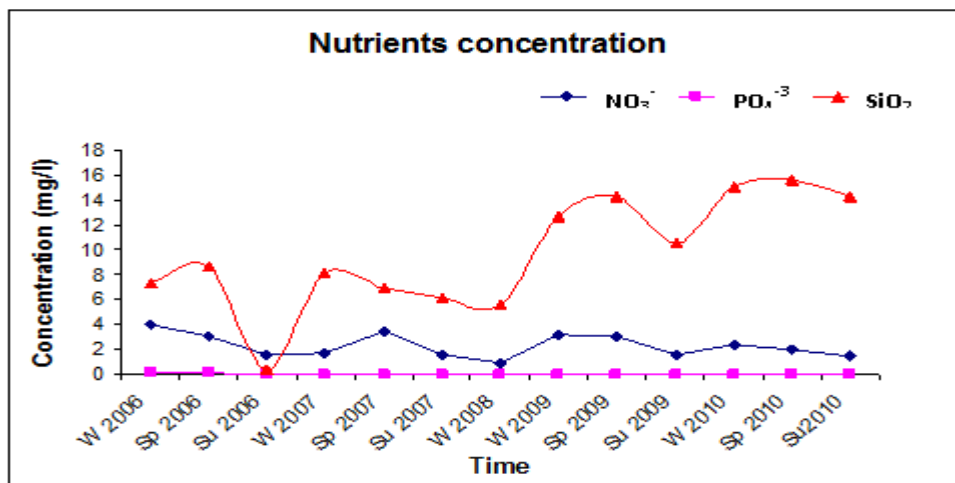


Figure 6. Temporal Variations of the average nutrients concentration of the Mujib Dam water

3.2.4. Trace Elements

Trace elements and heavy metals in Wadi Al Mujib dam water (Table 3) may be resulted from human activity such as mining and processing industrial, operation of

fuel-driven boat and weathering of rocks such as Oil shale in surrounding regions where the flow direction from Lajjoun area could reach Al-Mujib dam in a few hours (Al-Harashsheh *et al.*, 2010).

Table 3. Average concentration of Trace Elements in Mujib Dam water.

Time	B (µg/l)	Cd (µg/l)	Cr (µg/l)	Fe (µg/l)	Pb (µg/l)	Mn (µg/l)	Ni (µg/l)	Zn (µg/l)
W 2006	0.22	<0.003	<0.01	0.22	<0.01	<u>0.23</u>	<0.01	<0.04
Sp 2006	0.25	<0.003	<0.01	<0.1	<0.01	<0.01	<0.01	<0.06
Su 2006	<0.003	<0.003	<0.01	<0.1	<0.01	<0.01	<0.01	<0.06
W 2007	0.45	<0.02	<0.02	<0.2	<0.01	0.06	<0.02	<0.06
Sp 2007	0.28	0.02	0.02	<0.4	<0.01	<u>0.15</u>	<0.02	<0.06
Su 2007	0.3	<0.003	<0.02	<0.1	<0.01	<0.02	<0.02	<0.06
W 2008	0.22	<0.003	<0.01	<0.1	<0.01	<0.01	<0.01	<0.06
W 2009	0.4	<0.02	<0.02	<0.1	<0.01	<0.06	<0.02	<0.06
Sp 2009	0.34	<0.02	<0.02	0.24	<0.01	<0.06	<0.02	<0.06
Su 2009	0.33	<0.01	<0.02	<0.2	<0.01	<0.08	<0.02	<0.06
W 2010	0.2	<0.003	<0.02	<0.1	<0.01	<0.02	<0.02	<0.06
Sp 2010	0.3	<0.003	<0.01	<0.1	<0.01	<0.01	<0.01	<0.06

Table 3 shows that the concentration of trace elements and heavy metals were below the below the maximum permissible limits according to the Jordan Standards specification.

3.3. Dissolved Non-specific organic compounds.

The dissolved non-specific organic compound (Biological oxygen demand (BOD₅), Chemical oxygen demand (COD), Total organic carbon (TOC)), were analyzed in the Mujib dam water.

3.3.1. Biological oxygen demand (BOD₅)

The result of BOD₅ concentration in all samples for the 2006, 2007, 2008, 2009 and 2010 are less than 10 mg/l.

3.3.2. Chemical oxygen demand (COD)

The result COD concentration in all seasons are less than 20 mg/l except winter 2007 and winter 2008 are less than 30 mg/l but more than 20 mg/l.

3.3.3. Total Organic Carbon (TOC)

The result of TOC concentration analyses in all samples are less than 2 mg/l.

3.4. Biological parameters:

Chlorophyll "a", Plankton count, Total Coli forms and Escherichia cilia were analyzed to present the biological parameters in the Mujib dam water.

3.4.1. Chlorophyll "a" and Plankton count

The chlorophyll "a" concentrations show small variations between summer seasons and winter seasons, where the average value ranged between 0.86 ppb in winter 2006 to 1.24 ppb in summer 2007.

The concentration of chlorophyll "a" was found to be higher in the summer than in the winter due to high temperature, nutrients availability and high intensity of light. However, in general the concentration of chlorophyll "a" is very low in Mujib dam water compared with other dams in Jordan (e.g Wadi Al Arab, King Talal Dams and King Abdullallah Canal (KAC)) (Al-Harashsheh, 2007) (Figure 7).

Table 4 shows the result of plankton count analyses in all samples from winter 2006 to summer 2010, the Plankton count in the summer time higher than winter time where it is not seen in winter time except winter 2008 and 2009. The Plankton count in the summer time ranged between 4 in summer 2006 to 14 in summer 2010. The numbers of the Plankton count were found to be very low indicating that the concentration of the algae are very small and the occurrence of Eutrophication blooms is limited in Mujib dam.

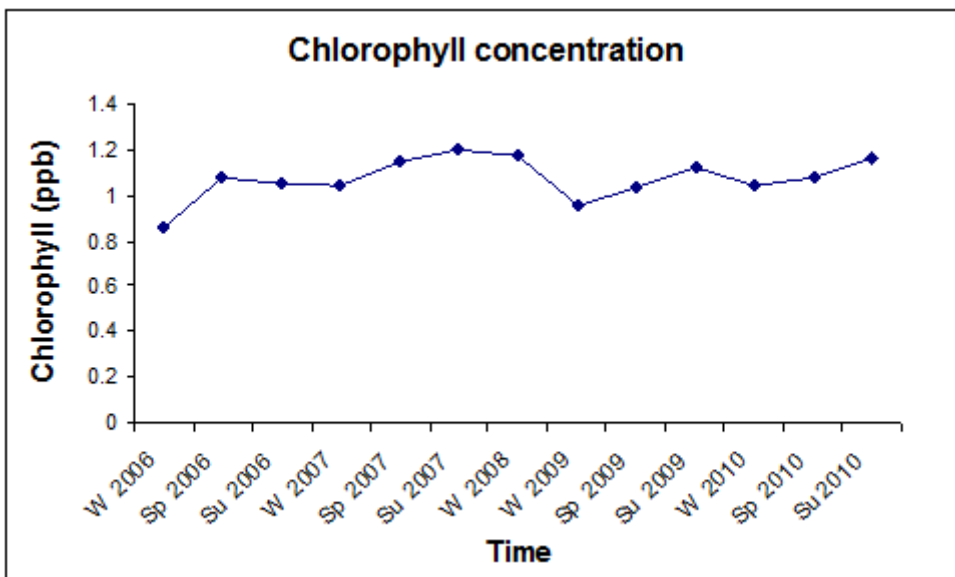


Figure 7. Temporal variations of the average Chlorophyll "a" concentration of the Mujib Dam water

Table 4. Average Plankton count in Mujib Dam water.

Time	Plankton count(unit/ml)
W2006	Not Seen
S2006	4
W2007	Not Seen
S2007	6
W2008	10
W2009	Not Seen
S2009	11
W2010	5
S2010	14

The bacterial count plays an important role in the biological process because heterotrophic bacteria break down organic matter into smaller molecules and carbon dioxide. The presence of Coliforms, particularly fecal Coliforms is an indication of the presence of associated pathogens. Thus, determination of Coli forms and fecal Coli forms in water is essential as water quality parameters (Al- Harahsheh, 2007). The analyses of Escherichia Coli and total Coli forms are presented in (Figure 8) for whole

samples. The average Escherichia Coli number ranged between 318 in winter 2009 to 7500 MPN/100ml in spring 2006, while the total Coliforms ranged between 255 in spring 2009 to 13667 MPN/100ml in spring 2007, the average Escherichia Coli number was higher in summer seasons than winter seasons and the average total Coli forms in winter seasons higher than summer seasons. The main sources of fecal Coli form and Escherichia Coli in lake water are unsewered houses and the livestock farms.

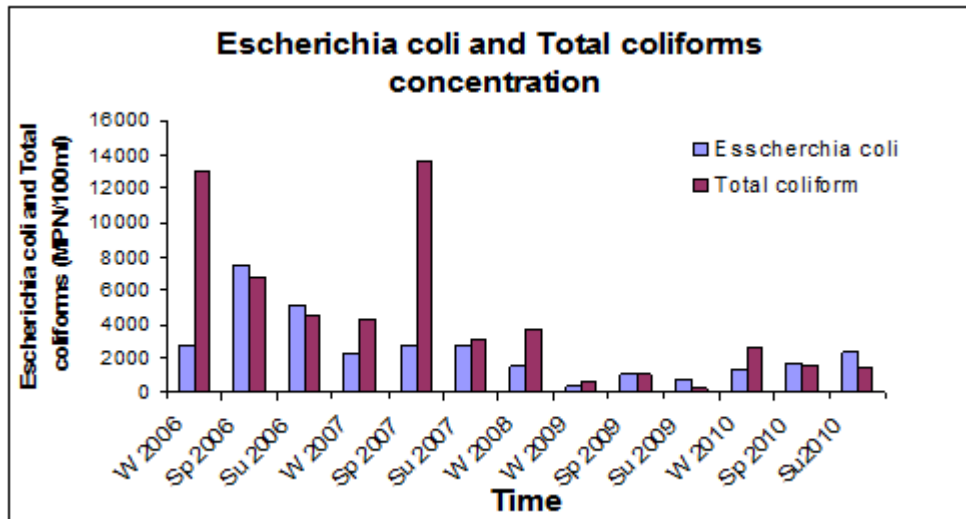


Figure 8. Temporal variations of the average Escherichia Coli and total Coli forms numbers value of the Mujib Dam water

4. Conclusions

- EC and pH showed small variation as a result of the feeding waters originating from the same geographic area.
- The major cations (Na^+ , K^+ , Ca^{2+} , Mg^{2+}), major anions (HCO_3^- , CO_3^{2-} , Cl^- , HCO_3^- , CO_3^{2-} , Cl^- and SO_4^{2-}), NH_4^+ and trace elements and heavy metals concentrations are less than permissible limits assigned by the Jordan Standard for drinking water, thus the Mujib dam water can be used as a drinking waters sources.
- Biological oxygen demands (BOD5), Chemical oxygen demand (COD), Total organic carbon (TOC), are lower than Jordan Standard for drinking water.
- The chlorophyll "a" concentration and Plankton count are very low and the mean the eutrophication is very limited in Mujib dam.
- All these factors (high nutrient concentration, high sun illuminations, suitable pH, high temperature, and the low velocity of water) are available to cause eutrophication processes. All these conditions provide ideal environment for big variations of algal species to grow and increase in numbers forming algal blooms. Nevertheless, the occurrence of Eutrophication blooms is limited in Mujib dam. The UV radiation which may restrict eutrophication process.
- The Mujib Dam water quality was affected by the climate and topography of the region (e.g. soil type and intensity of rainfall intensity...etc.) rather than with the effects of anthropogenic influence.

References

- Al-Ansari, N.A., Salameh, E., 1999. Water Resources in Mafraq and Al al-Bayt University Contribution, Workshop on Water Resources and Environment in the Badia Region organized by Al al-Bayt University and Coventry University. (U.K.), Mafraq 12-17 July.
- Al-Ansari, N.A, Salameh E., 2006. Jordan country study **In:** Efficient management of wastewater, its treatment and reuse in

four Mediterranean countries, Jordan, Palestinian Territories, Lebanon and Turkey, EMWter, Printed by Alshaeb Press. ashwa Amman. pp.14-73.

Al-Ass'ad, T.A, Abdulla, F. 2010. Artificial groundwater recharge to semi-arid basin: case study of Mujibaqufer, Jordan. *Environmental Earth Science*, 60:845-859.

Al-Harshsheh, S. T., 2007. Eutrophication process along King Abdullah Canal, chemistry, organisms, and resulting compound, PhD. Thesis, University of Jordan.

Al-Harshsheh S., Salameh E., 2010. Eutrophication processes in Arid climates, **In:** Eutrophication: Causes, Consequences and Control, Springer, Heidelberg, Germany.

Al- Harahsheh A., Al- Adamat R., Al-Farajat M., 2010. Potential impacts on surface water quality from the utilization of oil shale at Lajjoun areal southern Jordan using Geographic information system and leachability tests. *Energy Sources, Part A: Recovery Utilizations and Environmental Effects*, 32:1763-1776.

Al-Khoury, W. E. 2005. The water constituents of King Abdullah Canal and their role in the Eutrophication processes, unpublished M. Sc. Thesis, University of Jordan, Amman.

Anderson, D.M., 1994. Eutrophication, *Scientific American Journal*, 271: 62-68.

Bartram, J., Wayne, W., Carmichael, Ingrid, C., Gary, J., and Olav M., 1999. Cyanobacteria in water: A guide to their public health consequences, monitoring and management, **In:** World Health Organization.

Carpenter, S. R., Caraco, N. F., Correll, D. L., Howarth, R.W., Sharple, A. N., Smith, N. H., 1998. Non-point pollution of surface Waters with Phosphorus and Nitrogen, *Ecological Application*, 8 (3): 559-568.

DOM., 2010. Open files, Department of Metrology, Jordan.

Hailat .I.A., Manasreh, W. A, 2008. The study of the influence of Al- Lajoun basin on water quality of Al-Mujib Dam, Department of chemistry, Mutah University, Al-Karak, chem.yu.edu.jo/conf/finaly.

Hornung M., Sutton M .A., and Wilson R.B., 1995. Mapping and modeling of critical loads for nitrogen - a workshop report. Grange-over- Sands, Cumbria, UK. UN-ECE, Convention on Long Range Transboundary Air Pollution, Working Group for Effects, 24-26 October 1994. Published by Institute of Terrestrial Ecology, Edinburgh, UK.

- Lee, A.J., and Lee, G.F., 2005. Eutrophication (excessive fertilization), Water Surface and Agricultural Water, Wiley, published doctoral, NJ. Hoboken, NJ, pp.107-114, www.gfredlee.com.
- Mahasneh D., 2001. Water management in the Jordan Valley, JVA. Amman.
- [16] Manasreh W., Hailat I., El-Hasan T., 2009. Heavy metal and anionic contamination in the water and sediments in Mujib reservoir, Central Jordan, Environmental Earth Sciences, 60 (3): 613-621
- Margane, A., Borgstedt, A., Subah, A., Hajali, Z., Hamdan, B., Atrash, M., Jaber, A., Kouz, A., Jawad, F., 2008. Delineation of surface water protection zone for Mujib Dam, Federal Ministry for Economic Cooperation and Development (Bundesministerium. Fur wirtschaftliche zusammenarbeit and Entwicklung, BMZ 2008.
- National Water Master Plan (NWMP), 2004. Surface water resources: vol (4). Ministry of Water and Irrigation, Jordan and German Technical Cooperation (GTZ), Internal Report.
- Ongley D.E., 1996. Control of water pollution from agriculture, Gems/water Collaborating Canada, (FAO), Rome.
- Khalil, M. I, Jamal. J.O, 2007. Geochemistry and environmental impacts of retorted Oil shale from Jordan, Earth and Environmental Science, Environmental Geology, 52 (5): 979-984.
- Salameh, E., 1985. The potential of surface water utilization for domestic purposes in Jordan, Intern. T. Environmental Studies, 28: 291-300.
- Salameh, E., 2001. Water shortage and environmental Degradation, **In:** Living with water scarcity, water resources in Jordan badia region the way forward, Publication of Al al-Bayt University, Mafraq, Jordan. pp 71-87.
- Schramm W., 1999. Factors influencing seaweed responses to Eutrophication: some results from EU-project EUMAC, Journal of Applied Phycology, 11: 69-78.
- Sophia S.B., 2010. The Upper Jordan River algal communities are evidence of long-term climatic and anthropogenic impacts, J. Water Resource and Protection, 2:507-526.
- World Health Organization (WHO) Regional Office for Europe, 2002. Eutrophication and health, Office for Official Publications of the European Communities, vol. 4.



الجامعة الهاشمية



المملكة الأردنية الهاشمية

المجلة الأردنية
لعلوم الأرض والبيئة

JJEES

مجلة علمية عالمية محكمة

<http://jjees.hu.edu.jo/>

ISSN 1995-6681

المجلة الأردنية لعلوم الأرض والبيئة

مجلة علمية عالمية محكمة

المجلة الأردنية لعلوم الأرض والبيئة : مجلة علمية عالمية محكمة أسستها اللجنة العليا للبحث العلمي في وزارة التعليم العالي والبحث العلمي، الأردن، وتصدر عن عمادة البحث العلمي والدراسات العليا، الجامعة الهاشمية، الزرقاء، الأردن.

هيئة التحرير

رئيس التحرير

الأستاذ الدكتور عبد الرحيم أحمد حمدان
الجامعة الهاشمية، الزرقاء، الأردن.

الأعضاء

الأستاذ الدكتور أحمد أبو هلال
جامعة اليرموك.
الأستاذ الدكتور عيسى مخلوف
الجامعة الهاشمية
الأستاذ الدكتور طایل الحسن
جامعة مؤتة.

الأستاذ الدكتور عبد القادر عابد
الجامعة الأردنية.
الأستاذ الدكتور هاني خوري
الجامعة الأردنية.
الأستاذ الدكتور زهير العيسى
الجامعة الأردنية.
الأستاذ الدكتور سامح غرابية
جامعة اليرموك

فريق الدعم

تنفيذ وإخراج

الدكتور قصي الذبيان م.أسامة الشريط

المحرر اللغوي

ترسل البحوث إلى العنوان التالي:

رئيس تحرير المجلة الأردنية لعلوم الأرض والبيئة
عمادة البحث العلمي والدراسات العليا
الجامعة الهاشمية

الزرقاء ١٣١٣٣ - الأردن

فرعي: 4147 هاتف : 3903333 (5) +962

Email: jjees@hu.edu.jo

Website: www.jjees.hu.edu.jo